TRIBHUVAN UNIVERSITY

INSTITUTE OF ENGINEERING

PULCHOWK CAMPUS

THESIS NO: 075/MSWRE/020

Modeling the impacts of LULC change on Runoff and Sediment yield of Bagmati River Basin in Kathmandu Valley

by

Uttam Rokaya

A THESIS

SUBMITTED TO THE DEPARTMENT OF CIVIL ENGINEERING IN

PARTIAL FULFILLMENT OF THE REQUIREMENTS FOR THE DEGREE OF MASTER OF SCIENCE IN WATER RESOURCES ENGINEERING

DEPARTMENT OF CIVIL ENGINEERING

LALITPUR, NEPAL

SEPTEMBER, 2021

COPYRIGHT

TRIBHUVAN UNIVERSITY

INSTITUTE OF ENGINEERING

CENTRAL CAMPUS

DEPARTMENT OF CIVIL ENGINEERING

The undersigned certify that they have read, and recommended to the Institute of Engineering for acceptance, a thesis entitled **" Modeling the impacts of LULC change on Runoff and Sediment yield of Bagmati River Basin in Kathmandu Valley"** submitted by Uttam Rokaya in partial fulfillment of the requirements for the degree of Master of science in Water Resources Engineering.

_____

Supervisor: Dr. Suraj Lamichhane

Associate Professor

Department of Civil Engineering

M.Sc. Water Resources Engineering

_____

External Examiner: Er. Utsav Bhattarai

_____

Committee Chairperson: Dr. Pawan Bhattarai

Assistant Professor

Department of Civil Engineering

M.Sc. Water Resources Engineering

Date: September, 2021

ABSTRACT

Kathmandu valley (KV) is suffering from rapid land use change due to high rate of urbanization affecting hydrological process, which is crucial for sustainability of limited water resources. Land use/land cover (LULC) change in a watershed greatly affects the watershed hydrology and sediment yield. KV have a potential for a rapid LULC change in foreseeable future and requires attention. This study used Soil and Water Assessment Tool (SWAT) as a simulation tool for modelling the impact of LULC change on the catchment hydrological as well as sedimentological behaviour of the Bagmati river basin in the KV. This study incorporates hydrological and climate data from 2000 to 2016 for the analysis of LULC change effect on discharge and sediment yield. TerrSet software which incorporates Land Change Modeler (LCM), IDRISI GIS and image processing software was used for land cover change analysis and projection. LULC data of International Centre for Integrated Mountain Development (ICIMOD) for the year 1990, 2000 and 2010 A.D was used for land cover change analysis and validation of the projected LULC. Cellular Auromata-Markov Chain model was used for the LULC projection. The accuracy assessement of the projected LULC is done by Error Matrix analysis using IDRISI image processing tool. The overall Kappa Index of agreement gave 73 % accuracy. The LULC is projected for the year 2025, 2050, 2075 & 2100 A.D for impact assessment of LULC change on discharge and sediment yield.

Calibration, validation and sensitivity analysis was carried out using SWAT Calibration and Uncertainty Procedure (SWAT-CUP). The model result for both calibration and validation have shown good agreement with the observed values with Nash-Sutcliffe Efficiency (NSE), Coefficient of Determination (R^2), Modified Coefficient of Determination (bR^2), RMSE-Observations Standard Deviation Ratio (RSR) and Percentage Bias (PBIAS) for discharge as well as sediment. The prediction of LULC change using CA-Markov chain model indicates that built-up area is likely to increase by 2025, 2050, 2075 and 2100 at the expense of agricultural and forest areas, leading to an increase in river flow & surface runoff and decrease in lateral flow, groundwater flow and sediment yield.

Several studies has been carried out in the Bagmati basin of KV but most of those studies focused on implications of land use change on flow parameters only but this study assessed the implication of future LULC change on both water balance parameters and sediment yield. Quantification of

water balance and sediment yield within the urban watershed is more useful for the planning of water management as well as downstream projects for the engineer, environmentalist and others.

Keywords: Land use/land cover (LULC), Soil and Water Assessment Tool (SWAT), Cellular Automata – Markov Chain Model, SWAT Calibration and Uncertainty Procedure (SWAT-CUP), Discharge, Sediment yield

AKNOWLEDGEMENT

I express my sincere gratitude to my supervisor Assoc. Prof. Dr. Suraj Lamichhane sir for his valuable suggestions, continuous guidance, support and encouragement during the course of this study.

I would like to thank all the faculty members and colleague of Water Resources Engineering Program, Institute of Engineering, Pulchowk Campus for their support and constructive suggestions during the period of this study.

Also, lots of love and care to my parents and family members for their continuous inspiration and support throughout this study period.

Finally, thanks to all those persons who helped me directly or indirectly in accomplishing my thesis work.

Uttam Rokaya

September, 2021

Table of Contents

LIST OF TABLES

LIST OF FIGURES

LIST OF ANNEXES

ABBREVIATIONS

95PPU	95% Prediction Uncertainty
ASTER	Advanced Space-borne Thermal Emission and Reflection Radiometer
bR^2	Modified coefficient of determination
CA	Cellular Automata
CCAM	Climate Change Adaptation Modeler
CLUE-S	Conversion of land use and its effect at small regional extent
DEM	Digital Elevation Model
DHM	Department of Hydrology and Meteorology
ENVI	Environment for Visualizing Images
ESM	Ecosystem Services Modeler
ET	Evapotranspiration
ETM	Earth Trends Modeler
GLUE	Generalized Likelihood Uncertainty Estimation
HRU	Hydrologic Response Units
ICIMOD	International Center for Integrated Mountain Developement
IPCC	Intergovernmental Panel on Climate Change
KIA	Kappa index of agreement
KV	Kathmandu Valley
LCM	Land Change Modeler
LOADEST	Load Estimator
LULC	Land use/cover
MCMC	Markov Chain Monte Carlo
MLP	Multi layer perception

MUSLE	Modified Universal Soil Loss Equation
NSE	Nash Sutcliffe Efficiency
ParaSol	Parameter Solution
PBIAS	Percent Bias
PSO	Particle Swarm Optimization
R^2	Coefficient of determination
RMSE	Root mean square error
RSR	Standard deviation ratio
SOTER	Soil and Terrrain Database
SUFI-2	Sequential Uncertainty Fitting Version 2
SWAT	Soil and Water Assessment Tool
SWAT-CUP	SWAT Calibration and Uncertainty Program
USLE	Universal Soil Loss Equation

Chapter 1: INTRODUCTION

1.1. Background of the Study

Our natural environment has been modified over the years by different human activities. The dependence of human beings on natural resources has increased exponentially since the industrial revolution takes place. The rapid rate of urbanization, limited available resources, increasing demands and the constant overall earth mass has impacted the landmass and its natural ecosystem(Ndulue et al., 2015).

Nepal is among the least urbanized nations on the planet; however, it is among the top ten nations with the highest rate of urbanization (Bocquier, 2005). The urbanization rate of Nepal is highest in the Asia pacific region (R. B. Thapa & Murayama, 2010). Kathmandu Valley (KV), the capital city of Nepal is the most populous and rapidly growing urban area accounting 29% of the country's urban population. Increased population density, changes in LULC and changes in urban facilities & environment are the indicators of urbanization (Lamichhane & Shakya, 2019a).

The hydrologic cycle requires complex interactions and processes involving climate, land use, vegetation cover density, erosion rates and sediment load in the watershed. As a result of their complexity and unpredictability, natural systems such as the hydrologic cycle are difficult to understand, predict and manage. Hydrological models were created in response to the need for more scientifically sound analysis. It provides a framework to anticipate and foresee the relationships between climate, anthropogenic activities and water resources (Legesse et al., 2003).

LULC change is largely influenced by urbanization. Since the industrial revolution, the urban population has exploded resulting in significant environmental changes. The change in LULC impacts various areas of hydrology including socio-economics, ecology & environment (Ndulue et al., 2015). Additionally, it has a tendency to eliminate natural detention ponds and reroute river courses(Gomes & de Magalhaes, 2010). In this case, the discharge distribution changes over time, causing a change in flow pattern(Kashaigili, 2008). Agricultural based economics in developing countries are plagued by LULC changes (Tufa et al., 2014). As LULC changes from agriculture to settlement impervious surface increases, infiltration decreases, resulting in an increase in peak flow (Vildan Sahin, 1996). In addition, it accelerates soil erosion, which has a variety of negative

consequences on the natural ecosystem such as increased sedimentation and also causes water, soil & air pollution (Jokar Arsanjani et al., 2013).

Different hydrological models have been used for various watershed of Nepal to simulate models and to analysed impacts (Aryal et al., 2019; Shrestha et al., 2016; Thapa et al., 2017). SWAT model was selected for this study as this was used for the analysis of hydrological models in the Bagmati watershed before (Lamichhane & Shakya, 2019b; Pokhrel, 2018) and had proved to give reliable results. It is used all over the world for thousands of research and is regarded as one of the best model for analyzing hydrological responses (water, sediment and nutrient loss) caused by LULC change in the catchment with varying land use, soil and management conditions (Arnold & Fohrer, 2005) as well as its ability to characterize surface runoff and sediment yield producing mechanisms.

Some studies has been carried out in the past to analyse the impact of LULC change, climate change and their combined impacts on the Bagmati river. (Sharma & Shakya, 2006) analysed the impact of hydrological changes of the Bagmati river but their studies focused only on the hydrology and their study area was the whole watershed of the Bagmati river. (Lamichhane & Shakya, 2019b) studies the impact of both LULC change and climate change on the Bagmati watershed in KV but their study focuses only on the impacts on the hydrology.

Similar study was conducted by (Pokhrel, 2018) in the Bagmati basin of Kathmandu to analyze the impacts of LULC change on both flow & sediment yield. But the study focuses on historical change of LULC only and already published LULC data of 2000 and 2010 A.D from ICIMOD was used for change analysis. That study used sediment data projected from load estimater (LOADEST) and also the meteorological data used was only from two stations. Whereas this study used observed sediment data of the Khokana station from Department of Hydrology & Meteorology (DHM) and filled the missing data using sadiment rating curve. Also this study considered 21 rain gauge station, 6 temperature measurement station data, 8 relative humidtiy stations data, 2 solar radiation data & 2 wind station datas for the analysis. LULC is also projected for the future impact analysis of the LULC change on discharge and sediment yield. So this study will give us more realistic scenario of the LULC change impacts on both discharge and sediment yield.

In this study the impact of LULC change dynamics of KV, upper watershed of the Bagmati river in flow, water balance changed, soil erosion mechanism and sediment flow variation has been evaluated using hydrological model.

1.2. Objective of the Study

The overall objective of this study is to analyse the impacts of LULC change on the discharge and sediment yield of Bagmati basin in the Kathmandu valley. The specific objectives are:

- To model the potential changes in the LULC.
- To analyze the impacts of LULC change on hydrological process and sediment yield of the Bagmati basin.

To achieve these objectives, model selection, relevent literature review, data collection and methodology set up has to be carried out as discussed in the following sections.

1.3. Scope of the Study

The scope of the study, as per the objectives, contains methodology for estimation of discharge & sediment yield for present and future LULC with the application of hydrological modelling tool and GIS platform. It includes the acquisition, pre-processing and spatial analysis of DEM for catchment delineation and stream-network generation, preparation of hydro-meteorological data, Setting up of the physically based, semi-distributed hydrologic model (SWAT) to simulate the model, projection of LULC for future time periods and SWAT Calibration and Uncertainty Program (SWAT-CUP) for calibration, validation, sensitivity analysis and uncertainty analysis of the flow & sediment concentration, and finally the analysis of results. This can be summarized as follows:

- Acquisition and processing of data
- Watershed delineation and discretization
- Land use/land cover and Soil parameterization
- Writing precipitation, temperature and other weather generator files for model input
- Writing parameter files and running the chosen model
- Model calibration, validation and sensitivity analysis

- Projection of LULC for different time periods
- Projection of future Flow and Sediment yield for the projected LULC
- Result analysis

Use of tools like Arc GIS, Arc SWAT, SWAT-CUP and TerrSet Software for different purposes falls under the scope of the study.

1.4. Significance of the Study

Land use/land cover (LULC) changes in a watershed greatly affects the flow and sediment concentration of the river flowing through that watershed. Due to rapid urbanization in the Kathmandu valley most of the agricultural fields are converted into housing plots. Cutting down of steep slopes which was stable initially for construction works further accelerates erosion of soils. All these factors contribute greatly to the erosion of soils and ultimately increases sediment load of the river. Due to conversion of agricultural fields and forest into impermeable concrete surfaces for physical infrastructure decreases the infiltration of rain water into the ground subsurface, which ultimately accelerates the surface flow of water causing flash floods during heavy rainfall.

The findings of this research will give policy makers the insight of the present scenerio of Kathmandu valley and other urban areas of Nepal and helps to undertake effective measures to prevent the negative impacts of the land use change.

1.5. Layout of the Thesis Work

This Thesis report consists of five chapters which are illustrated in the following order:

Chapter 1:

This chapter gives the introduction of the thesis work as well as the objectives of the study. It also provides the scope of the work and explains the significance of the study.

Chapter 2:

This chapter gives the brief overview of different literatures reviewed which relates to my study. Review of past studies related to LULC change, hydrological watershed models and the description of different tools used for the LULC projection and hydrological modelling.

Chapter 3:

This chapter explains the study area and its characteristics.

Chapter 4:

This chapter explains the methodology adopted for study, data used, various process involved and the description of the models used.

Chapter 5:

This chapter summarizes the results and analysis of the study and discussions of the obtained results.

Chapter 6:

This chapter finally gives the brief conclussion of this Thesis work and recommendations for the further works.

Chapter 2: LITERATURE REVIEW

2.1. Watershed Hydrological Models

It is possible to simulate the flow of water and sediments in a given watershed using watershed/hydrological models. These models can also be used to quantify the impact of human activities on these processes. Water resources, environmental, and social problems can all be addressed by simulating these processes. Hydrological models have become a key tool to address a wide range of environmental and water resources issues including its planning, design, development, operation and management (Zhang et al., 2020). Flooding, droughts, upland erosion, stream bank erosion, coastal erosion, sedimentation, nonpoint source pollution, water pollution from industrial, domestic, agricultural and energy industry sources, migration of microbes, salinity and alkalinity of soils, deterioration of lakes, acid precipitation, disappearances of beaches, desertification of land, degradation of land, decay of rivers, irrigation of agricultural lands, proper management of water resources, conjunctive use of surface and groundwater, reliable design of the hydraulic structure and justifying the need for river training works are some of the critical environmental problems which are solved using the watershed model.

Watershed models help to understand the dynamic interaction between climate and land surface hydrology (Nyatuame et al., 2020). To protect the environment and water resources, watershed models are used to quantify the impacts of watershed management strategies linking human activities within the watershed to water quantity and quality of the receiving streams or lakes. Assessment of the impact of climate change on national water resources and agricultural productivity is also made possible by the use of watershed models.

2.2. Types of Hydrological Models

Hydrological models are classified based on the model inputs, parameters, and the extent to which physical principles are applied. Depending on the model parameters as a function of space and time, it can be categorized as a lumped or distributed model, and deterministic or stochastic models based on the other criteria.

As opposed to deterministic models, where a single input gives a single output; stochastic models can produce a variety of outputs from the same set of inputs. Lumped models ignore the spatial variability and assume an entire river basin as a single unit (Moradkhani & Sorooshian, 2008)

whereas a distributed model divides the entire watershed into small units usually square cells or a triangular irregular network to accommodate the spatial variability in the analysis and gives different outputs to each parameter.

Hydrological models can also be classified as static or dynamic based on the time factor. Dynamic model considers the temporal variation of the model parameters while it is excluded in the static model. One of the most important classifications is empirical model, conceptual models and physically-based models based on process representation.

2.2.1. Empirical Models

Empirical models are data-driven models also called observational models; that rely solely on existing data and ignore the features and processes of the hydrological system. Mathematical equations are used to correlate the time-series input and output data. Physical processes in the watershed is ignored while generating the mathematical equations, so the mathematical relationship obtained from the analysis is only valid within the confines of the boundaries they were created. Unit hydrograph method can be taken as an example of this model. Regression and correlation models are used to determine the functional relationship between inputs and outputs. Artificial neural networks and fuzzy regression are two of the machine learning techniques that are widely used in research.

2.2.2. Conceptual Models (Parametric models)

This model describes all the hydrological processes that make up a watershed. It considers the whole watershed as an interconnected reservoir which are recharged by precipitation, percolation & infiltrations and drained by evaporation & runoff. This method uses semi-emperical equaitons. Model parameters are determined by field data and also by calibration. A large record of hydrological and meteorological data are needed to calibrate the model. Calibration entails curve fitting, which complicates interpretation and makes it difficult to predict the effects of land-use change.

Many conceptual models of varying complexity have been developed. The Stanford Watershed Model IV (SWM) was the first major conceptual model developed by (NH Crawford, 1966) and has 16 to 20 parameters.

2.2.3. Physically Based Models

This is a mathematically idealized representation of the real phenomenon. This method primarily focuses on the physical process of the watershed, so it is also known as the mechanistic model. Both time and space-dependent and measurable state variables are used. Finite difference equations are used to represent the hydrological processes of water movement. Their calibration does not necessitate extensive hydrological and meteorological data, but a large number of parameters describing the catchment's characteristics must be evaluated (Abbott et.al., 1986). Many variables, such as soil moisture content, initial water depth, topography, topology and dimensions of river network must be considered in this method. Due to the use of physical parameters, the physical model can overcome many of the shortcomings of the other two models. As a result of its versatility, it can be used to provide a large amount of information, even outside the boundary. An example is the SHE (MIKE SHE) model.

Table 1: Comparison of Empirical, Conceptual and Physically based model

Empirical Model	Conceptual Model	Physically Based Model
Data based or metric or black box model	Parametric or grey box model	Mechanistic or white box model
Involve mathematical equations, derive value from available time series data	Based on modeling of reservoirs and include semi empirical equations with a physical basis	Based on spatial distribution, Evaluation of parameters describing physical characteristics
Little consideration of features and processes of system	Parameters are derived from field data and calibration	Require data about initial state of model and morphology of catchment.
High predictive power, low explanatory depth	Simple and can be easily implemented in computer code	Complex model. Require human expertise and computation capability.
Cannot be generated to other catchments	Require large hydrological and meteorological data	Suffer from scale related problems
ANN, Unit hydrograph	HBV model, TOPMODEL	SHE or MIKESHE model, SWAT
Valid within the boundary of given domain	Calibration involves curve fitting make difficult physical interpretation	Valid for wide range of situations

2.3. **Hydrological Model Selection**

There is a range of possible model structures within each class of models. Hence, choosing a particular model structure for a particular application is one of the challenges of the model user community. Four criteria for selecting model structures are as below: (Beven, 2001)

i. Consider models which are readily available and whose investment of time and money appeared worthwhile.
ii. Determine whether the particular model will produce the outputs to meet the goal of the project.
iii. Prepare a list of assumptions made by the model and check the assumptions likely to be limiting in terms of what is known about the response of the catchment. A relative assessment, or at best a screening to eliminate those models that are clearly wrong in their representations of catchment processes will be made.
iv. List all the inputs that the models requires and decide whether all the information required by the model can be provided within the time and cost constraints of the project.

Thousands of studies have been carried out using SWAT all around the world. A comparison of SWAT, HSPF and DWSM by (D. K. Borah et al., 2003) have found 17 applications of SWAT and conclude that it can be applied for continuous simulations of flow, soil erosion, nutrient and sediment transport etc. Using the SWAT model, (Easton et al., 2010) determined the runoff and erosion in the Blue Nile basin in order to determine the respective sources. They concludes that, the SWAT model requires very less calibration to get the good hydrologic prediction and also the model can predict sediment peaks.

Therefore, a semi-distributed physically-based hydrological model SWAT is selected for this particular study by considering the factors stated above and it is a basin-scale model used to simulate rainfall-runoff to predict the future environmental change impacts.

2.4. **SWAT for Watershed Modelling**

Among the above mentioned models, the physically based, basin scale, continuous time, semi-distributed SWAT model is a well-established model that operates on a daily/sub-daily time step for

analyzing the water, sediment, and agricultural chemical yields in large complex watersheds. It is one of the watershed models for long term impact analysis.

It is a river basin model developed by Dr. Jeff Arnold for the United States Department of Agriculture (USDA) Agricultural Research Service (ARS) (Arnold et al., 1995). This model uses comprehensive data and was developed to assess the impact of land management practices in large complex basins with varying soil types & land use conditions. The inbuilt algorithms of SWAT model are useful tools for generating missing climate data for basins. Currently the model is being applied worldwide with reported success. The use of SWAT model in USA, to support total maximum daily load analysis, as well as, in studies of climate change, hydrologic processes, land use change and water use and water quality applications, increased (P. W. Gassman et al., 2007). Recently, SWAT model has been also applied in catchments of Asian (Peng et al., 2021; Singh & Saravanan, 2020; Li et al., 2009b) African countries (Getachew et al., 2021; Nyatuame et al., 2020; Briak et al., 2016) for various applications.

The SWAT model is widely used in the United States and in some European countries to solve water management problems. It has been used for a variety of applications, including water balance calculation, sediment transport and stream-aquifer interaction. SWAT was integrated in GIS with Arc View 10.5. The different types of data required by the model were added, allowing the model to run. The calibration permitted the prediction of the behavior of the basin depending on different conditions.

This study demonstrated that SWAT:

- Is capable of operating on a watershed scale with several sub-basins.
- Allowed topographical, land use and management differences.
- Is capable of simulating several management practices.
- Could simulate long periods of time.
- Could be calibrated through field testing.

Major short comings of SWAT model are:

- Extensive data input requirements.
- Difficulties of selecting appropriate parameters for calculation.
- Subjectivity of selecting coefficients.
- Limitations in simulating short-term events.

Despite the complexity of the model, major benefits include: SWAT is applicable to decision-making in land management and is able to model the impacts on water quality and quantity such as cropping patterns, fertilizer applications, pesticide applications and timing and amount of irrigation.

Uncertainties in predictions are an important factor to consider when predicting hydrology, sediment yield, and water quality. The primary sources of uncertainty are:

- Simplifications in the conceptual model. For example, the simplifications in a hydrologic model, or the assumptions in the equations for estimating surface erosion and sediment yield, or the assumptions in calculating flow velocity in a river,
- Processes occurring in the watershed but not included in the model. For example, wind erosion, soil losses caused by landslides
- Processes that are included in the model, but their occurrences in the watershed are unknown to the modeler or unaccountable; for example, reservoirs, water diversions, irrigation, or farm management affecting water quality,
- Processes that are not known to the modeler and not included in the model. These include dumping of waste material and chemicals in the rivers, or processes that may last for a number of years and drastically changes the hydrology or water quality such as constructions of roads, bridges, tunnels and dams and
- Errors in the input variables such as rainfall and temperature.

2.5. **Land Use and Land Cover**

When referring to land use and land cover, the terms are often used interchangeably and incorrectly. It's possible to define land use as a series of activities undertaken in order to produce a goods or services. In this way, land use is determined by its purpose (Ndulue et al., 2015). According to the IPCC (2001), the term land use encompasses a wide range of direct management activities that affect agricultural soils, result in land-use change, alter forest management, or have an impact on long-term carbon storage. Inherently, all of these activities are caused by humans. Land uses include agriculture, forestry, recreation, etc.

Land cover refers to the physical cover of the earth's surface as seen from the ground or via remote sensing, which includes vegetation (natural or planted) and human structures (buildings, roads, etc)(Ndulue et al., 2015). Water, ice or sand surfaces are examples of land cover.

2.5.1. LULC Projection

Different supevised, unsupervised classificaton methods and softwares has been developed for the classification and projection of LULC. (Ampomah et al., 2020) performed a supervised image classification using Environment for Visualizing Images (ENVI). software for geospatial imagery processing to detect land development changes within the Cuyahoga River watershed in Ohio (Naikoo et al., 2020) performed K means clustering technique using ERDAS Imagine Software on the Landsat data for the LULC classification and then the change detection technique was used to quantify the LULC change in Delhi NCR. (Getachew et al., 2021) performed LULC change model of Lake Tana Basin of Ethiopia using Cellular Automata (CA) Markov Chain model to project LULC. (Lamichhane & Shakya, 2019b) used Conversion of land use and its effects at small regional extent (CLUE-S) for future LULC projection of the Kathmandu Valley.

Most of these LULC classification and projection works included the use of Satellite imagery. These satellite images need to be corrected radiometrically and geometrically before use and most of these data contains varying percentages of cloud coverage (Ampomah et al., 2020). The satellite images collected should be cloud free for the accurate classification of LULC. This condition limits the time at which the data should be collected which leads to decrease in accuracy of the work.

So, this study have used LULC map from (ICIMOD, 2013) which is highly recognised and provides accurate representation of LULC of the study area and TerrSet software which incorporates Land Change Modeler (LCM), IDRISI GIS and image processing software for change analysis and LULC projection.

2.6. **TerrSet**

TerrSet is an integrated geospatial software system for monitoring and modelling the earth system for sustainable development. TerrSet incorporates the IDRISI GIS and Image Processing tools and

offers a constellation of vertical applicationc focused on monitoring and modelling the earth system for sustainable development (J Ronald, 2020).

TerrSet provides an unprecedented set of tools for monitoring and modelling the earth system. At present, the full TerrSet constellation includes:

- IDRISI GIS Analysis
- IDRISI Image Processing
- The Land Change Modeler (LCM)
- The Earth Trends Modeler (ETM)
- The Ecosystme Services Modeler (ESM)
- The Climate Change Adaptation Modeler (CCAM)
- GeOSIRIS

2.6.1. Land Change Modeler (LCM)

The Land Change Modeler is an integrated software environment within TerrSet which is used as an innovative land planning and decision support software tool that simplifies the complexities of change analysis, resource management and habitat assessment. It is used to rapidly analyze the land cover change and to simulate the future land change scenarios.

1. **Land Change Analysis**

   Two historical land cover map layers is needed to evaluate the changes in the land cover including gain and losses in certain types of land cover, persistence to change and the potential variables that contributes to the change.

2. **Transition Potential Modeling**

   Modeling the potential of land to experience specific transitions such as forest to agriculture area or agriculture area to built-up area lies at the very heart of land change modeler. It identify the dominant transitions which can be grouped and modeled, these are known as submodels. The transitions of these submodel can be analysed seperately but ultimately each submodel are combined together for the final change prediction.

Different driver variables can be assigned to each submodel. This is where we have to specify what variables drive the transitions contained within the sub model we are evaluating.

3. Change Prediction

LCM uses Markov Chain analysis to project the expected amount of change and a competitive land allocation model to determine scenarios for a specified future date based on the transition potential models. Planned interventions such as incentives and constraints, proposed reserve areas, and infrastructure changes can be incorporated into the planning process.

Chapter 3: DESCRIPTION OF THE STUDY AREA

3.1. **Study Area**

Bagmati river flows through the heart of KV, the capital city of Nepal. Six major tributaries; Hanumante, Manohara, Dhobi Khola, Bishnumati, Balkhu and Nakhhu rivers drained into the Bagmati river. All the tributaries are spring-fed and rain-fed rivers flowing from north to south direction (Pokhrel, 2018). The Bagmati river originates from Shivapuri at an altitude of 2669 m and its watershed is surrounded by Mahabharat hills. The catchment of Bagmati river as shown in figure 1 covers an area of 613 km^2 at Khokana station, which is situated at a Latitude of $27^0$37'4", Longitude of $85^0$17'41", and an altitude of 1190 m.

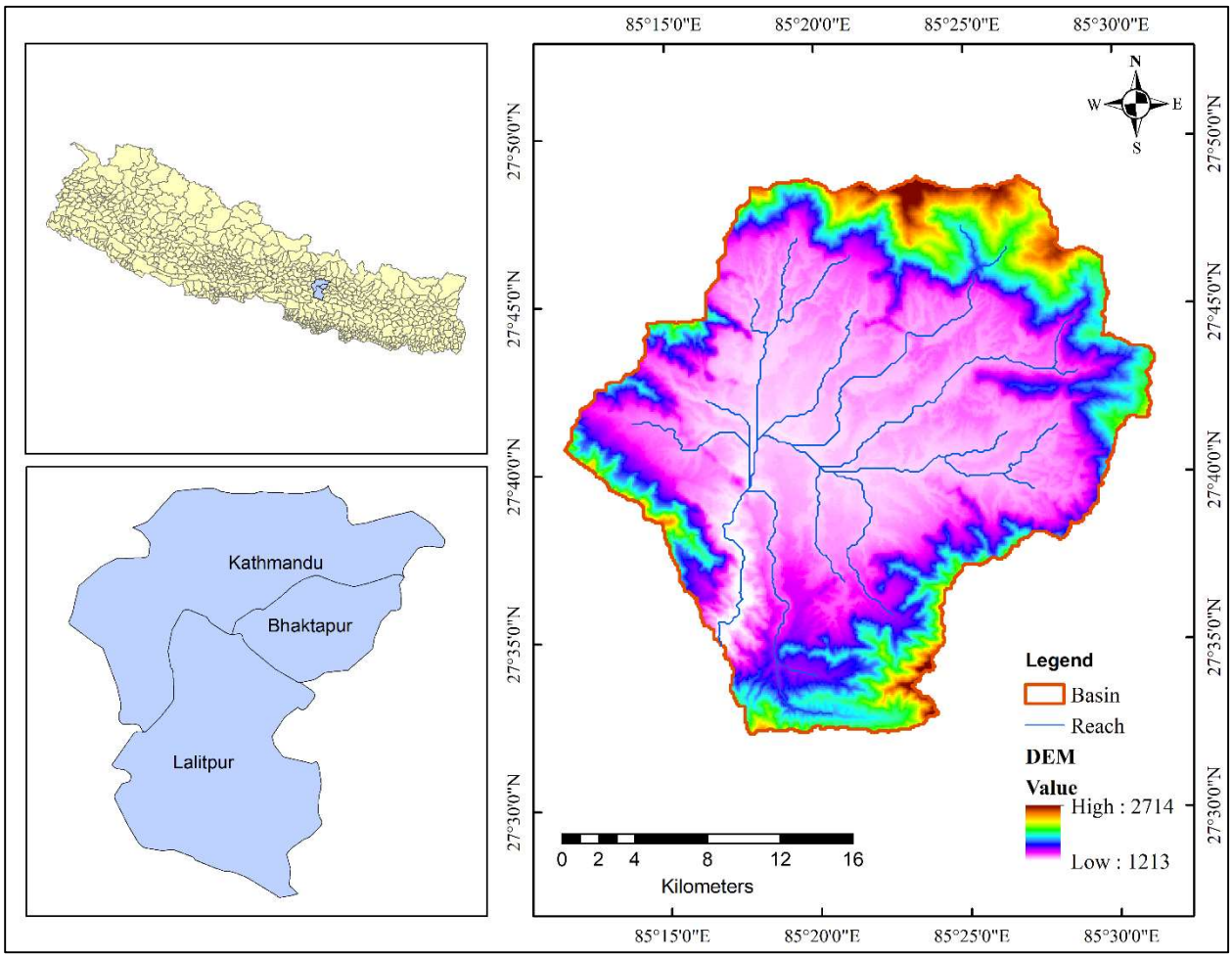

Figure 1: Location map of the Study Area

The climate of KV region is fairly pleasant and is categorized as a warm temperate zone. The average monthly air temperature during summer seasons reaches up to 29.3^{0}C and during winter seasons the average monthly temperature falls up to 0.9^{0}C (DHM). The analysis of data for the study period (2000 – 2016 A.D) shows the average monthly maximum precipitation of 402.1 mm in the month of July and average monthly minimum precipitation of 4.2 mm in December. The maximum precipitation over that period recorded was 300.100 mm on 23rd July 2002, while the average relative humidity and wind speed recorded were 64.8% and 2.381 Km/Hr. The precipitation in the KV is mostly monsoon based and over 80% of the total average annual rainfall occurs during the monsoon season that is from the month of June to September. So the Bagmati river and its tributaries experienced a very high variation of discharge during the wet and dry period (Lamichhane & Shakya, 2020). The total average annual rainfall over the study period(2000 to 2016) is 1533 mm/year.

3.2. **Catchment Characteristics**

The watershed delineation and HRU definition in the Bagmati River Basin gave effective watershed area of 61310 hectares which resulted in 65 sub-basins with 1210 HRUs. The area coverage by the major land use types in the Basin is presented in Table 2 below:

Table 2: Area under different land use types of Bagmati Basin

Land Use	**SWAT Code**	**Area (Ha)**	**% Watershed Area**
Forest - Mixed	FRST	20091.34	32.77
Residential	URBN	10557.38	17.22
Agricultural Land - Generic	AGRL	29547.57	48.19
Barren	BARR	929.34	1.52
Water	WATR	184.89	0.30

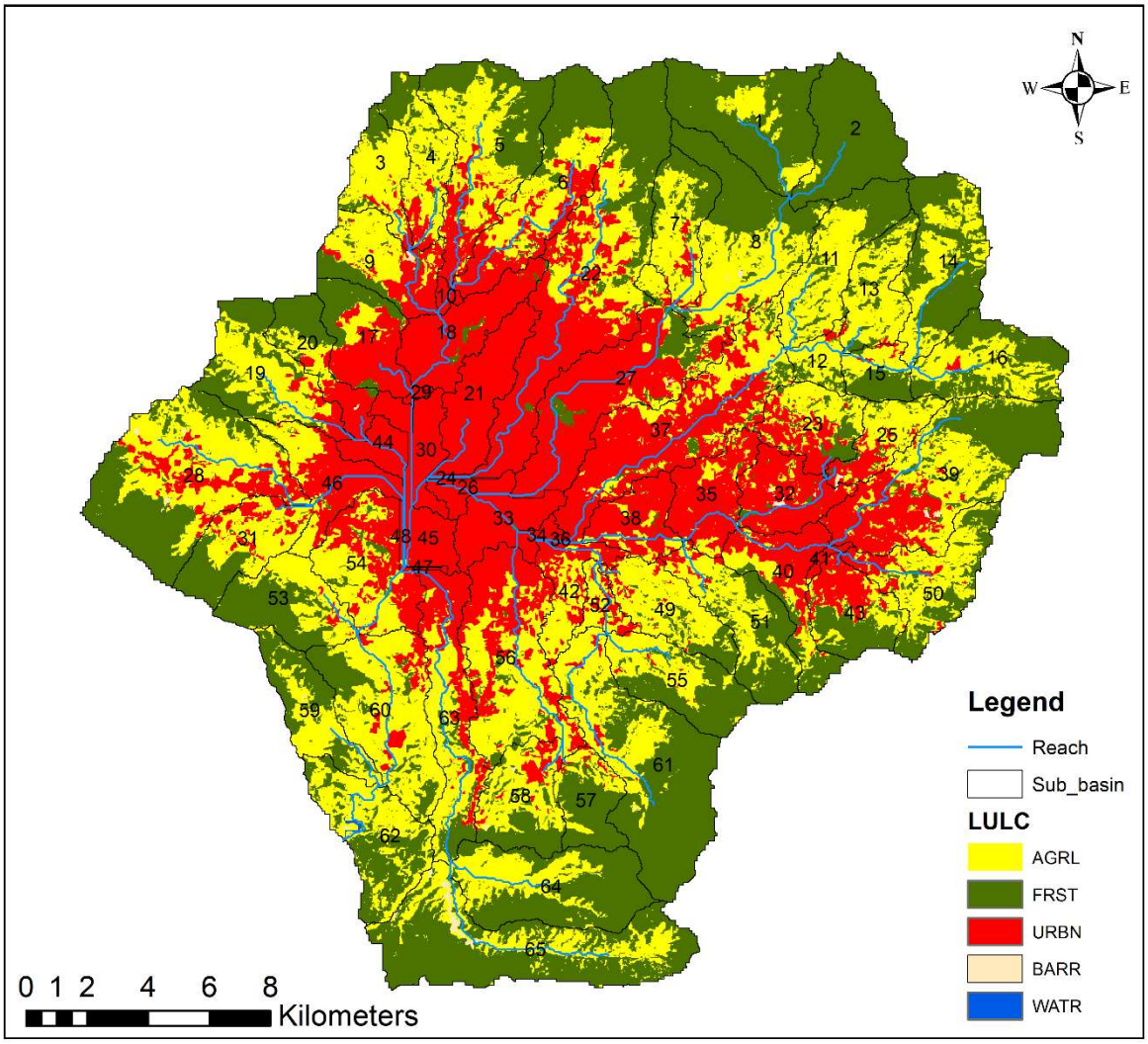

Figure 2: Land use types of Bagmati River Basin ((ICIMOD, 2013)

As it is observed in the given Table 2, the major portion of the watershed is covered by agricultural land area which accounts for 48.19% of the total watershed area. Forest covers the second largest area with 32.77% and Urban area covers 17.22%. The area covered by Barren land and Water surface is insignificant.

Similarly, the major soil types of Bagmati River Basin are presented in Table 3 below:

Table 3: Areas under different soil types of Bagmati Basin

Soil Name	Area (Ha)	% Watershed Area
Chromic Cambisols	17130.95	28.32
Eutric Cambisols	9396.64	15.53
Gleyic Cambisols	18271.90	30.20
Chromic Luvisols	15700.56	25.95

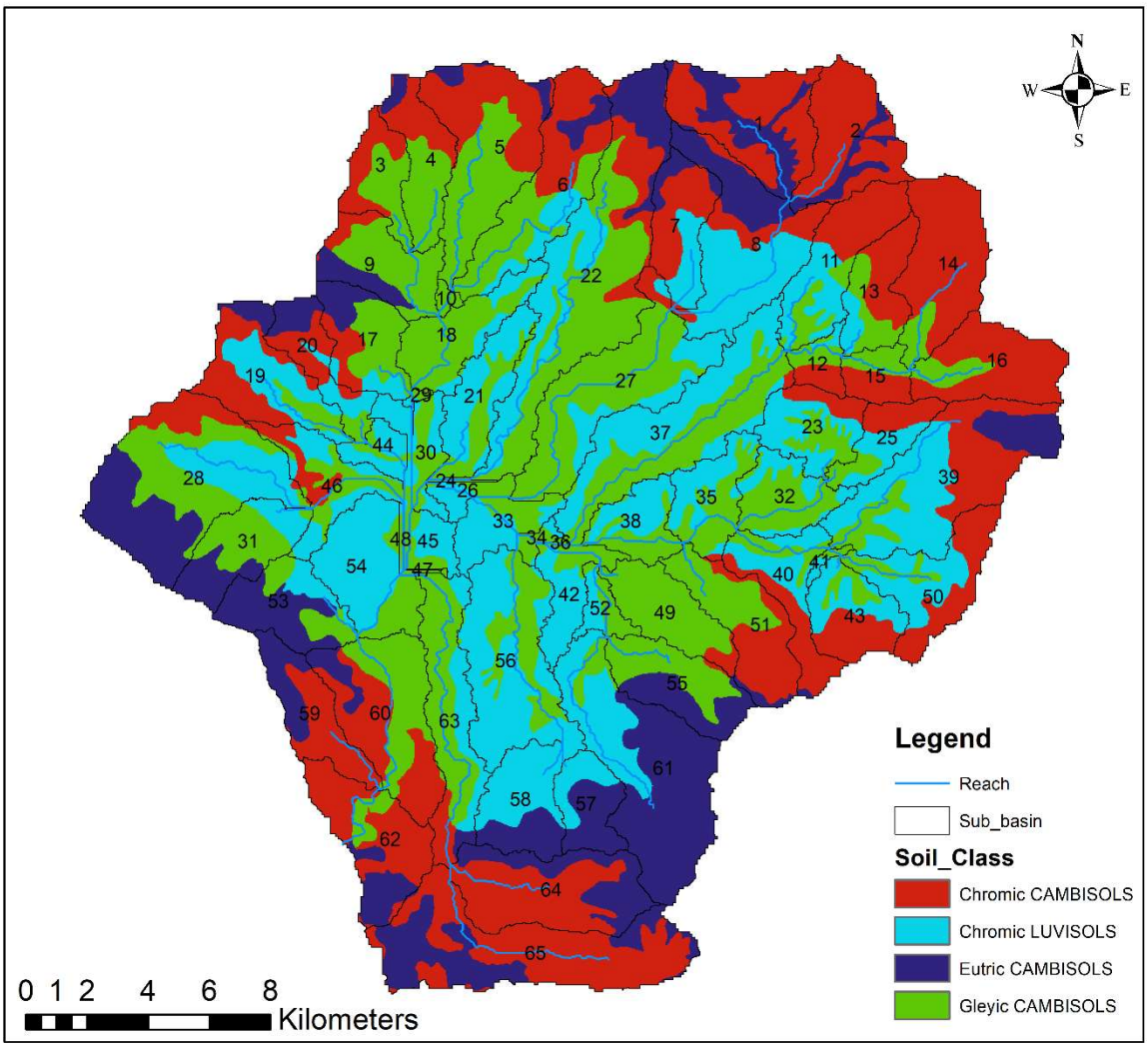

Figure 3: Soil types of Bagmati River Basin

Four classes of soils represent the whole Bagmati river basin in Kathmandu valley. Gleyic Cambisols is observed to be the dominant soil type which accounts for 30.20 % of the total watershed area followed by Chromic Cambisols, Chromic Luvisols and Eutric Cambisols which accounts for 28.32 %, 25.95 % & 15.53 % of the watershed area respectively.

Table 4 shows the areas in the Basin under different slope categories. From that table, it is clear that the majority of the catchment area lies under the slope of <20%. It accounts to a total value of 54.88%.

Table 4: Areas under different slope categories of Bagmati River Basin

Slope Category (%)	**Area (Ha)**	**% Watershed Area**
0 – 20	33199.99	54.88
20 – 40	14314.92	23.66
>40	12985.1386	21.46

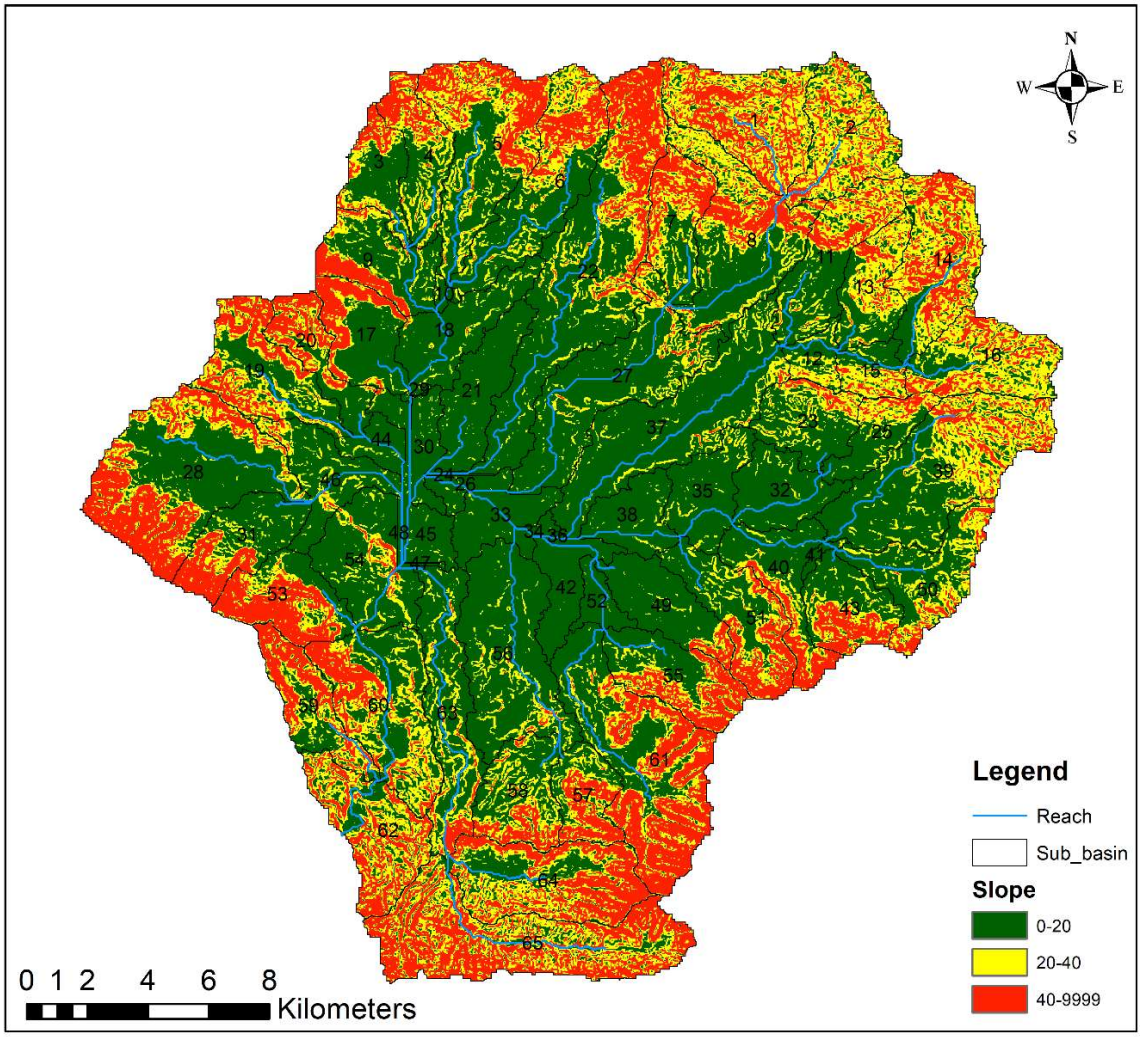

Figure 4: Slope Classification of Bagmati River Basin

Chapter 4: METHODOLOGY

4.1. Framework of Methodology

The methodological framework of the study is as shown in the Figure 5 below. The detail description of the methodology is discussed in the following sections.

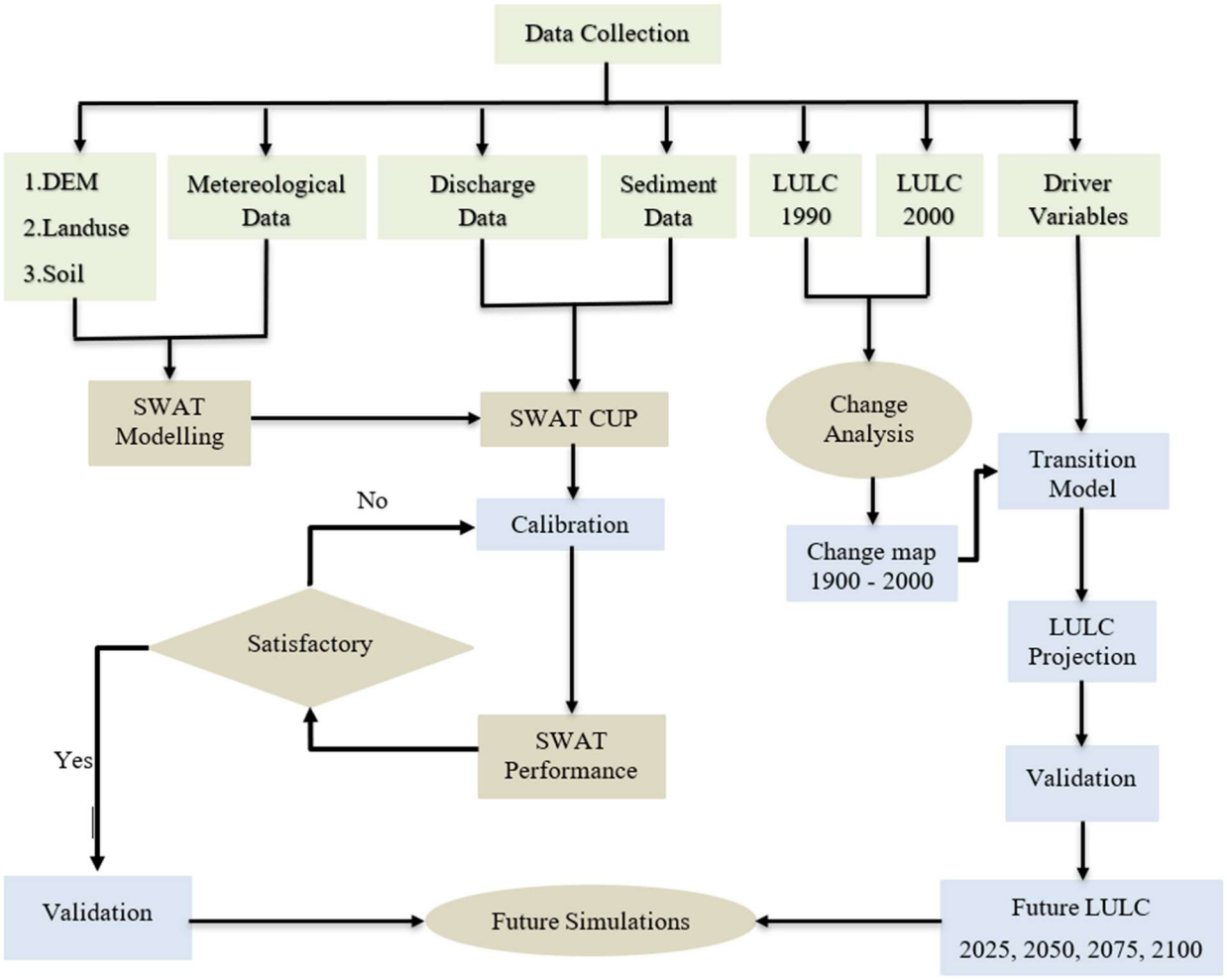

Figure 5: Methodological Framework of the study

4.2. Data Collection

A SWAT model requires different types of data to simulate the hydrological processes of the watershed. These data can be obtained from different sources. The Digital Elevation Model (DEM) data of 30 m spatial resolution was downloaded from ASTER (Advanced Space-borne Thermal Emission and Reflection Radiometer) satellite data (GDEM) (https://earthdata.nasa.gov/), which is required to delineate the watershed and to generate the stream reaches. It is also used to analyze

the stream length/width, drainage pattern of the watershed and to categorize the slope of the basin (Chaplot, 2005). The LULC data of 1990, 2000 and 2010 was downloaded from International Center for Integrated Mountain Development (ICIMOD, https://rds.icimod.org/). Road Network data of the Bagmati basin in Kathmandu valley and National Parks & Protected areas data was also obtained from ICIMOD. The Soil and Terrain (SOTER) database for Nepal at scale 1:1 million was downloaded from ISRIC World Soil Information (https://www.isric.org/).

Sediment and discharge data of the Khokana Gauging Station and other meteorological data such as daily precipitation, maximum & minumum temperature, relative humidity, wind speed & solar radiation data of the Bagmati basin was obtained from Department of Hydrology and Meteorology (DHM).

In this study, the GIS interface ArcSWAT will be used to set up a SWAT model of the Bagmati watershed. To simulate hydrological processes, the SWAT model requires input data for topography, soil, and land use, as well as hydro-meteorological data (Aghsaei et al., 2020). The model calculations are based on hydrologic response units (HRUs), which are lumped areas within a sub-basin that have a unique land use, soil, and slope class combination.

Different data that has been used for this study, their duration, resolution and sources are shown in Table 5 below:

Table 5: Input Data and their Sources

S.N	Input Data	Duration	Resolution	Source
1.	Digital Elevation Model		30 m x 30 m	ASTER-GDEM (Global Digital Elevation Map)
2.	Land use / Land Cover	1990, 2000 & 2010 A.D	30 m x 30 m	ICIMOD
3.	Soil Data	2009 A.D	30 m x 30 m	Soil & Terrain Database (SOTER) for Nepal
4.	Metereological Data	2000 – 2016 A.D		Department of Hydrology and Meteorology (DHM)
5.	Discharge Data	2000 – 2016 A.D		DHM
6.	Sediment Data	2000 – 2016 A.D		DHM

7.	Road Network Data	2009 A.D	30 m x 30 m	Road Network of Nepal from ICIMOD
8.	Protected Area Data	2007 A.D	30 m x 30 m	Nepal National Parks & Protected Areas Data from ICIMOD

4.3. SWAT Model Setup

The Soil and Water Assessment Tool (SWAT) (Arnold et al., 2012) is a continuous, semi-distributed, parametric model used by many researchers all over the world for the hydrologic analysis (Santos et al., 2021). This model is physically based, and is very efficient for the simulation of the long term continuous databases(Tang et al., 2012). The major components of the SWAT includes hydrology, weather, erosion/sedimentation, soil temperature & properties, plant growth, nutrients, pesticides, land management, stream routing and pond/reservoir routing(Arnold & Fohrer, 2005).

The SWAT simulates the hydrologic model using water balance equation (Quyen et al., 2014):

$$SW_t = SW_0 + \sum_{i=1}^{n} (R_{day} - Q_{surf} - E_a - w_{seep} - Q_{gw})$$

Where,

SW_t = Final soil water content (mm)

SW_0 = Initial soil water content (mm)

R_{day} = Days Rainfall (mm)

Q_{surf} = Quantity of surface runoff (mm)

E_a = Evapotranspiration (mm)

W_{seep} = Seepage from the bottom soil layer (mm)

Q_{gw} = Ground water flow (mm)

There are two methods to calculate surface runoff using the SWAT model. One is SCS curve number procedure and the other is Green & Ampt infiltration model procedure (Tang et al., 2012). We have selected SCS curve number procedure for the analysis.

For sediment flow analysis, SWAT uses Modified Universal Soil Loss Equation (MUSLE)(Chaplot, 2005, Choto & Fetene, 2019). The MUSLE equations to calculate the sediment erosion from the watershed is:

$$S = 11.8(Q * Area * pr)^{0.56} * K * C * P * LS * R$$

Where,

S = Sediment load (mt)

Q = Surface runoff (cu.m)

pr = Peak runoff rate (cu.m)

K = USLE soil erodibility factor

C = Cover and management factor

P = Support practice factor

LS = Topographic factor (gradient, length)

R = Coarse fragment factor

For each day with rainfall and runoff, sediment generation is estimated by applying this equation for each HRU in the watershed.

A watershed delineation and a hydrologic response units (HRUs) determination function were used in ArcSWAT to preprocess GIS data for the SWAT model. This is outlined in the next subtopics in detail:

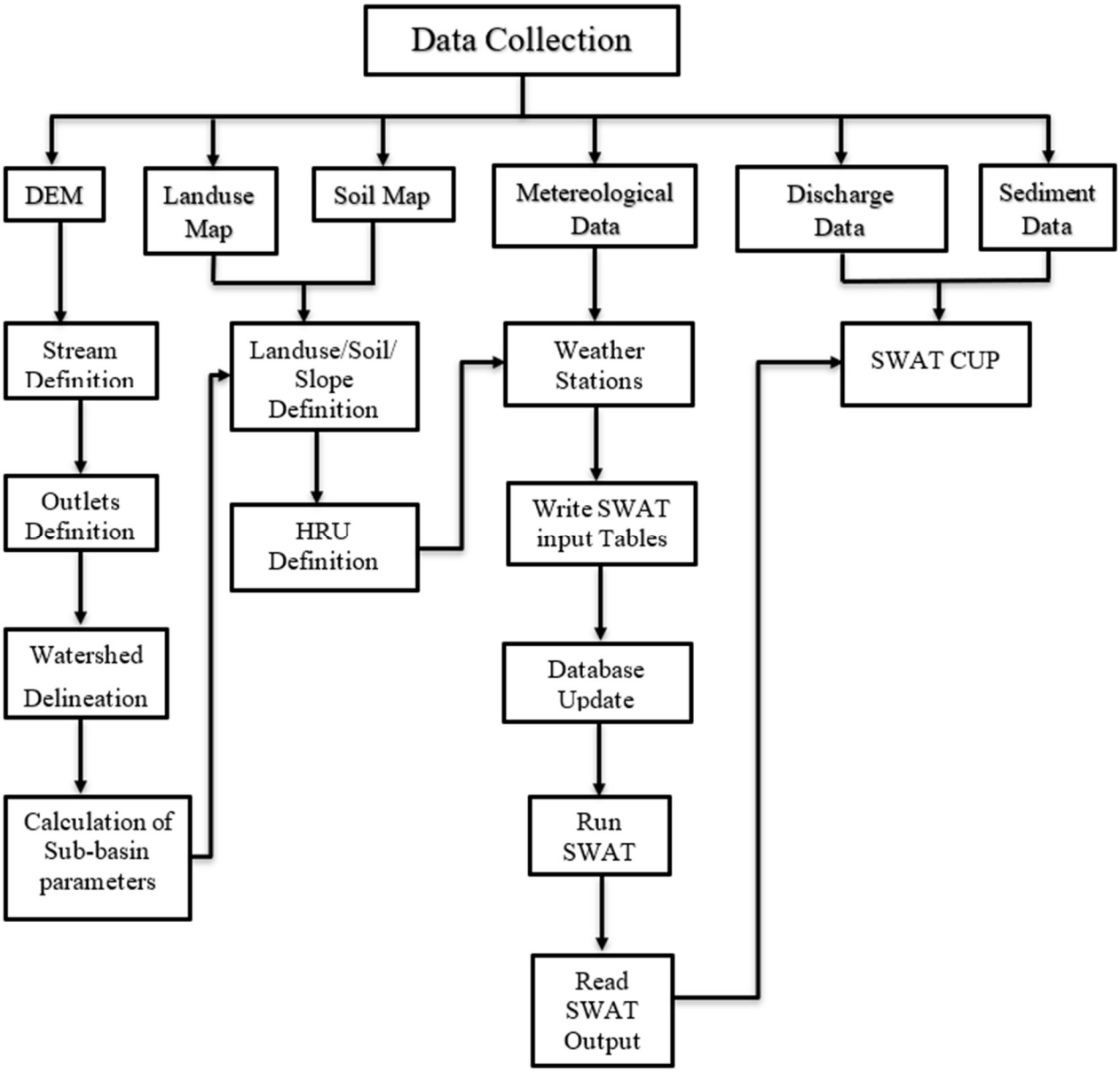

Figure 6: Methodological Flowchart in SWAT Model

4.3.1. Watershed Delineation

It is the process of dividing the watershed into discrete sub-basins and stream reaches. DEM data is used by the SWAT to delineate the watershed. The Watershed delineation process provides the geographic relationship between upstream & downstream and also enables researchers to give the specific location of input and output so that it can be used for scientific research and management purposes. Before the delineation process the DEM data should be projected and also the pits and depressions should be filled if required.

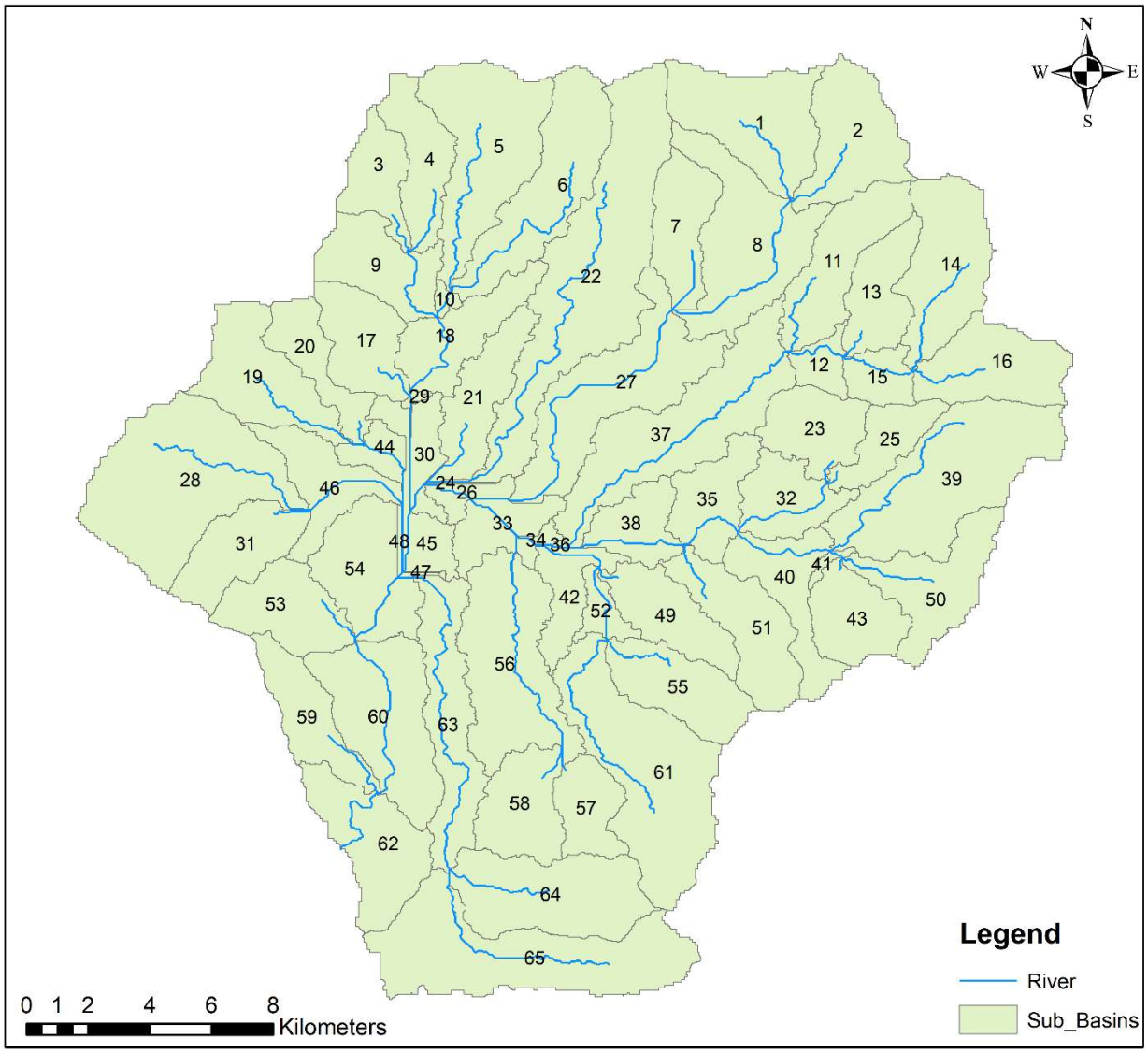

Figure 7: Watershed with sub-basins

Water Delineation process in the study area creates 65 sub-basins. A 500 hectares of threshold is given to define a beginning of stream.

4.3.2. Hydrologic Response Unit Analysis

Hydrologic Response Units (HRUs) are the areas of land that are assumed to respond similarly to weather inputs and are unique combinations within each sub-basin of land use, soil and slope. For different land cover and soil types HRUs allow the model to take into account differences in evapotranspiration, as well as other hydrologic conditions. Runoff and sediment are estimated separately for each HRU and routed to obtain the total runoff for the watershed. This improves the flow prediction accuracy and provides a more accurate physical description of the water balance.

To determine the area and hydrologic parameters of each land soil category simulated within each sub-watershed, the land use and soil data in a projected Grid file format were loaded into the ArcSwat interface. The land cover and soil classes are defined using the look-up table. After assigning a land use SWAT code to each map category, the area covered by each land use was calculated and reclassified. Similarly, the user soil database information was linked to the soil layer in the map by loading the soil look up table and applying reclassification.

The land slope classes were also integrated in defining the hydrologic response units. The sediment transport capacity is directly proportional to the slope of the land surface. The Bagmati basin in Kathmandu Valley is a bowl shaped surrounding by hills and more or less flat terrain in the center. More than 55% of land is below 20 % slope. So based on the suggested minimum, maximum, mean and median slope statistics of watershed, only three classes of slope has been defined; (0 – 20) %, (20 – 40)% & greater than 40% and slope grids reclassified. Using the same DEM data that was used for the watershed delineation, slope reclassification was performed. The land use, soil and slope grids were overlaid.

The last step in the HRU analysis was the HRU definition. The HRU definition in this study was determined by assigning multiple HRU to each sub-watershed. In multiple HRU definition HRU Thresholds are kept zero so that every unique combination of land use, soil and slope will be considered a unique HRU. The HRU definition process creates 1210 HRU's in our study area.

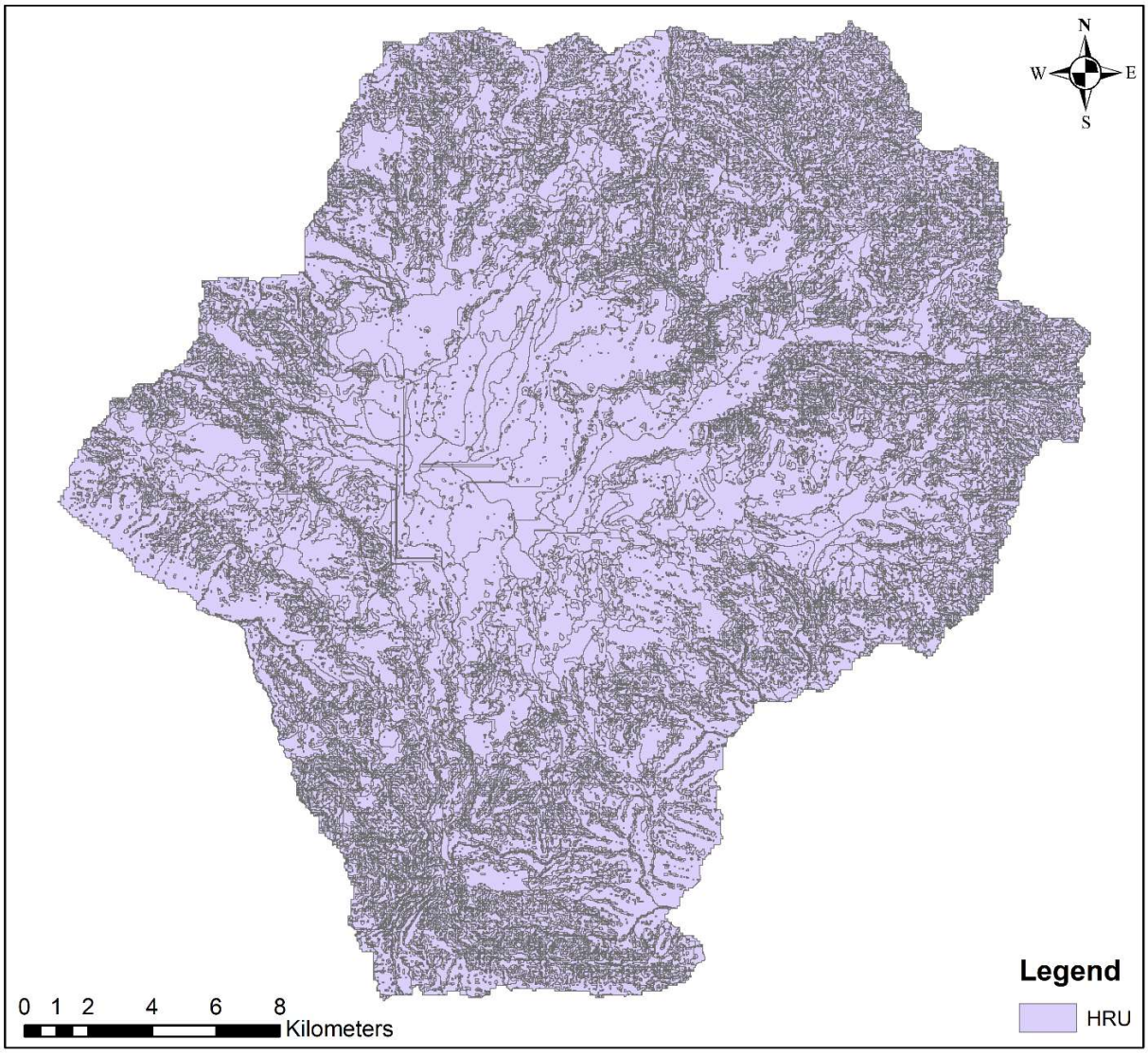

Figure 8: Hydrologic Response Units

4.3.3. Importing Climate Data

Climatic variables are the essential components of the hydrologic cycle which affects the overall water balance of the watershed. Five most important weather database is needed for the analysis of the model; precipitation, temperature (max/min), solar radiation, wind speed and relative humidity. The weather databases required should be in a specific file format. Solar radiation, wind speed and relative humidity data are needed for the calculation of potential evapotranspiration. A Solar radiation database is also needed to analyze the plant growth but that is not the part of our study. A continuous high quality daily weather database is needed for the accurate analysis of the

model. So, we have imported only those stations database which has the required qualities together with their weather location in the model. A total of 21 rain gauge stations, 7 meteorological stations and 1 hydrological station in and around the Bagmati watershed is used in our study. Their station number and location is shown in Figure 9 below.

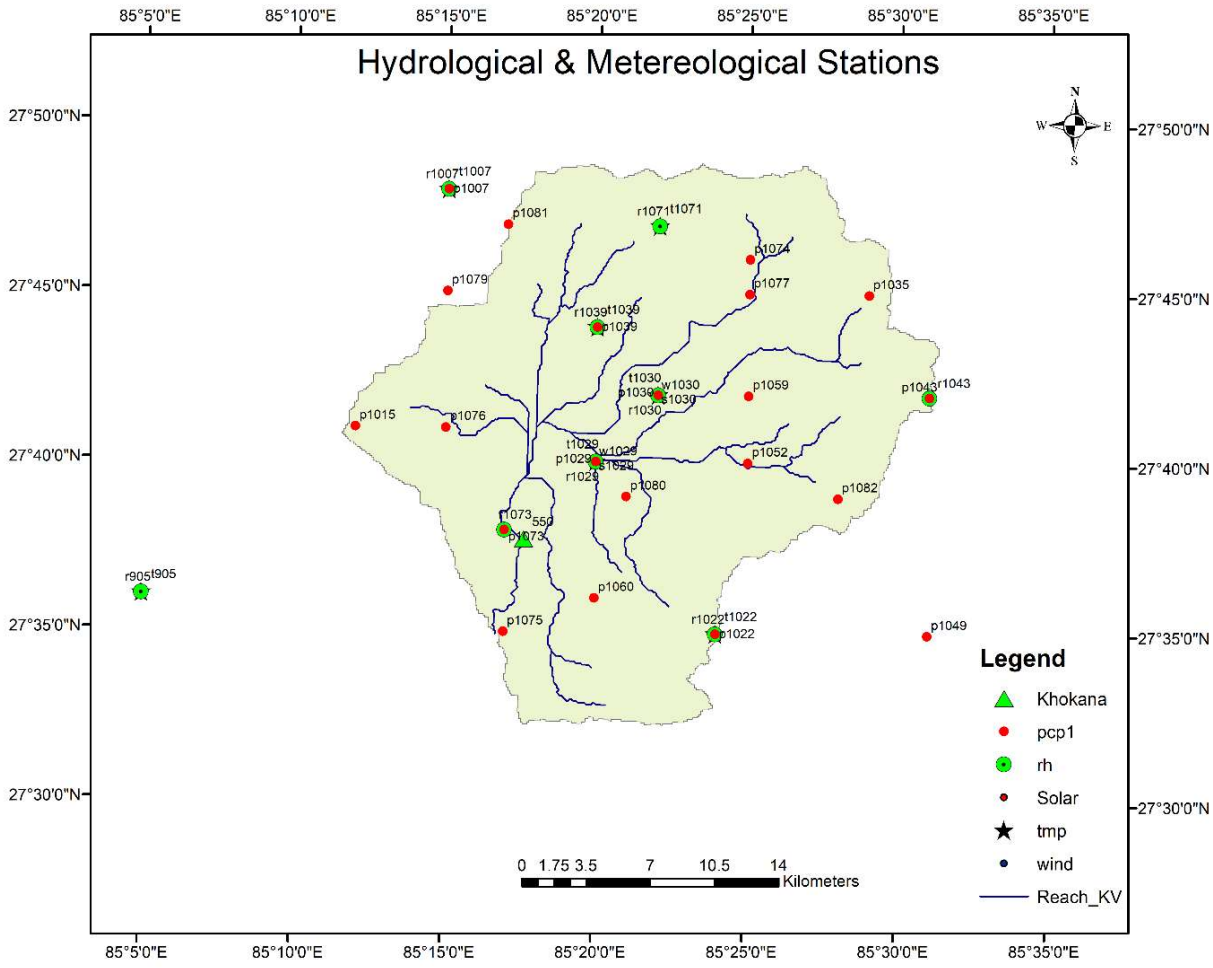

Figure 9: Hydrological and Meterological Stations

The weighted average rainfall representing all 21 rain gauge station data is calculated by applying Thissien polygon (Annex 3) method to correlate the discharge and sediment yield from the river at a particular time with corresponding rainfall

4.3.4. Model Simulation

After gathering all the input data together and processing some of the data to create sub-basins and HRUs, very specific input files with precise formatting is created. Thus created SWAT formatted input files were used in running the SWAT model and creating the outputs. The model is simulated

from 2000 to 2016 with three years warm up period. The values of many variables at the beginning of the simulation are also important. There is an amount of water in the soil moisture, in reservoir and aquifers at the beginning of the simulation for which we often do not have data, so the model was run for three years at the beginning of the simulation as a warm-up period to get the hydrologic cycle fully operational.

4.4. **SWAT-CUP Model setup**

SWAT- CUP (Karim C. Abbaspour, 2015) is an automatic calibration tool used worldwide for fitting the model parameters and their uncertainty analysis. Uncertainty analysis is a process of propagating and quantifying the errors in the model inputs through the calibration process. Various factors can be responsible for the uncertainty in the model. The uncertainty can be due to the variables used, error in the input data (discharge, sediment, soil, landuse, rainfall etc.) for the analysis, simplifications of the processes included in the model, unknown model parameters or the missing processes (wetland, dam, glacier melts etc.)(Tang et al., 2012). Various analysis programs like Particle Swarm Optimization (PSO), Sequential Uncertainty Fitting version 2 (SUFI-2), Parameter Solution (ParaSol), Markov Chain Monte Carlo (MCMC) and Generalized Likelihood Uncertainty Estimation (GLUE) are integrated in the SWAT-CUP (Khalid et al., 2016). The integration of these algorithms makes the program exceptionally flexible to analyze various aspects of the model. The quality of the model output for the SWAT-CUP calibration and uncertainty analysis is measured by the P factor and R factor at a 95% prediction uncertainty (95PPU) (Karim C. Abbaspour, 2015). The P factor represents the percentage of measured data captured by 95PPU and its value of 1 indicates the perfect model simulation. The R factor measures the quality of the calibration results and its value of zero represents the direct fit of the observed and simulated data (discharge, sediment or nutrients) (Khalid et al., 2016). TxtInOut file formed after the SWAT simulation in ArcSWAT is given as an input for the SWAT-CUP. SUFI-2 analysis program is considered to give the widest margin of the parameter uncertainty (Briak et al., 2016), so it is used for our study.

The methodological flow chart for the execution of SWAT-CUP analysis program is shown in Figure 10 below.

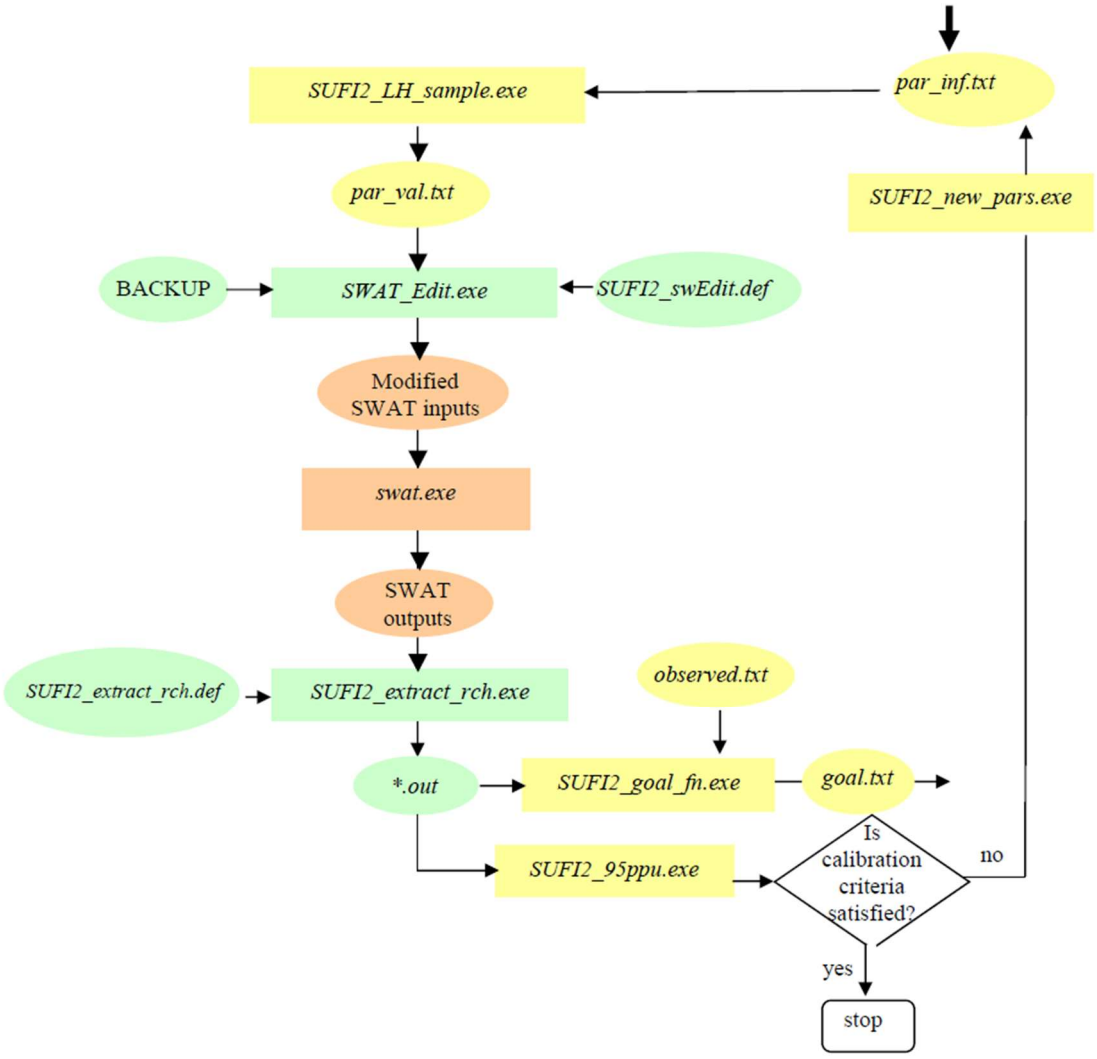

Figure 10:Methodological Flowchart for SWAT-CUP SUFI-2 Optimization Program
(Karim C. Abbaspour, 2015)

4.4.1. Sequential Uncertainty Fitting (SUFI-2)

In SUFI-2, paramter uncertainty accounts for all the sources of uncertainties such as uncertainty in driving variables (e.g., rainfall), conceptual model, parameters and measured data.(Tang et al., 2012). According to (Karim C. Abbaspour, 2015), In SUFI-2, the P-factor is used to quantify the degree to which all uncertainties are taken into account which is the percentage of measured data bracketed by the 95% prediction uncertainty (95PPU). Another measure quantifying the strength of a calibration/uncertainty analysis is the R factor, which is the average thickness of the 95PPU

band divided by the standard deviation of the measured data. Therefore, SUFI-2 aims to bracket the vast majority of measured data with a small uncertainty band. Using Latin hypercube sampling, the 95PPU is calculated at 2.5 percent and 97.5 percent of the cumulative distribution of an output variable to eliminate 5 percent of the worst simulations. Theoretically, the value of the P factor ranges between 0% to 100% while the R-factor ranges from 0% to infinity. A P-factor of 1 and R-factor of zero is a simulation that exactly corresponds to the measured data (Khalid et al., 2016).

A short step-by-step description of SUFI-2 algorithm (K. C. Abbaspour et al., 2004; Tang et al., 2012) is as follows:

i. To begin with, an objective function must be defined.

ii. A physical minimum and maximum range for the parameters that are being optimized is established. It's important to keep absolute parameter ranges as large as possible while still being physically meaningful.

iii. "Absolute sensitivity analysis" is optional, but highly recommended for all parameters at the early stage of calibration.

iv. For the first round of Latin hypercube sampling, initial uncertainty ranges are assigned to the parameters. In general, the above ranges are smaller than the absolute ranges, and depend upon experience. The sensitivity analysis in step iii can provide a valuable guide for selecting appropriate ranges.

v. Following that, Latin hypercube sampling is used to generate n parameter combinations, where n is the number of simulations desired.

vi. As a first step in assessing the simulations, the objective function is calculated.

vii. The sensitivity matrix J and the parameter covariance matrix C are then calculated using Latin Hypercube sampling in the hypercube, the corresponding objective functions are evaluated, and the sensitivity matrix J and the parameter covariance matrix C are calculated using:

$$J_{ij} = \frac{\Delta g_i}{\Delta j_i} \quad i = 1...C_2^n, j = 1...m \qquad (1)$$

where C_2^n is the number of rows in the sensitivity matrix (equal to all possible combinations of two simulations), and j is the number of columns (number of parameters).

Where S_g^2 is the variance of the objective function values resulting from m model runs.

$$C = s_g^2 (J^T J)^{-1} \quad (2)$$

viii. A 95 % predictive interval of a parameter bj is computed as follows:

$$b_{j,lower} = b_j^* - t_{V,0.025} s_j \quad (3)$$

$$b_{j,lower} = b_j^* + t_{V,0.025} s_j \quad (4)$$

where b_j^* is the parameter bj for the best estimates and v is the degrees of freedom (m-n).

ix. The 95PPU is calculated. Then two indices i.e, the p-factor and the r-factor is calculated:

$$r - factor = \frac{\bar{d}_X}{\sigma_X} \quad (5)$$

where σ_x is the standard deviation of the measured variable X. A value less than 1 is desirable measure for the r-factor

$$\bar{d}_X = \frac{1}{k} \sum_{l=1}^{k} (X_U - X_L)_l \quad (6)$$

where k is the number of observed data points and X_L (2.5^{th}) and X_u (97.5^{th}) represent the lower and upper boundary of the 95PPU.

x. The value of d tends to be quite large during the first sampling round because parameter uncertainties are initially large. As a result, additional sampling rounds are required, with updated parameter ranges calculated from:

$$b'_{j,\min} = b_{j,lower} - Max\left(\left(\frac{b_{j,lower} - b'_{j,\min}}{2}\right),\left(\frac{b'_{j,\max} - b'_{j,upper}}{2}\right)\right) \quad (7)$$

$$b'_{j,\max} = b_{j,upper} + Max\left(\left(\frac{b_{j,lower} - b'_{j,\min}}{2}\right),\left(\frac{b'_{j,\max} - b'_{j,upper}}{2}\right)\right) \quad (8)$$

where b' indicate updated values. Parameters of the best simulation are used to calculated $b_{j,lower}$ and $b_{j,upper}$.

The above criteria ensure that the updated parameter ranges are always centered on the best estimates, despite producing narrower parameter ranges for subsequent iterations. SUFI-2 is also linked to SWAT (in the SWAT-CUP software) via an interface that includes the GLUE, Parasol, and MCMC algorithm programs. SWAT-CUP was created by the Swiss Federal Institute of Aquatic and Technology, the Naprash Company, and Texas A & M University.

4.4.2. Sensitivity Analysis

Sensitivity analysis is actually carried out to determine which processes as well as model calibration parameters are dominant in a watershed. For that, we have to determine the significance of one or a combination of parameters with respect to the objective function or a model output. There are two different methods for sensitivity analysis.

i. Local (one at a time) Sensitivity analysis

In this type of analysis, all the parameters are fixed or kept constant and change only one parameter at a time. This anlysis also helps to get an idea of the paramter range.

ii. Global Sensitivity analysis

In Global sensitivity analysis all the paramters are changing at the same time. This is advantageous than the local sensitivity analyses as sensitivity of one parameter depends on the values of other paramters.

Sensitivities are obtained by performing multi-regression computation expressed as:

$$g = \alpha + \sum_{i=0}^{m} \beta i.\, bi$$

A t-test is then used to identify the relative significance of each parameter b_i. The above sensitivities are estimates of the average changes in the objective function caused by changes in each parameter while all other parameters change. This provides relative sensitivities based on

linear approximation and thus only provides partial information about the objective function's sensitivity to model parameters. In this analysis, the greater the absolute value of the t-stati and the lower the p-value, the more sensitive the parameter (Karim C. Abbaspour, 2015).

A multiple regression analysis is used to get the statistics of parameter sensitivity. The t-stat is the coefficient of a parameter divided by its statndard error. It is a measure of the precision with which the regression coefficient is measured. If a coefficient is large compared to its standard error, then it is probably different from zero and the paramter is sensitive.

In each case, the p-value is used to test the null hypothesis that the coefficient is zero (no effect). A low p-value (0.05) indicates that the null hypothesis can be rejected. Low-p-value predictive variables are likely to add value to the model because changes in the predictor's value are related to changes in the response variable. A higher p-value, on the other hand, indicates that changes in the predictor are unrelated to changes in the response. As a result, that parameter isn't particularly sensitive. With a p-value of 0.05, there's only a 5% chance that the results you're seeing would have appeared in a random distribution, so you can say with 95% certainty that the variable is having some effect. (Karim C. Abbaspour, 2015)

Global sensitivity analysis is carried out by selecting all parameters which may affects the flow of Sediment and Discharge. Initially 25 parameters are considered based on the studies carried out by different researchers most notably by (Pokhrel, 2018) who studied in the same watershed as mine and the parameters suggested by (Karim C. Abbaspour, 2015). After carrying out Global Sensitivity Analysis, of those parameters with 2000 iterations; only 20 sensitive parameters were considered for the analysis.

4.4.3. Parameters used in the Study

As described above; Global Sensitivity analysis is carried out to determine the most sensitive parameters. The parameters used in our study after the sensitivity analysis for the model calibration & validation are as follows (Arnold et al., 2012):

i. **Initial SCS Curve Number for moisture condition II (CN2):**

   The SCS curve number is a function of the soil's permeability, land use and antecedent soil water conditions. The increased value of this factor offers higher contribution to the surface runoff.

ii. Available Water Capacity of the Soil Layer (mm H2O/mm soil) (Sol-AWC):

The plant available water, also known as the available water capacity, is the fraction of water content present between field capacity and permanent wilting point. It is calculated as the difference between the fractions of water present at the permanent wilting point from that present field capacity.

iii. Base flow alpha factor (days) (Alpha_BF)

The base flow recession constant (αgw), is a direct index of ground waterflow response to changes in recharge. Lower values of this factor can be assessed as the slower response of the land to ground water recharge. Higher values depict the faster response to the recharge. The values may vary from 0.1 -0.3 for land with slow response to 0.9 – 1.0 for land with faster response.

iv. SPCON

SPCON is the linear parameter for calculating the maximum amount of sediment that can be re-entrained during the channel sediment routing. The values for this parameter vary in between 0.0001 to 0.01.

v. SPEXP

SPEXP is the exponent parameter for calculating the sediment re-entrained in the channel sediment routing. The values normally vary between 1 and 2. It was set at 1.5 in the original Bagnold Stream Power equation.

vi. CH_COV2

The channel cover factor, CH_COV2, is defined as the ratio of degradation from a channel with a specified vegetative cover to the corresponding degradation from a channel with no vegetative cover. The vegetation influences degradation by lowering stream velocity and, as a result, the erosive power near the bed surface. Its value ranges from 0 to 1, where 0 equals to channel is completely protected from erosion by cover and 1 equals to no vegetation cover on channel.

vii. CH_ERODMO

CH_ERODMO is set to a value from 0.0 to 1.0. A value of 0.0 indicates a non-erosive channel while a value of 1.0 indicates no resistance to erosion.

viii. USLE_P

The support practice factor, P_{USLE}, is defined as the ratio of soil loss with a specific support practice to the corresponding loss with up and down slope culture. Support practices include contour tillage, stripcropping on the contour and terrace systems.

ix. CH_N2

CH_N1 represents Manning's "n" value for the main channels. Its value also ranges between 0.01 to 0.3.

x. SOL_K (mm/hr)

The saturated hydraulic conductivity (SOL_K) relates soil water flow rate to the hydraulic gradient and is a measure of the ease of water movement through the soil.

xi. GW_DELAY

Groundwater delay time (days) is the lag between the time that water exits the soil profile and enters the shallow aquifer.

xii. GWQMN

Threshold depth of water in the shallow aquifer required for return flow to occur (mm H2O). Groundwater flow to reach is allowed only if the depth of water in the shallow aquifer is equal to or greater than GWQMN.

xiii. GW_REVAP

Groundwater “revap” coefficient. The value of GW_REVAP should be between 0.02 to 0.2.

xiv. REVAPMN

Threshold depth of water in the shallow aquifer for “revap” or percolation to the deep aquifer to occur (mm H2O).

This variable along with GW_REVAP is the reason a different groundwater file is created for each HRU rather than each subbasin.

xv. RCHRG_DP

Deep aquifer percolation fraction is the fraction of percolation from the root zone which recharges the deep aquifer. The value for RCHRG_DP should be between 0.0 to 1.0.

xvi. ESCO

Soil evaporation compensation factor.

This coefficient has been incorporated to allow the user to modify the depth distribution used to meet the soil evaporative demand to account for the effect of capillary action, crusting and cracks. ESCO must be between 0.01 and 1.0.

xvii. EPCO

Plant uptake compensation factor.

The amount of water uptake that occurs on a given day is a function of the amount of water reqired by the plant for transpiration and the amount of water available in the soil. The plant uptake compensation factor can range from 0.01 to 1. As epco approache 1.0, the model allows more of the water uptake demand to be met by lower layers in the soil. As epco approaches 0.0, the model allows less variation from the original depth distribution to take place.

xviii. SURLAG

Surface runoff lag coefficient.

In large subbasins with a time of concentration greater than 1 day, only a portion of the surface runoff will reach the main channel on the day it is generated. SWAT incorporates a surface runoff storage feature to lag a portion of the surface runoff release to the main channel.

If no value for SURLAG is entered, the model will set SURLAG = 4.0.

xix. CANMX

Maximum canopy storage (mm H2O).

SWAT allows the maximum amount of water that can be held in canopy storage to vary from day to day as a function of the leaf area index. CANMX is the maximum amount of water that can be trapped in the canopy when the canopy is fully developed (mm H2O).

xx. CHK2

Effective hydraulic conductivity in main channel alluvium (mm/hr).

For perennial streams with continuous groundwater contribution, the effective conductivity will be zero. For bed material of high silt-clay content its value is in the range of 0.025 – 2.5 mm/hr.

4.4.4. Model Peformance Analysis in SWAT-CUP

The parameters selected from the Global Sensitivity analysis were used for calibration of the model in SWAT-CUP. The model performance was evaluated on the basis of objective functions. Ten objective functions are currently allowed in the SUFI-2 algorithm. Five of the ten were selected to evaluate the model performance owing to their popularity and available details on accessibility.

The following objective functions were considered for the model evaluation.

i. Coefficient of determination (R^2)

It describes the level of variance between the simulated and observed data. It is not suggested to use as a single criteria for the evaluation of the model performance as it can give same R^2 value for different magnitude data set.Where, Q is a variable (eg., discharge), m and s stands for measured and simulated, i and i^{th} measured or simulated data.

$$\text{Maximize:} \qquad R^2 = \frac{\left[\sum_i \left(Q_{m,i} - \overline{Q}_m\right)\left(Q_{s,i} - \overline{Q}_s\right)\right]^2}{\sum_i \left(Q_{m,i} - \overline{Q}_m\right)^2 \sum_i \left(Q_{s,i} - \overline{Q}_s\right)^2}$$

If there are more than one variable, then the objective function is defined as:

Where w_j is the weight of j^{th} variable.

ii. Modified coefficient of Determination (bR^2)

This function takes into account the magnitude of data sets as well as their linearity by multiplying the magnitudes by regression constant (b). So, this function is considered better than R^2.

$$\text{Maximize:} \qquad \phi = \begin{cases} |b|R^2 & if \quad |b| \le 1 \\ |b|^{-1}R^2 & if \quad |b| > 1 \end{cases}$$

If there are more than one variable, the objective function is expressed as:

Where wj is the weight of j^{th} variable.

$$g = \sum_j w_j \phi_j$$

iii. Nash – Sutcliffe Efficiency (NSE)

It indicates the goodness of fit of the plot between the measured and simulated datasets.

$$\text{Maximize:} \qquad NS = 1 - \frac{\sum_i (Q_m - Q_s)_i^2}{\sum_i (Q_{m,i} - \overline{Q}_m)^2}$$

Where Q is a variable (eg., discharge), m and s stands for measured and simulated respectively, and the bar stands for average.

If there are more than one variable, then the objective function is defined as:

$$g = \sum_j w_j NS_j$$

Where w_j is the weight of j^{th} variable.

iv. RMSE – observations standard deviation ratio (RSR)

RSR is calculated by dividing the RMSE (Root Mean Square Error) by the standard deviaton of measured data.

$$\text{Minimize:} \qquad RSR = \frac{\sqrt{\sum_{i=1}^{n}(Q_m - Q_s)_i^2}}{\sqrt{\sum_{i=1}^{n}(Q_{m,i} - \overline{Q}_m)^2}}$$

Where Q is a variable (e.g., discharge), m and s stand for measured and simulated respectively.

RSR is the standardizes the RMSE using the observation standard deviation. It varies from zero to large positive values. The lower the RSR the better the model fit.

In case of multiple variables, g is defined as:

$$g = \sum_j w_j RSR_j$$

Where wj is the weight of jth variable.

v. Percent bias (PBIAS)

The tendency for observed data to be greater (or lesser) than the simulated data is measured by PBIAS. The optimum value is zero, where low magnitude values indicate better simulations. Positive values indicate model under estimation and negative values

$$\text{Minimize:} \qquad PBIAS = 100 * \frac{\sum_{i=1}^{n}(Q_m - Q_s)_i}{\sum_{i=1}^{n} Q_{m,i}}$$

indicate model over estimation.

Where Q is a variable (eg., discharge), m and s stand for measured and simulated respectively .

4.5. **Model Evaluation Guidelines**

Different literature has been published to evaluate the SWAT model performance. A review of published literatures are done to develop a range of values for performance evaluation of model

during calibration and validation for surface runoff and sediment flow. General model evaluation guidelines developed by (Moriasi et.al., 2007) is shown in Table 6 below:

Table 6: General Performance ratings for recommended statistics for a monthly time steps

Performance Rating	RSR	NSE	PBIAS (%)	
			Streamflow	Sediment
Very good	$0.00 \leq RSR \leq 0.50$	$0.75 < NSE \leq 1.00$	$PBIAS < \pm 10$	$PBIAS < \pm 15$
Good	$0.50 < RSR \leq 0.60$	$0.65 < NSE \leq 0.75$	$\pm 10 \leq PBIAS < \pm 15$	$\pm 15 \leq PBIAS < \pm 30$
Satisfactory	$0.60 < RSR \leq 0.70$	$0.50 < NSE \leq 0.65$	$\pm 15 \leq PBIAS < \pm 25$	$\pm 30 \leq PBIAS < \pm 55$
Unsatisfactory	$RSR > 0.70$	$NSE \leq 0.50$	$PBIAS \geq \pm 25$	$PBIAS \geq \pm 55$

4.6. LULC change analysis using TerrSet Software

1. **Land Change Analysis**

   Two historical land cover map layers is needed to evaluate the changes in the land cover including gain and losses in certain types of land cover, persistence to change and the potential variables that contributes to the change.

The land cover map of 1990 and 2000 A.D from (ICIMOD, 2013) is used in our study to evaluate the changes in the land cover. LCM analyse each pixel to identify the changes that occur between those two time periods. It also analysed the gain and loss of each category of land use, net change experienced by each category and the contributors to that change. The transition which happens for a small quantity or the transition of less significace can be ignored by applying the threshold for transitions. The changes that are identified are transitions from one state of land cover to another state. It is most likely that with many land cover classes the potential combination of transitions can be very large. The Figure 11 below shows the historical maps published by ICIMOD which are used in our study for land change analysis and validation of the projected land use map.

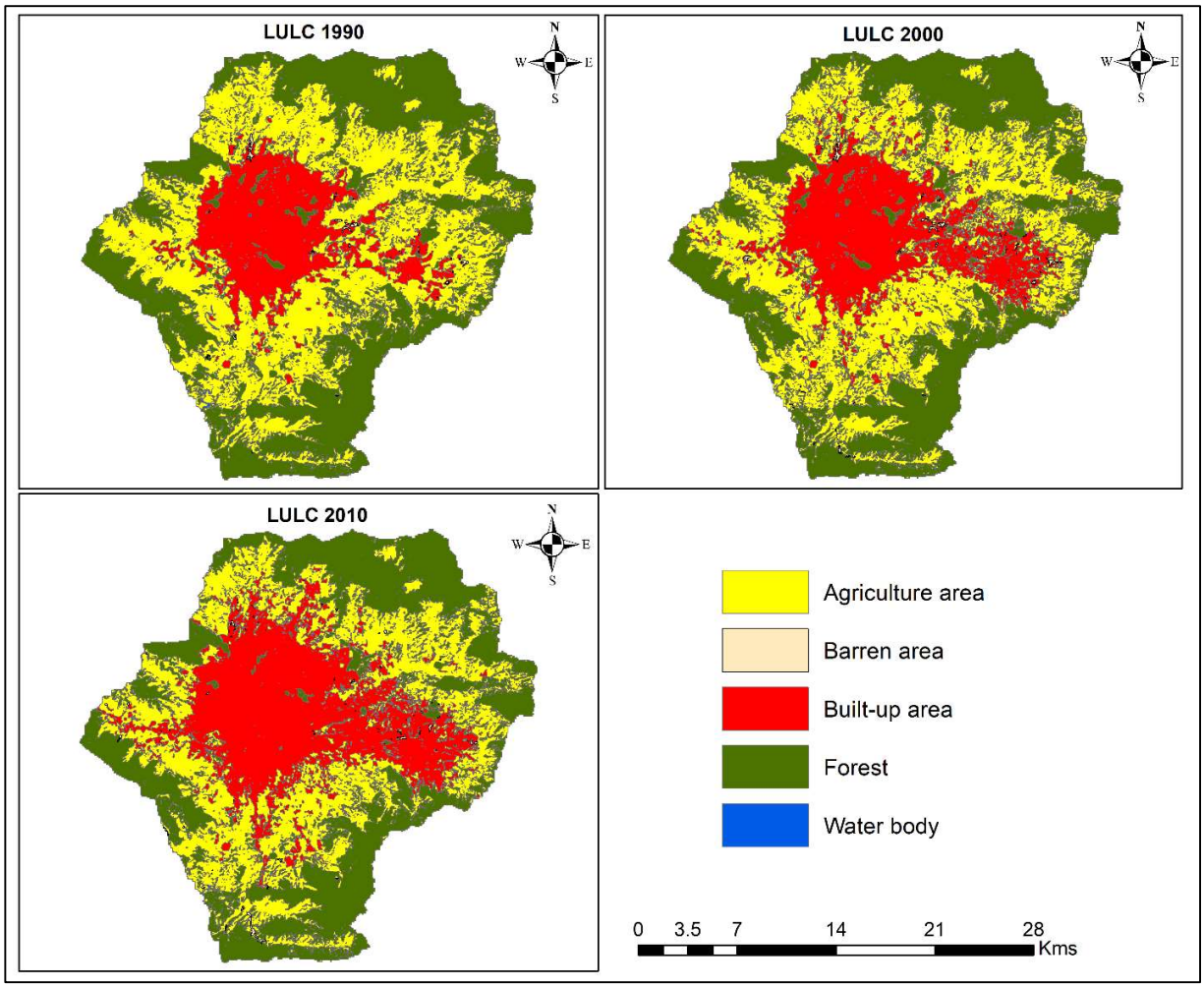

Figure 11: ICIMOD LULC data used for change analysis and validation of projected LULC

2. Transition Potential Modeling

Cellular Automata (CA) Markov model is used to project the land use land cover transition of 2025, 2050, 2075 and 2100 A.D. For the projection of LULC transition, different driver variables needed to be assigned to each submodel. This is where we have to specify what variables drive the transitions contained within the sub model we are evaluating. In this research, i have used variables such as distance from road, distance from river, slope, elevation, protected area, population density etc (Figure 12). These driver variables are used to model the historical change process.

Roads can provide access to previously remote areas promoting anthropogenic disturbance near roadways. Urban areas tends to grow when population increases. Since environmental gradients such as temperature and precipitation change with elevation it is often a good predictor of areas that are suitable for agriculture and thus are vulnerables to conversion to agricultural land. Slope is important in determining whether land is useful to humans for example agriculture and building require fairly gentle slopes so areas with these slopes may be more likely to experience land cover change. The choice of driver variables should be based on the knowledge of the study area.

Transition potentials describe the probability of a particular transition occuring on the modelled landscape and will be used in predicting the future change. Transitions are modeled using either a Multi-Layer Perception (MLP) neural network, Sim-Weight or Logistic Regression to create transition potentials. Sim Weight and Logistic Regression can only be used to model one transition at a time such that each transition must also have its own sub model. The Multi-Layer Perceptron can handle multiple transitions at once. There are many parameters tha can be set for the MLP neural network. After running the sub model, the MLP will first select random sample of pixels that went through each transitions we are modelling and pixels that could have gone through each transition. Half of the sampled pixels will be used to train the model and the other half will be used to test how well the model is doing at predicting change. MLP creates a multivariate function that can predict the potential of a pixel to transition based on the valuses of the driver variables for that pixel.

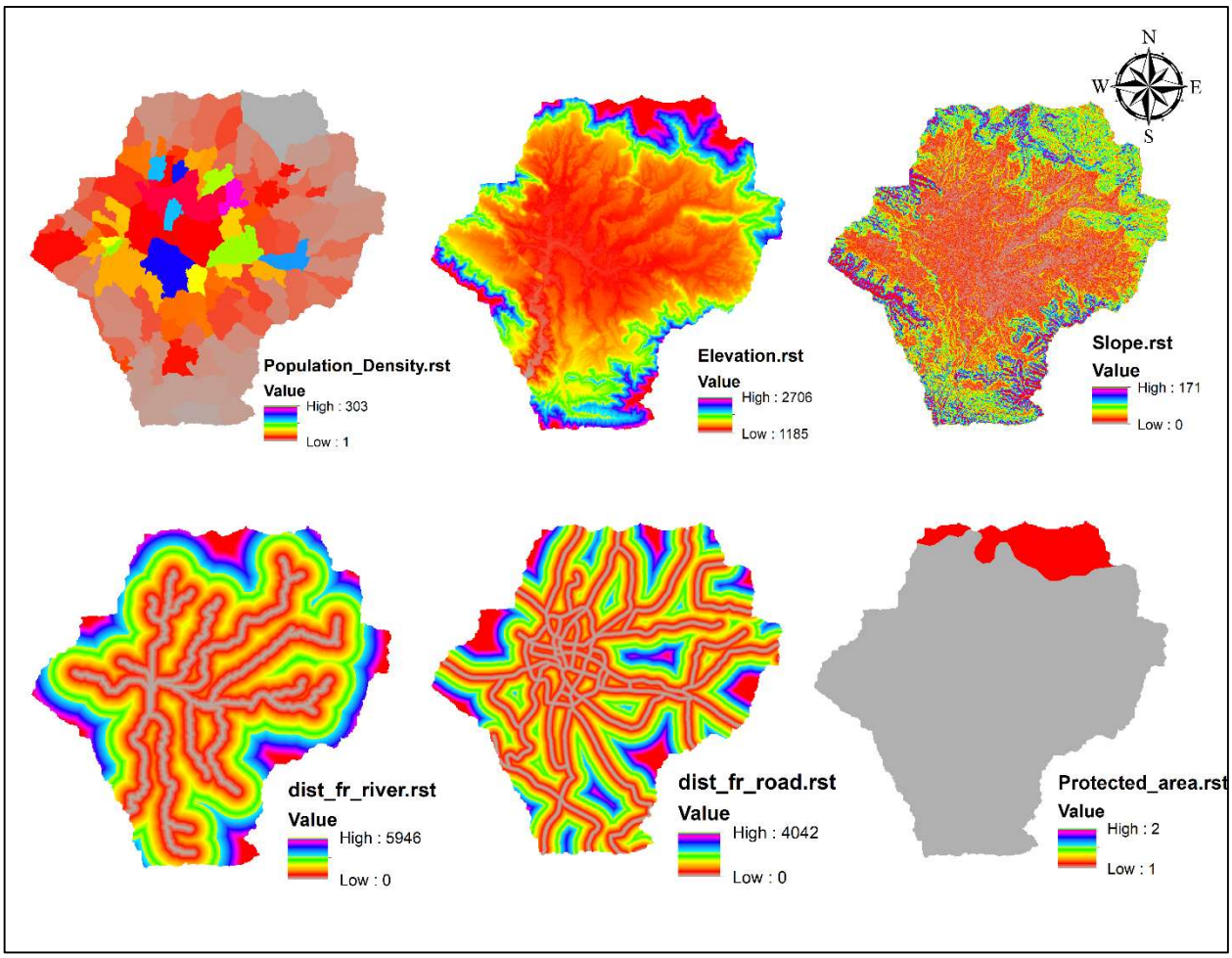

Figure 12: Driver Variables for Land Use Change

3. Change Prediction

Using the historical rates of change and the transition potential model, LCM can predict a future scenario for a specified future date. Essentially, the model will determine how the variables influence future change, how much change took place between time 1 and 2, then calculate the relative amount of transition to the future date (J Ronald, 2020). In our case, the input land cover images are for 1990 and 2000 A.D and we will predict for the year 2010 A.D.

Options are available to incorporate planning interventions such as incentives and constraints, proposed reserve areas and infrastructural changes. The transition can be modeled either through a Markov Chain analysis or through a transition probability matrix

from an external model. After running the model we will get two outputs; a hard prediction output and a soft prediction output. The soft prediction depicts the vulnerability of each pixel to transition to a different land cover class during the time period specified. The hard prediction predicts a specific land cover class for each pixel. The validation panel available in this tab helps to determine the quality of the predicted map by comparing it to an actual landuse map. The validation output will show misses, false alarms and hits and can be used to evaluate the accuracy of the model results.

According to J Ronald, 2020;

A |B| B = Hits (green) - Model predicted change and it changed

A |A| B = Misses (red) - Model predicted persistance and it changed

A |B| A = False Alarms (yellow) - Model predicted change and it persisted

Table 7: Land Use area transfer Matrix (2000 – 2010) in percentage using Markov Chain

	Agriculture area	Built-up area	Forest	Barren area	Water body	Total
Agriculture area	84.58	11.35	3.79	0.16	0.12	100
Built-up area	1.64	97.66	0.53	0.14	0.03	100
Forest	9.85	0.68	89.44	0.01	0.01	100
Barren area	6.72	8.8	0.8	83.68	0	100
Water body	65.89	3.97	2.98	1.16	25.99	100

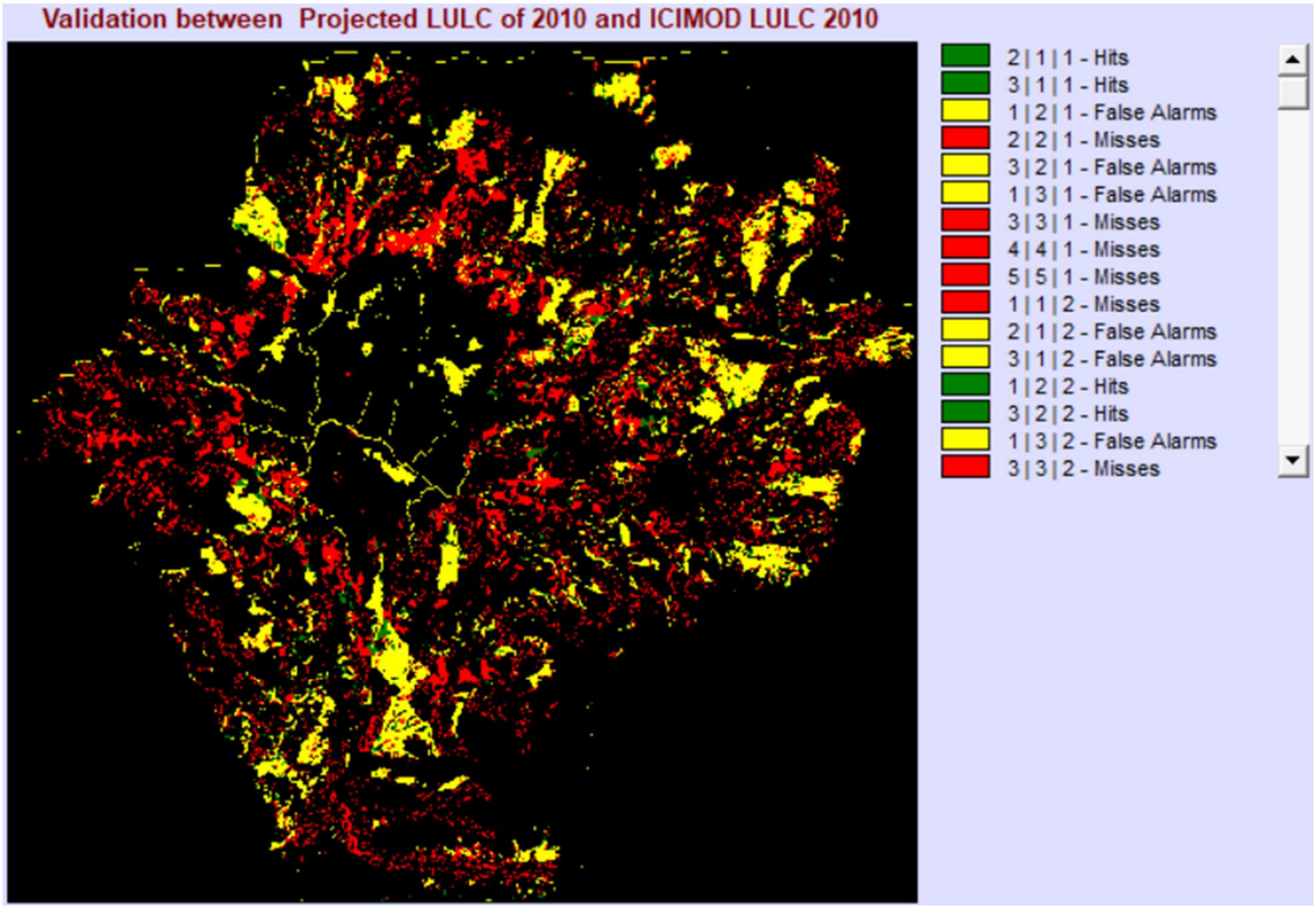

Figure 13: Hits, Misses and False Alarms for LULC Prediction

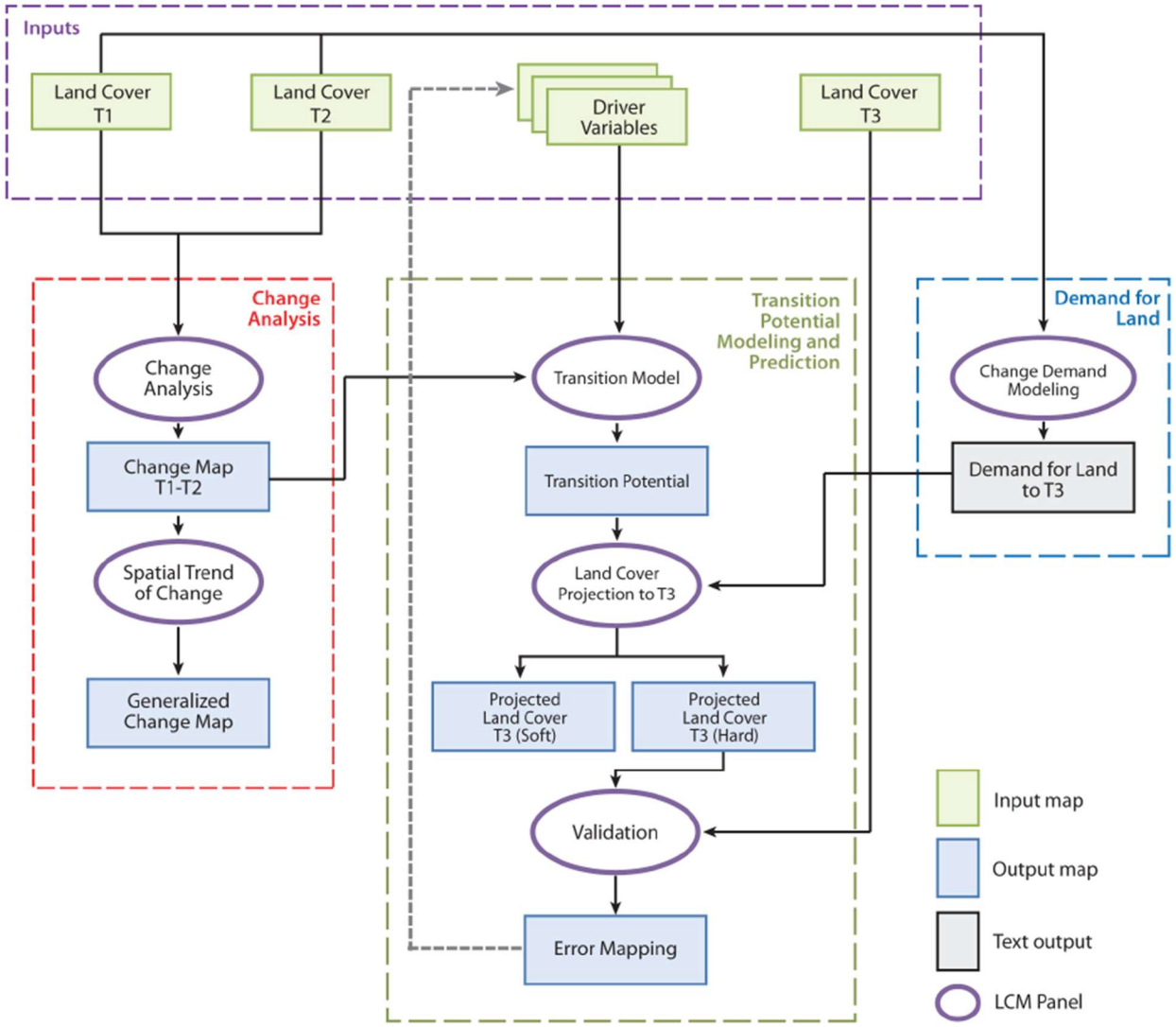

Figure 14: Methodological Flow chart for LULC Projection in TerrSet

(J Ronald, 2020)

4.6.1. IDRISI GIS Analysis

It consists of broad spectrum of fundamental tools for GIS analysis, primarily oriented to raster data. One of IDRISI's most notable features is a suite of multi-criteria and multi-objective decision procedures, in addition to a wide range of analytical and statistical tools for change & surface analysis. There are also graphical modeling environments for dynamic modeling and decision support.

4.6.2. IDRISI Image Processing

An extensive set of procedures for the restoration, enhancement, transformation and classification of remotely sensed images. IDRISI has the broadest set of classification procedures including both hard and soft classificatin procedures based on machine learning (such as neural networks) and statistical characterization.

4.6.3. Accuracy Assessment

The post processing accuracy assessment is an important part of the LULC calssification and mapping which is used to analyze the precision of the classified maps (Manandhar et al., 2009). The classification accuracy quantifies the quality of maps produced and it helps to evaluate the applicability of a map for a particular use. The techniques like Kappa coefficient, error matrix and indices-based techniques have already been used in several studies for the accuracy assessment of LULC maps produced (Rahman et al., 2019), (Manandhar et al., 2009).

In our study Kappa index of agreement (KIA) is used to evaluate the accuracy of projected LULC map. This is a very effective method to represent accuracy in which each category is plainly described along with both the errors of inclusion (commision errors) and errors of exclusion (omission errors) present in the classification.

Omission error estimates the probability of a pixel being accurately classified. This is the result from dividing the number of training pixels determined from ground truth data. This reveals how well training set pixels of the given LULC type are classified. Commision error shows the probability that a pixel represents the class for which it has been assigned. This is computed by dividing the number of correctly classified pixels in each category by the total number of pixels in that category. The relationship between these two sets of information (classified pixels and commision error) is usually summarized in an error matrix, also named a confusion matrix (Santos et al., 2021). The number of rows and columns in the error matrix should be equal to the number of categories whose classification accuracy is being assessed. In the error matrix the pixels located along the diagonal (from the upper left to the lower right) represent the pixels classified into the proper category. The non-diagonal values in the columns represent the omission error, while the non-diagonal values in the rows represent the comission error.

$$Kappa = \frac{Total\ Accuracy - Random\ Accuracy}{1 - Random\ Accuracy}$$

Or, $$Kappa = \frac{N\Sigma_{i=1}^{n} m_{i,i} - \Sigma_{i=1}^{n} G_i C_i}{N^2 - \sum_{i=1}^{n} G_i C_i}$$

Where, N is the total numbers of classified values to compared to truth value, i is the class number, $m_{i,i}$ is the number of values belonging to the truth class i that have also been classified as class i (i.e., values found along the diagonal of the confusion matrix). C_i is the total number of predicted values belonging to class i. G_i is the total number of truth values belonging to class i.

Chapter 5: RESULTS AND DISCUSSIONS

5.1. Sensitivity Assessment of the SWAT Model

SWAT parameters have to undergo sensitivity analysis first before model calibration to help in identifying and ranking parameters that have significant impact on specific model outputs such as stream flow and sediment yield (Choto & Fetene, 2019). Global sensitivity analysis was carried out to determine the processes which are dominant in a watershed and also to optimize them to achieve the objective function. Initially 24 parameters were considered based on literature review, preliminary sensitivity analysis, study area conditions and their known role on hydrologic processes. The studies carried out by different researchers are also considered most notably by (Pokhrel, 2018) who studied in the same watershed as mine and the parameters suggested by (Karim C. Abbaspour, 2015). The selected parameters were also chosen to reflect as much as possible. all the hydrological processes that might be occurring within the Bagmati watershed. After carrying out Global Sensitivity Analysis, of those parameters with 2000 iterations; only 20 sensitive parameters were considered for the analysis. These 20 parameters were iterated or adjusted until the optimum performance efficiency factors (R^2, NSE, bR^2, RSR and PBIAS) were obtained, indicating a good model simulation.

Of those selected parameters, the most sensitive parameters were the Manning's roughness coefficient for the main channel (CH-N2), soil evaporation compensation factor (ESCO), Saturated hydraulic conductivity (Sol-K), SCS runoff curve number (CN2), available soil water capacity (SOL- AWC), surface runoff lag coefficient (SURLAG) from the surface runoff parameters and baseflow alpha factor (ALPHA-BF), groundwater revap co-efficient (GW-REVAP), threshold depth of water in the shallow aquifer for return flow (GWQMN) from the subsurface response parameters.

Among channel erosion parameters, linear parameter for calculating the maximum amount of sediment that can be re-entrained during channel sediment routing (SPCON) and exponent parameter for calculating sediment re-entrained in channel sediment routing (SPEXP) were leading the group among all sediment parameters with second and third rank among overall parameters followed by Channel erodibility factor (CH-ERODMO) and Channel cover factor (CH-COV2).

Universal Soil Loss Equation (USLE) support practice factor (USLE-P) has been found to be the most sensitive landscape soil erosion variable.

According to (Karim C. Abbaspour, 2015) higher the absolute value of t-stat and smaller the p-value, the parameter is considered more sensitive. The t-stat indicates the degree of sensitivity and p-value, on the other hand, determines the significance of the sensitivity of the parameters. A multiple regression analysis is used to get the statistics of parameter sensitivity. The result of the sensitivity analysis is shown in Table 8 in descending order.

Table 8: Global sensitivity analysis result of the parameters

S.N	Parameter Name	t-Stat	P-Value
1	CH_N2	18.89	0.00
2	SPCON	-10.45	0.00
3	SPEXP	-2.98	0.00
4	ESCO	-2.23	0.03
5	SOL_K	-2.23	0.03
6	ALPHA_BF	-2.06	0.04
7	GW_REVAP	-1.39	0.16
8	CN2	-1.32	0.19
9	SOL_AWC	-1.06	0.29
10	SURLAG	-1.02	0.31
11	CH_ERODMO	-0.88	0.38
12	CH_COV2	-0.86	0.39
13	GWQMN	-0.84	0.40
14	REVAPMN	-0.51	0.61
15	GW_DELAY	0.50	0.61
16	RCHRG_DP	-0.46	0.64
17	USLE_P	-0.25	0.80
18	CANMX	0.21	0.83
19	CH_K2	0.20	0.84
20	EPCO	0.09	0.93

Above data shows that CH_N2, SPCON, SPEXP, ESCO and SOL_K are the five most sensitive parameters.

5.2. **Model Calibration, Validation and Evaluation of Model Performance**

In this study, the calibration is done using SWAT-CUP software with SUFI-2 optimization program. Table 11 shows the list of parameters and their fitted values obtained after the calibration. Figure 15 & Figure 19 shows the monthly simulation of the discharge and sediment yield for the calibration period respectively.

The validation of the parameters obtained from the calibration of the model was done by using so obtained parameters value for the known monthly discharge and sediment data from 2011 to 2016 A.D. Figure 17 & Figure 21 shows the validation period of the discharge and sediment yield respectively.

Based on the performance criteria by (Moriasi et.al., 2007), the values obtained shows very good result in the calibration period with (NSE = 0.9, R^2 = 0.9, PBIAS = 2.7) for discharge and good result with (NSE = 0.73, R^2 = 0.74, PBIAS = -9.4) for sediment yield. The simulated discharge follows the observed patterns to an extent except some peak discharges, where there were discrepancies. The simulated sediment yield also shows good agreement with observed data to the large extent. The peak sediment yield in the first year of simulation period slightly over predicted and the opposite happens in the last two years. The simulated base flow for both discharge and sediment shows good agreement with measured flow. Overall the hydrographs in the calibration period for both discharge and sediment shows better representation of peak flows, base flow & median flows.

The validation period also shows good performance of the model. The NSE and R^2 values obtained during validation for both discharge (NSE = 0.89, R^2 = 0.92) and sediment yield (NSE = 0.83, R^2 = 0.85) can be classified as very good and the PBIAS value of -16.7% & -23.2% for discharge and sediment respectively as satisfactory and good. The simulated discharge is consistant with the observed discharge with slightly more base flow in certain period. The simulated sediment flow is also consistant with the observed sediment flow with better statistical parameters than that of the calibration period. Overall the calibrated parameters seems quite fit for validation.

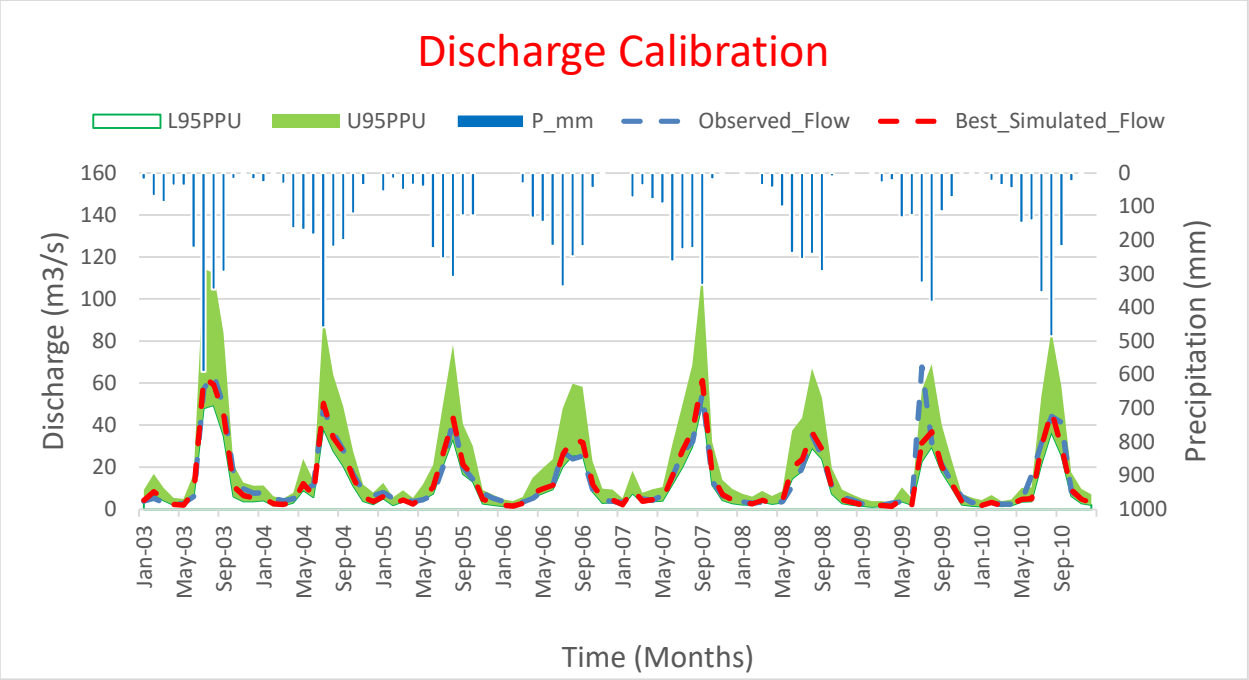

Figure 15: Calibration of Discharge at Khokana Station of Bagmati Basin

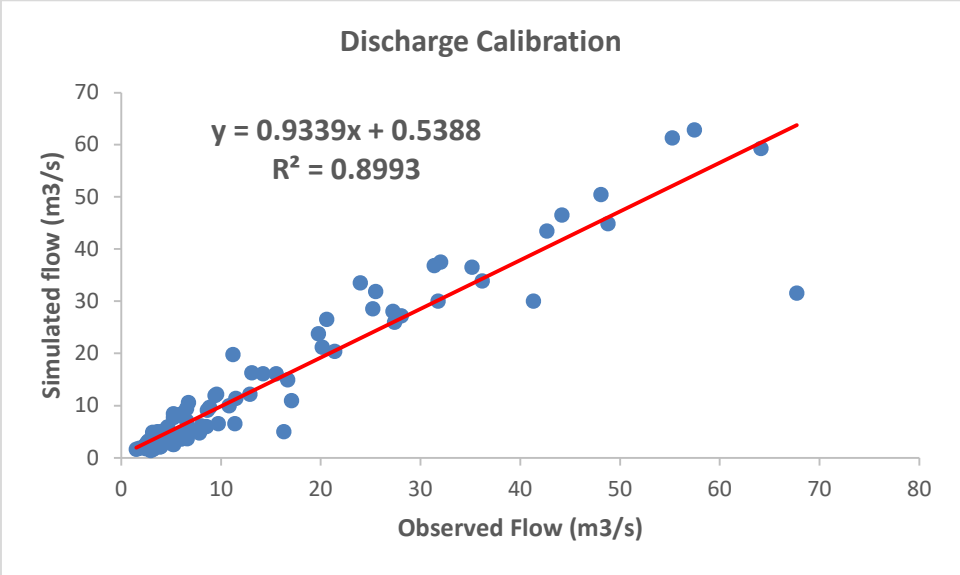

Figure 16: Correlation performance of Discharge during Calibration

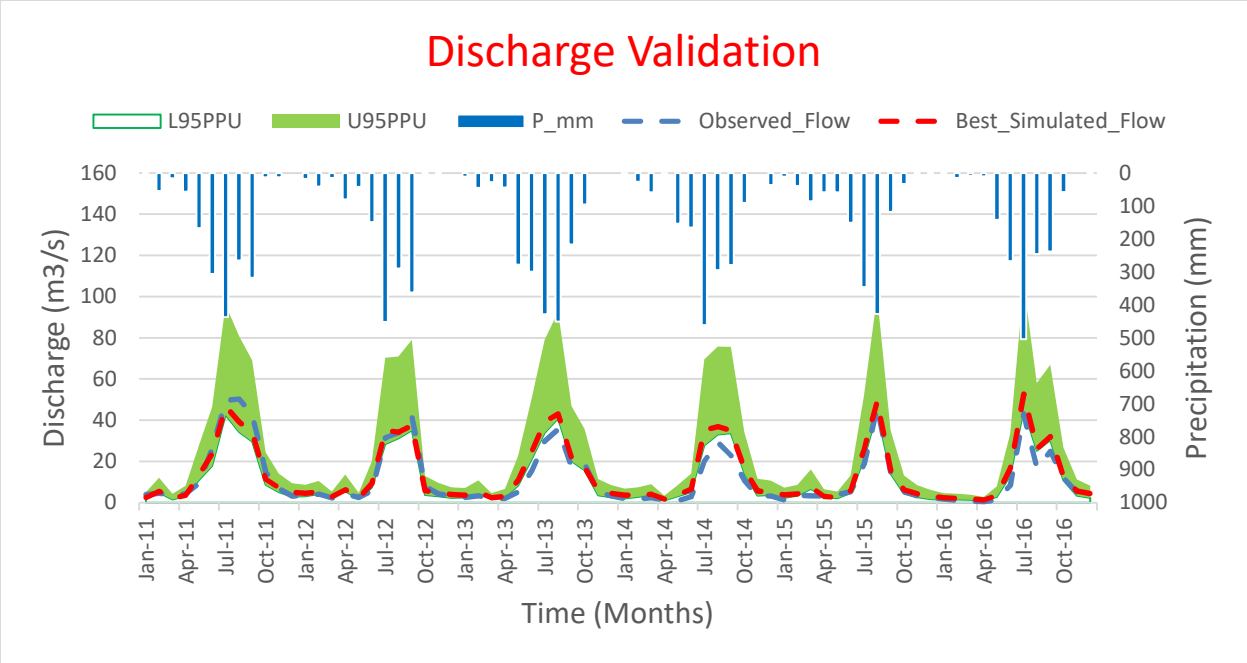

Figure 17: Validation of Discharge at Khokana Station of Bagmati Basin

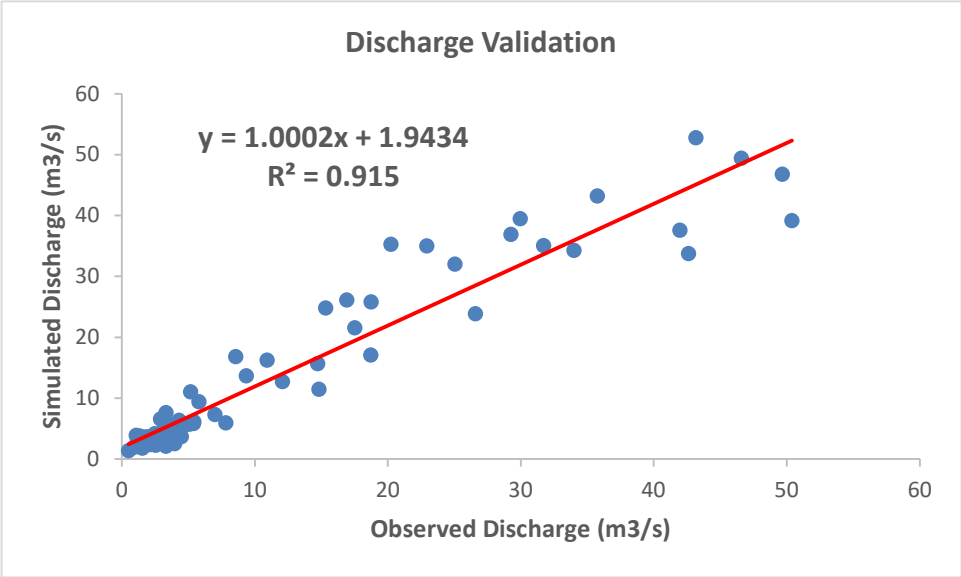

Figure 18: Correlation performance of discharge during Validation

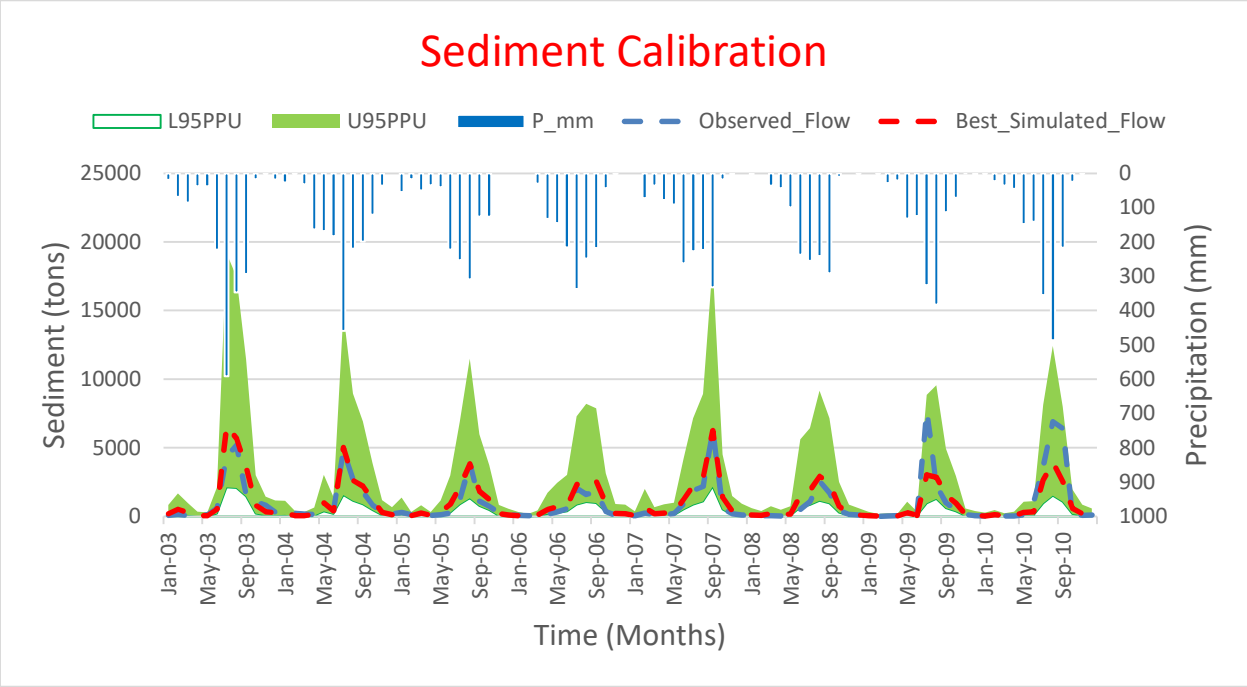

Figure 19: Calibration of Sediment at Khokana Station of Bagmati Basin

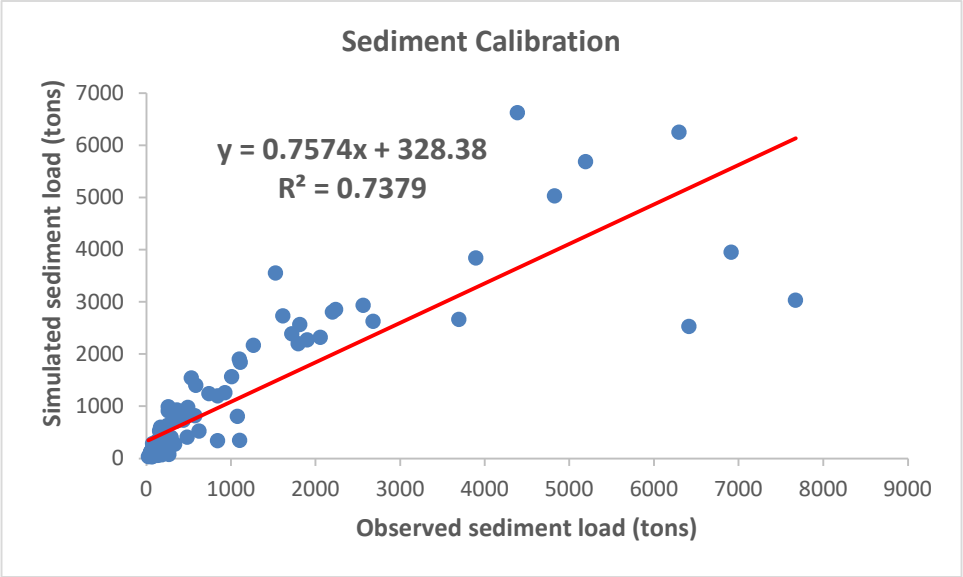

Figure 20: Correlation performance of Sediment during Calibration

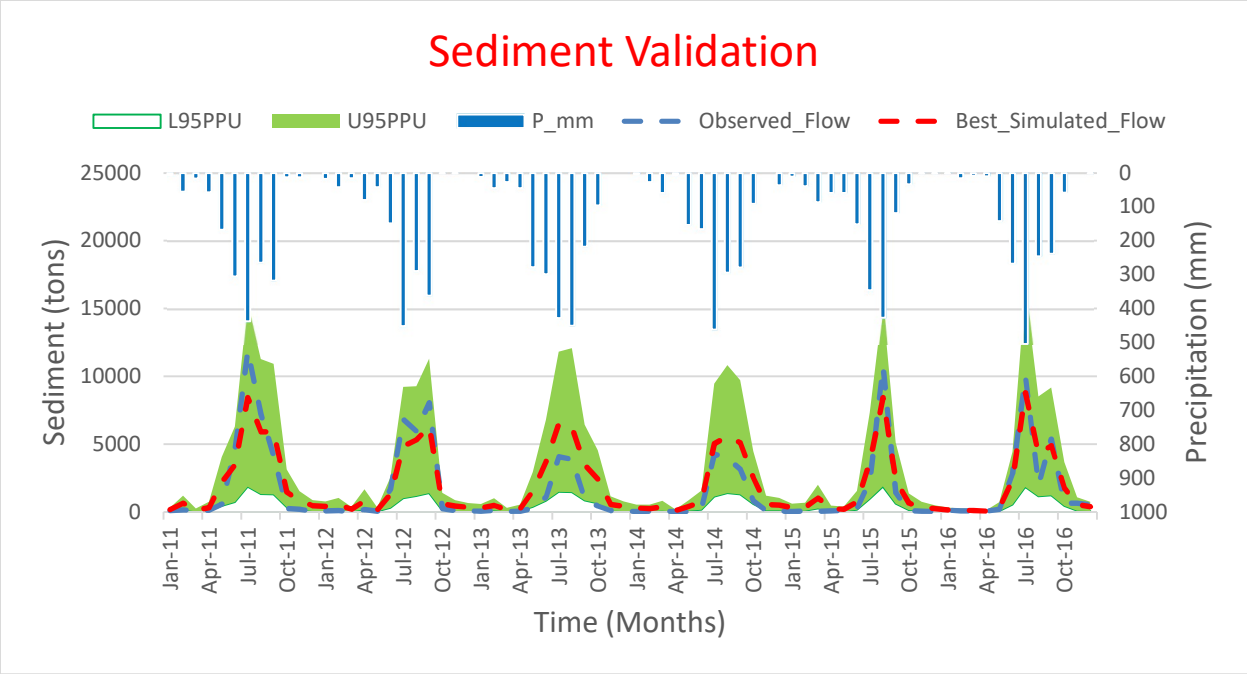

Figure 21: Validation of Sediment at Khokana Station of Bagmati Basin

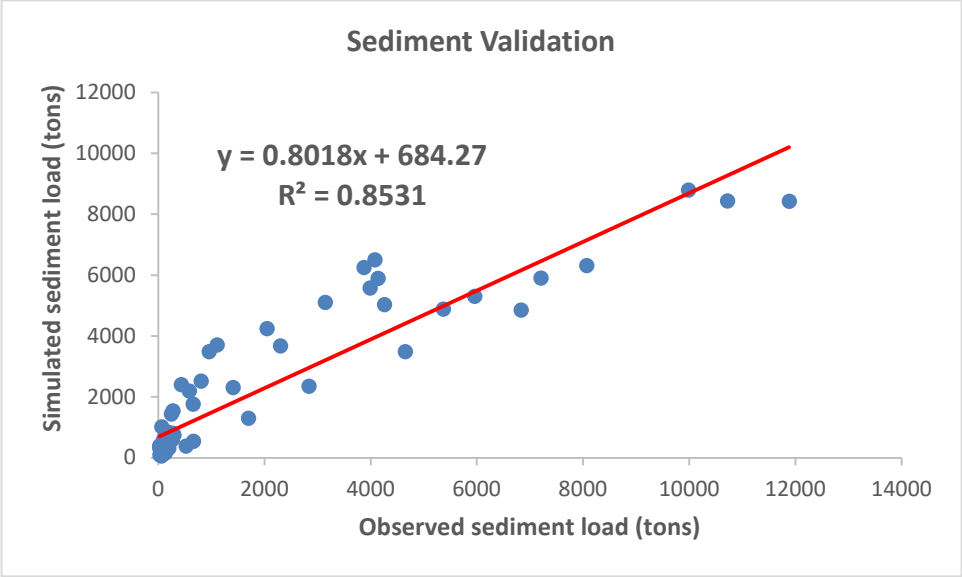

Figure 22: Correlation performance of sediment during Validation

Table 9: Calibration & Validation Statistics of the SWAT model using monthly Discharge data

Stage of Model	Evaluated Parameters						
	p-factor	r-factor	R^2	NSE	bR^2	RSR	PBIAS
Calibration (2000 - 2010)	0.79	0.32	0.9	0.9	0.84	0.32	2.7
Validation (2011 - 2016)	0.56	0.38	0.92	0.89	0.91	0.34	-16.7

Table 10: Calibration & Validation Statistics of the SWAT model using monthly Sediment data

Stage of Model	Evaluated Parameters						
	p-factor	r-factor	R^2	NSE	bR^2	RSR	PBIAS
Calibration (2000 - 2010)	0.99	1.61	0.74	0.73	0.56	0.52	-9.40
Validation (2011 - 2016)	0.94	1.03	0.85	0.83	0.68	0.41	-23.2

Table 11: List of Calibrated Parameters and their values

S.N	Parameters used to calibrate stream flow	Description of Parameters	Range of values	Fitted Values
1	CN2.mgt	SCS runoff curve number	-0.1 to 0.1	0.008
2	ALPHA_BF.gw	Baseflow alpha factor (days)	0 to 1	0.851
3	GW_DELAY.gw	Groundwater delay time (days)	0 to 500	40.875
4	GWQMN.gw	Threshold depth of water in the shallow aquifer for return flow (mm)	0 to 5000	1918.75
5	CH_N2.rte	Manning's roughness coefficient for the main channel	- 0.01 to 0.3	0.16
6	SOL_AWC.sol	Available soil water capacity	0 to 1	0.3
7	SOL_K.sol	Saturated hydraulic conductivity (mm/hr)	0 to 2000	409.5
8	ESCO.hru	Soil evaporation compensation factor	0 to 1	0.06
9	EPCO.hru	Plant uptake compensation factor	0 to 1	0.904
10	GW_REVAP.gw	Groundwater revap coefficient	0.02 to 0.2	0.131
11	RCHRG_DP.gw	Deep aquifer percolation fraction	0 to 1	0.197

12	REVAPMN.gw	Threshold depth of water in the shallow aquifer for "revap" or percolation to the deep aquifer to occur (mm)	0 to 500	238.875
13	SURLAG.bsn	Surface runoff lag coefficient	0.05 to 24	1.002
14	CANMX.hru	Maximum canopy storage	0 to 100	41.725
15	CH_K2.rte	Effective hydraulic conductivity in the main channel	-0.01 to 500	135.618

S.N	**Parameters used to calibrate sediment yield**	**Description of Parameters**	**Range of values**	**Fitted Values**
1	SPEXP.bsn	Exponent parameter for calculating sediment reentrained in channel sediment routing	1 to 1.5	1.469
2	SPCON.bsn	Linear parameter for calculating the maximum amount of sediment that can be reentrained during channel sediment routing	0.0001 to 0.01	0.000172
3	CH_ERODMO.rte	Channel erodability factor	0 to 1	0.365
4	USLE_P.mgt	USLE equation support parameter	0 to 1	0.009
5	CH_COV2.rte	Channel cover factor	-0.001 to 1	0.442

5.3. **Model Validation for LULC Change**

The land use land cover map is projected using IDRISI GIS analysis and Land Change Modeler extension in the TerrSet software. The landuse map given by ICIMOD for the year 1990 A.D and 2000 A.D is used as input for the change analysis and transition potential analysis for the preparation of land use map of 2010 A.D. A comparision of predicted land use land cover map of 2010 A.D with land use land cover map given by ICIMOD for the same year is made (Table 12) for the validation of the predicted LULC map.

The accuracy assessement of the projected LULC is done by Error Matrix analysis using IDRISI image processing model. The overall Kappa Index of agreement gives 73 % accuracy.

Table 12: Comparision between Actual & Projected Land Use

LULC Class	Icimod_LULC_2010		LULC_2010_Projected		Error %
	Area (sq.km)	Percentage (%)	Area (sq.km)	Percentage (%)	
Built-up area	172.391	28.118	160.584	26.221	1.897
Agriculture area	224.228	36.573	238.272	38.906	-2.334
Forest	215.165	35.094	211.575	34.547	0.547
Barren area	1.211	0.198	1.509	0.246	-0.049
Water Body	0.110	0.018	0.487	0.080	-0.062

The comparision of actual LULC map with projected LULC map for the year 2010 A.D shows more or less same area for different LULC class. The built-up area and forest area shows slightly more in actual LULC map. Agricultural area, barren area and water body in the actual LULC map is slightly less than the projected map. The result shows the maximum error of less than 2.4 % so we can say that the validation result is quite good.

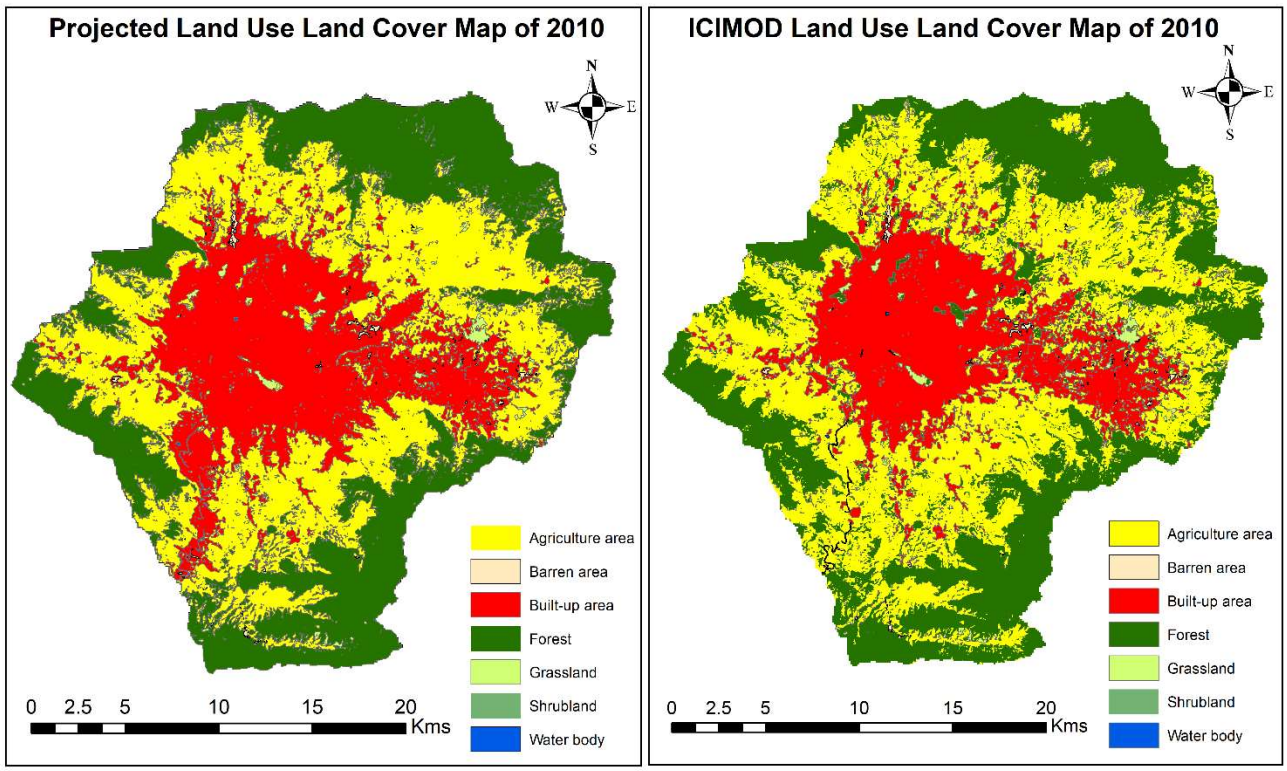

Figure 23: Validation of Land Use Land Cover Change

5.4. **Projection of Future LULC**

After the validation of the LULC map; future LULC map is projected (Figure 24) using CA markov model for the year 2025 A.D, 2050 A.D, 2075 A.D and 2100 A.D. The comparision (Table 13 & Figure 25) of the projected LULC for different time periods shows the gradual increase of built-up area in the expense of agricultural area and forest area. The comparison of LULC change for the period from 2000 to 2100 A.D shows the overall increase of Built-up area of the Kathmandu valley by 186.709 Sq.km (30.3%). All the other land use classes are in decreasing trend. Increasing urbanization pattern can be seen in Figure 24, mostly affects the agriculture area and forest area which shows 15.4% and 15.2% decrease from 2000 to 2100 A.D. Area of the water bodies are also decreasing. The water body area in the year 2010 shows the rapid decrease and then increase in the 2025 A.D. and finally the continious decrease in the following years. This may be due to the size of the grid and also the area and width of the water bodies in the valley are less so the chance of miscalculaiton is also high. The future projection of LULC is based on 2000 A.D LULC map of ICIMOD, so the projected area of water bodies after the 2010 A.D shows the gradual decrease. The barren area seems to increase gradually with contradicting result in the year 2010 A.D; this may be also due to the same reason as that of suddent decrease of water body in that year.

The trend of changing LULC shows the central urban area to increase rapidly and almost completely filled with built-up area till 2025 A.D. The trend of built-up area shows the continuous increase towards the outer periphery. The forest area also shows the decreasing trend. The forest area in the plain areas seems to be converted into first the agricultural area and then to built-up area. The forest area in the sorrounding hills seems to remain constant and presence of Shivapuri Nagarjun National park also helps to control the the complete degradation of the forest area.

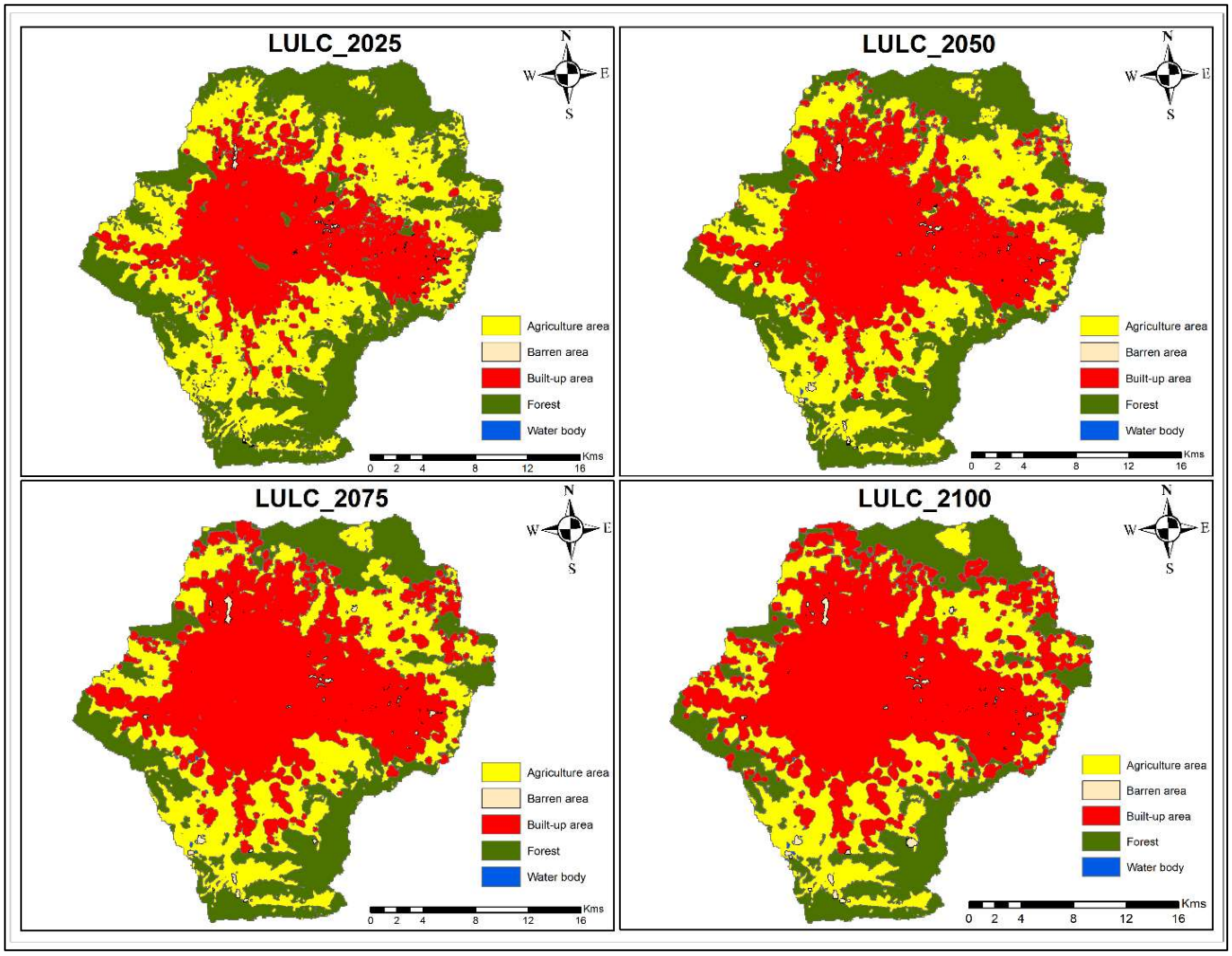

Figure 24: Projected LULC maps for future time periods

Table 13: LULC Change Dynamics (Area in percentages)

LULC Class	Historical LULC			Projected LULC			
	1990	2000	2010	2025	2050	2075	2100
Built-up area	16.6	21.5	28.1	32.0	39.8	46.0	51.8
Agriculture area	44.2	41.6	36.6	36.1	32.2	29.5	26.2
Forest	38.9	36.6	35.1	31.6	27.5	24.0	21.4
Barren area	0.2	0.2	0.2	0.2	0.4	0.5	0.6
Water Body	0.1	0.1	0.0	0.1	0.1	0.1	0.1

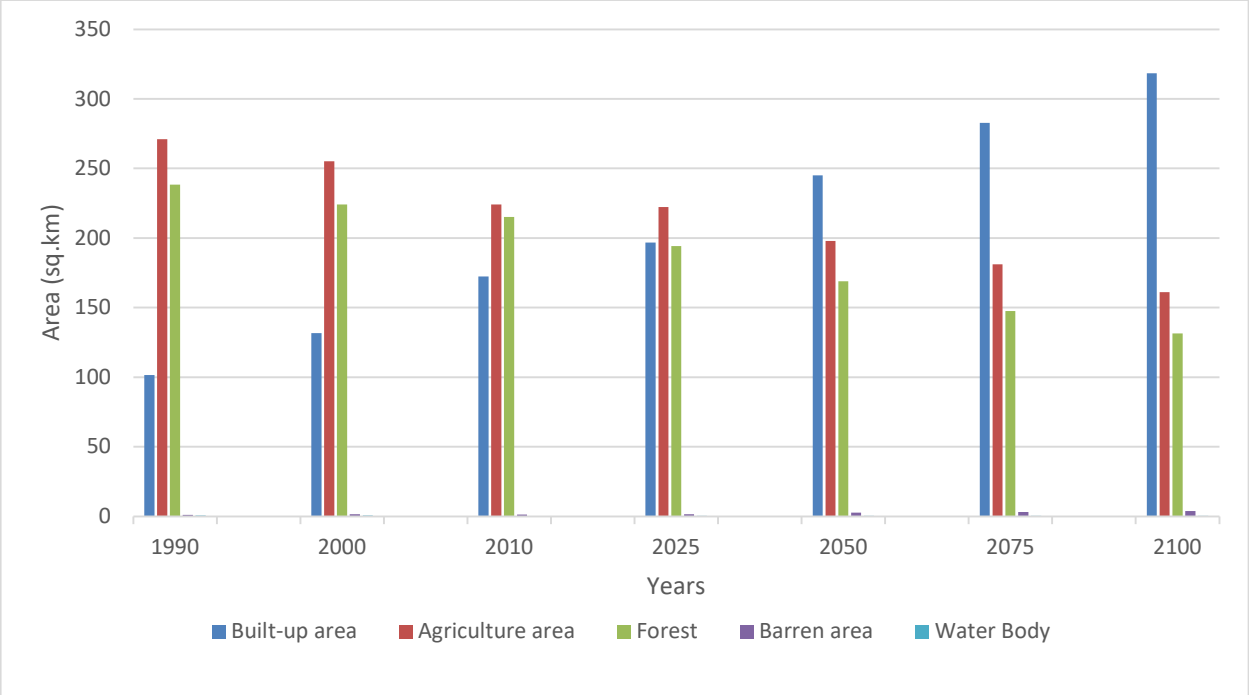

Figure 25: Land use dynamics from 1990 A.D to 2100 A.D

5.5. LULC change Impact Analysis

Land use land cover data of 2000, 2025, 2050, 2075 and 2100 A.D is used for the impact assessment of the LULC change on the hydrology and sediment yield of the Bagmati basin. The LULC of 2000 A.D is considered as the baseline data for the LULC change impact analysis. The impact of this change of LULC classes on the discharge and sediment yield was examined after the calibration and validation of the model. The annual, seasonal and monthly average values of the six parameters (surface flow, lateral flow, ground water flow, evapotranspiration, water yield and sediment yiedl) was analysed for the impact assessment of the LULC change.

5.5.1. Impact of LULC change on Hydrology

1. Annual Impact Analysis

The impact of LULC change on the hydrology of the watershed is examined after the validation of the SWAT model. Figure 26 shows the comparison of future average annual water yield, sediment yield, surface runoff (SURQ), lateral flow (LATQ), groundwater flow (GWQ) and evapotranspiration (ET) under different scenarios of LULC change. The average annual analysis of the result shows the increase of surface runoff(SURQ) by 48% from 2000 to 2100 A.D. While

the lateral flow contribution to steam flow(LATQ) and ground water contribution (GWQ) to the stream flow shows the decrease by 9% & 17.7% respectively. Overall the increase of surface runoff with simultaneous decrease of lateral flow and groundwater flow compensated each other with only 1.1 % runoff increase from 2000 to 2100 A.D. The evapotranspiration (ET) for all the LULC period shows the decreasing trend.

This results shows the negative impact of the urbanization on the water balance of the Bagmati watershed. Increase of impervious surfaces due to urbanization decrease the percolation of rain water into the ground sub-surface resulted in decrease of ground water recharge. While it contributes to increase in surface runoff. The implication of this findings are the threating flood hazards and the challenges that are associated with it during the rainy months. Also the lack of reliable water supply in the KV and the dependency on ground water for water supply purpose further reduces the ground water table which finally contributes to low ground water flow (GWQ). The decrease of agricultural area and forest area contributes to the decrease in evapotranspiration. According to (Costa et al., 2003) & (Li et al., 2009a) forests generally produces more evapotranspiration than other land use types due to higher leaf area and deeper rooting depth so the rapid decrease of forest area and the corresponding decrease of ET value shows the correlation between them.

Table 14: Estimated average annual discharge and sediment yield for different LULC

Component	Year (A.D)				
	2000	2025	2050	2075	2100
Water Yield / Runoff (mm)	782.87	784.64	787.15	789.71	791.80
Sediment yield (T/Ha)	5.59	5.5	5.64	5.41	5.03
Surface runoff contribution to stream flow SURQ (mm)	171.39	198.64	220.52	238.92	253.72
Lateral flow contribution to stream flow LATQ (mm)	399.27	393.19	384.16	373.38	363.52
Ground water contribution to stream flow GWQ (mm)	212.21	192.81	182.47	177.41	174.55
Evapotranspiration ET (mm)	595.80	593.80	591.90	590.10	588.90

Table 15: Percentage change of average annual values for projected LULC considering LULC of 2000 A.D as base period

Component	Year (A.D)			
	2025	2050	2075	2100
Water Yield / Runoff (%)	0.2	0.5	0.9	1.1
Sediment yield (%)	-1.6	0.9	-3.2	-10.0
Surface runoff contribution to stream flow SURQ (%)	15.9	28.7	39.4	48.0

Lateral flow contribution to stream flow LATQ (%)	-1.5	-3.8	-6.5	-9.0
Ground water contribution to stream flow GWQ (%)	-9.1	-14.0	-16.4	-17.7
Evapotranspiration ET (%)	-0.3	-0.7	-1.0	-1.2

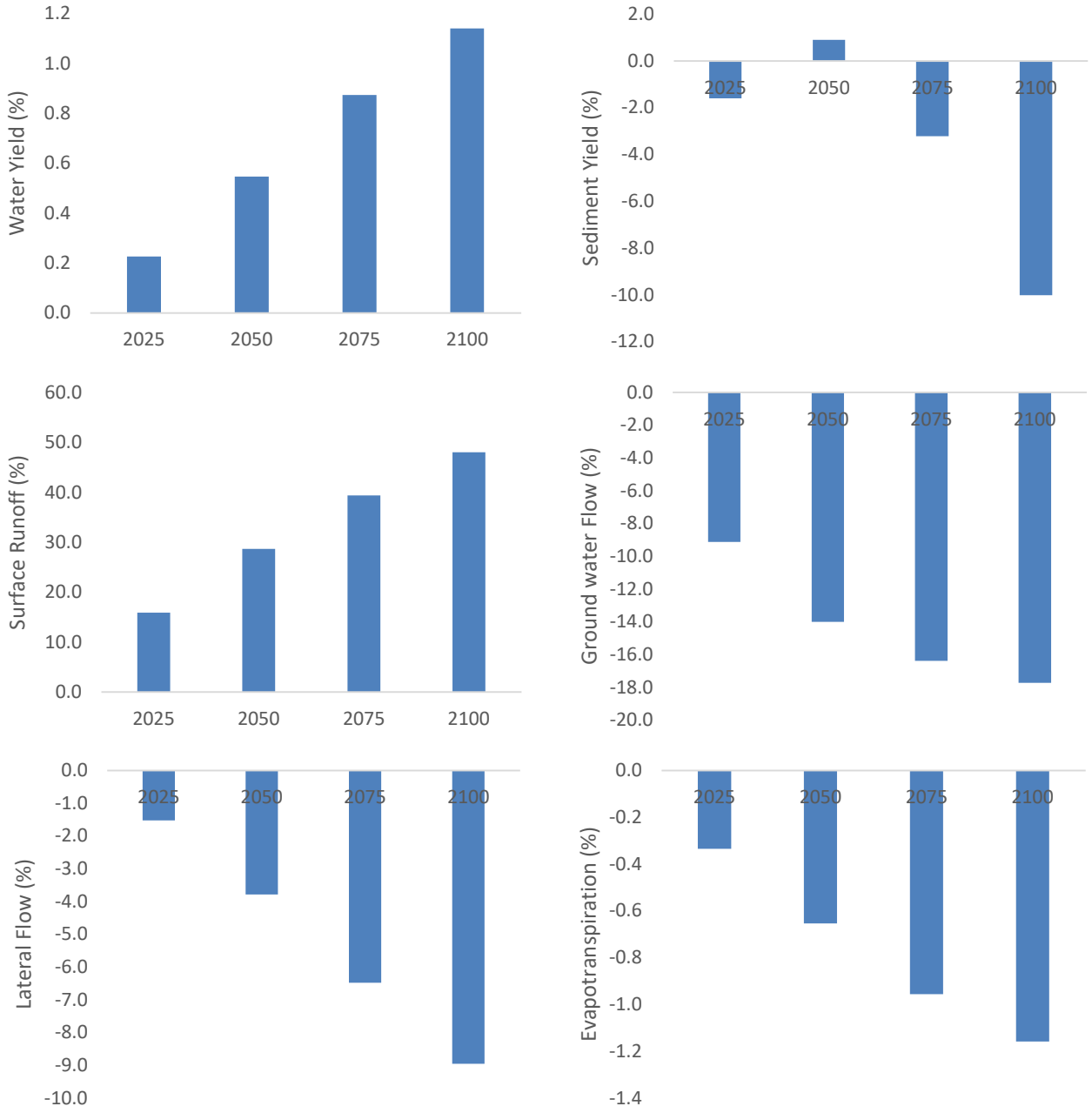

Figure 26: Percentage change of average annual values for different hydrological parameters for projected LULC (2025, 2050, 2075 & 2100) campared with baseline (LULC 2000)

2. Seasonal Impact Analysis

Seasonal impact assessment is carried out considering month from March to May as pre-monsoon period, month form June to September as monsoon period and month from October to February as post-monsoon period. The analysis (Table 15, Table 16 & Figure 27) shows the increase of water yield for pre-monsoon and monsoon period while for the post monsoon period water yield is decreasing. The surface runoff shows the increasing trend for all seasons while lateral flow and groundwater flow shows the decresing trend for all seasons. For evapotranspiration the pre-monsoon and post-monsoon period shows the decreasing trend for all the LULC but for monsoon period ET value is more or less constant.

Surface runoff is increasing during all seasons. The results shows the possibility of flood hazards during monsoon season. So, during this season flood disaster prevention measures such as building of diversion structures to safely convey the storm water to its outfall should be put in place to prevent the economic loss due to submergence which can be seen regularly in Kathmandu each year during monsoon season.

Table 16: Seasonal Impacts Analysis of LULC change on hydrology

Year	Water Yield (mm)			Surface Runoff (mm)			Lateral Flow (mm)			Evapotranspiration (mm)			Groundwater Flow (mm)		
	S1	S2	S3	S1	S2	S3	S1	S2	S3	S1	S2	S3	S1	S2	S3
2000	23.6	139.1	31.3	2.8	38.4	1.9	12.7	83.9	5.1	49.6	85.9	20.8	8.1	16.7	24.3
2025	24.0	141.3	29.6	3.7	44.0	2.3	12.7	82.5	5.1	49.0	86.0	20.7	7.6	14.8	22.2
2050	24.3	142.8	28.7	4.5	48.5	2.6	12.6	80.5	5.0	48.5	86.0	20.5	7.3	13.8	21.1
2075	24.6	143.7	28.3	5.1	52.3	2.9	12.3	78.1	4.8	48.2	86.0	20.4	7.2	13.3	20.6
2100	24.8	144.4	28.1	5.7	55.3	3.1	12.1	76.0	4.7	47.9	86.0	20.3	7.1	13.1	20.2

Table 17: Seasonal Impacts of LULC change on hydrology in percentages considering baseline data of 2000 A.D LULC

Year	Water Yield (%)			Surface Runoff (%)			Lateral Flow (%)			Evapotranspiration (%)			Groundwater Flow (%)		
	S1	S2	S3	S1	S2	S3	S1	S2	S3	S1	S2	S3	S1	S2	S3
2025	1.7	1.6	-5.5	33.3	14.5	23.4	-0.3	-1.7	-1.3	-1.2	0.2	-0.7	-6.3	-11.3	-8.5
2050	3.2	2.7	-8.3	59.9	26.2	40.8	-1.1	-4.1	-3.1	-2.1	0.2	-1.3	-9.8	-17.2	-13.1
2075	4.3	3.4	-9.6	82.3	36.1	55.0	-2.7	-7.0	-5.3	-2.8	0.2	-1.9	-11.7	-20.0	-15.4
2100	5.1	3.8	-10.2	102.5	43.9	66.9	-4.9	-9.5	-7.4	-3.4	0.2	-2.4	-12.9	-21.4	-16.7

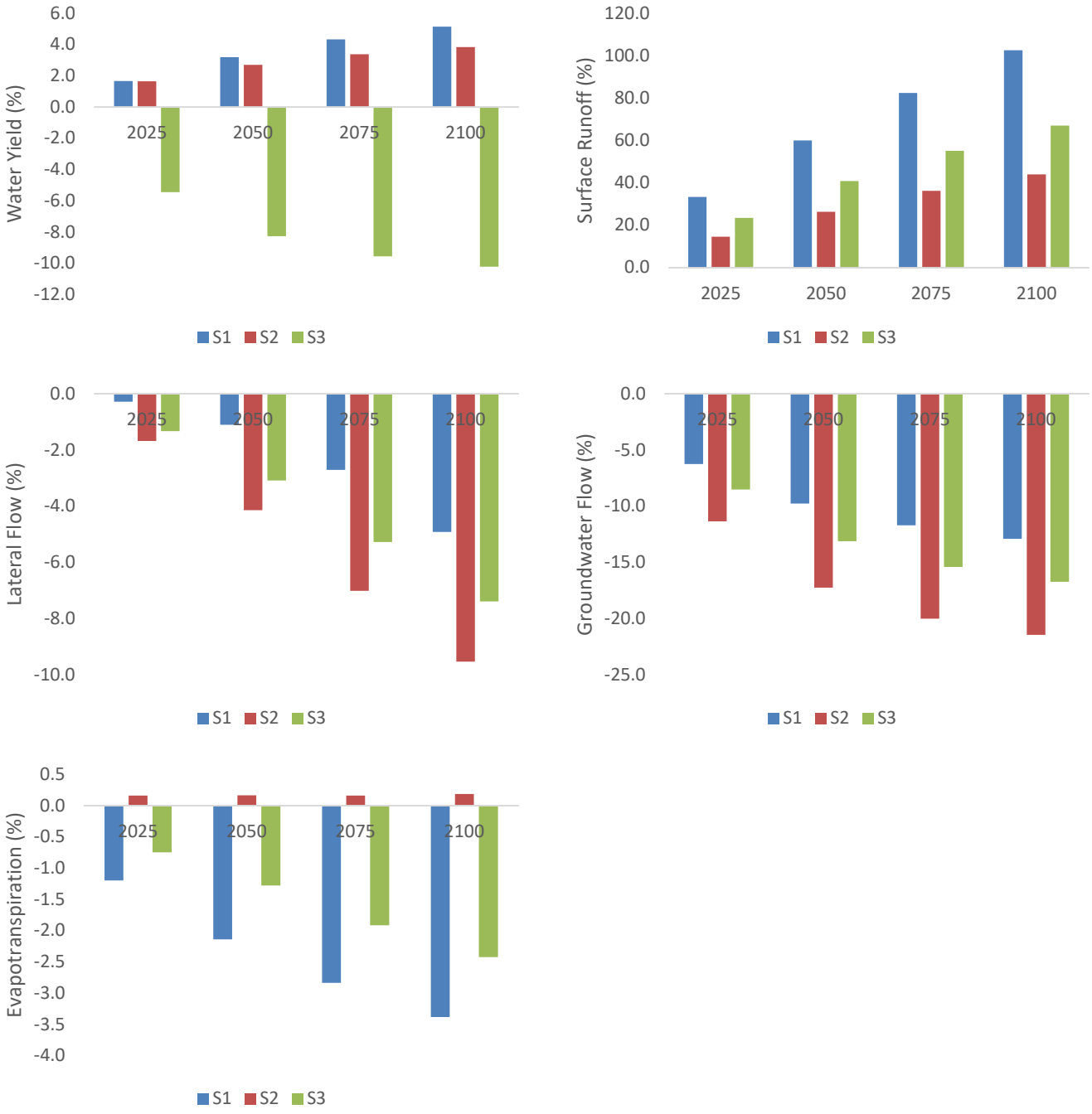

Figure 27: Percentage change in average seasonal values for different hydrological parameters for projected LULC (LULC of 2025, 2050, 2075 & 2100) compared with baseline LULC of 2000 A.D

3. Monthly Impact Analysis

The assessment of the water balance components for the monthly time period (Table 18) shows the increasing trend of water yield from month of march to september which falls under pre-monsoon and monsoon period while month from october to february shows the decreasing trend. It shows the runoff is increasing in the wet months but decreasing in the dry months. The surface runoff is increasing during all months under all LULC scenarios. All the other water balace components shows the decreasing trend for all LULC scenarios. The implication of this will be lowering of overall base flows and the surface runoff during rains will be excessive. The ground water table will decrease due to less percolation of water to the soil sub-surface which is the cause of increase impervious surfaces due to urbanization. The evapotranspiration is also decreasing in almost every months.

Table 18: Monthly impact assessment of LULC change on hydrology in percentages compared to the base year LULC of 2000 A.D

Year	Total Water Yield (%)											
	Jan	Feb	Mar	Apr	May	Jun	Jul	Aug	Sep	Oct	Nov	Dec
2025	-5.9	-1.6	-0.1	1.7	2.6	3.2	2.5	1.4	0.2	-4.4	-8.2	-7.3
2050	-9.0	-2.3	0.2	3.7	4.6	5.2	3.9	2.4	0.4	-6.7	-12.5	-11.2
2075	-10.4	-2.5	0.8	5.1	5.9	6.5	4.6	3.1	0.8	-7.6	-14.7	-13.1
2100	-11.2	-2.5	1.3	6.1	6.7	7.6	5.1	3.5	1.0	-8.0	-15.8	-14.2

Year	Surface Runoff (%)											
	Jan	Feb	Mar	Apr	May	Jun	Jul	Aug	Sep	Oct	Nov	Dec
2025	45.2	43.0	43.2	42.6	27.3	20.8	13.3	14.1	14.4	17.4	28.6	42.1
2050	83.3	76.1	74.7	76.7	50.0	37.2	24.3	25.8	25.6	29.7	46.4	78.9
2075	111.9	102.8	100.0	104.5	69.8	51.0	33.4	35.7	35.1	40.1	60.7	110.5
2100	138.1	126.1	124.0	131.3	86.7	62.5	40.6	43.4	42.6	48.4	71.4	136.8

Year	Lateral Flow (%)											
	Jan	Feb	Mar	Apr	May	Jun	Jul	Aug	Sep	Oct	Nov	Dec
2025	-1.1	-1.1	-0.4	0.6	-0.6	-1.5	-1.8	-1.6	-1.7	-1.6	0.0	-1.0
2050	-2.5	-2.8	-1.0	1.0	-2.0	-3.6	-4.4	-4.0	-4.2	-3.5	-1.8	-1.0
2075	-4.3	-5.1	-2.1	0.2	-4.1	-6.0	-7.5	-6.7	-7.2	-5.9	-1.8	-2.0
2100	-6.1	-7.4	-3.7	-1.8	-6.6	-8.1	-10.1	-9.2	-10.0	-8.2	-1.8	-3.0

Year	Ground Water Flow (%)											
	Jan	Feb	Mar	Apr	May	Jun	Jul	Aug	Sep	Oct	Nov	Dec
2025	-7.8	-7.1	-6.1	-6.3	-6.5	-7.0	-10.9	-13.3	-11.0	-9.6	-8.7	-8.0
2050	-12.0	-11.0	-9.6	-9.7	-10.1	-11.1	-16.3	-20.0	-16.7	-14.8	-13.3	-12.3
2075	-14.1	-13.0	-11.5	-11.6	-12.1	-13.2	-18.9	-23.1	-19.4	-17.2	-15.6	-14.5
2100	-15.4	-14.2	-12.8	-12.7	-13.2	-14.6	-20.4	-24.6	-20.8	-18.6	-16.9	-15.8

Year	Evapotranspiration (%)											
	Jan	Feb	Mar	Apr	May	Jun	Jul	Aug	Sep	Oct	Nov	Dec
2025	-1.4	-1.5	-2.0	-1.6	-0.7	-0.3	0.0	0.1	1.1	0.1	-1.3	-1.9
2050	-2.4	-2.6	-3.5	-2.8	-1.3	-0.6	-0.1	0.0	1.7	0.1	-2.3	-3.2
2075	-3.2	-3.4	-4.8	-3.7	-1.6	-0.7	-0.1	0.0	2.0	-0.1	-3.4	-4.4
2100	-4.0	-4.3	-5.9	-4.4	-1.9	-0.9	-0.1	-0.1	2.4	-0.2	-4.3	-5.6

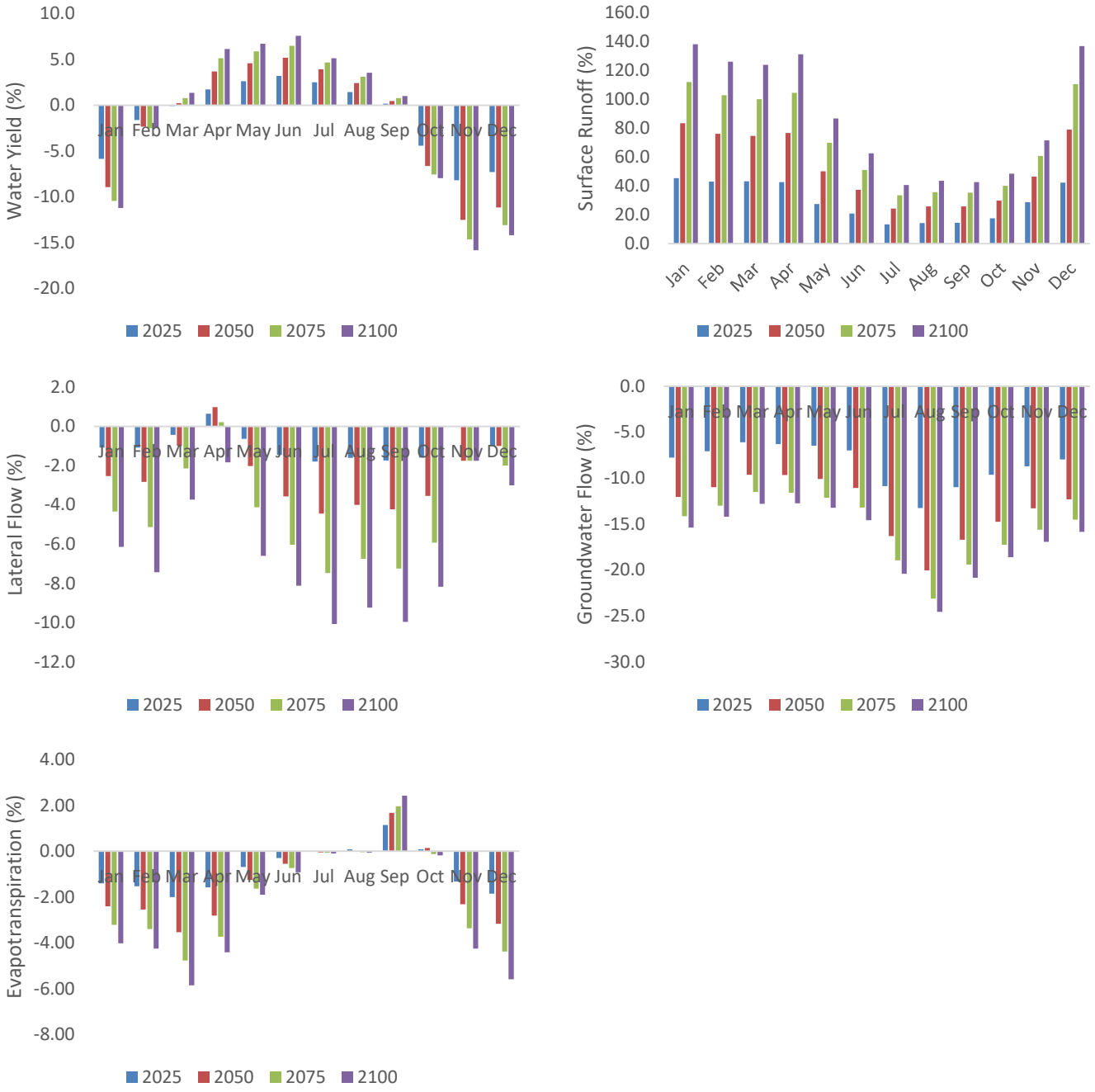

Figure 28: Percentage change in average monthly values for different hydrological parameters for projected LULC (LULC of 2025, 2050, 2075 & 2100) compared with baseline LULC of 2000 A.D

5.5.2. Impact of LULC change on Sediment yield

1. Annual Impact Analysis

The annual impact analysis of LULC change on the sediment yield is evaluated for base year period (LULC 2000) as well as projected time periods (LULC of 2025, 2050, 2075 & 2100) using the validated sediment yield results. The annual sediment yield of the Bagmati watershed was decreased from 5.59 mt/ha for 2000 LULC to 5.03 mt/ha for 2100 LULC with overall decrease of 10% due to land cover changes.

The decrease of sediment yield is likely due to the conversion of agricultural land and forest land into built-up areas. Agricultural areas and barren lands are more susceptible to erosion. The conversion of those land into residential areas casues reduction in erosion process inspite of increase in surface runoff. Table 14, Table 15 and Figure 26 shows the the values of sediment yield for different LULC. The result clearly shows the decreasing trend of sediment yield for all the projected scenarios except for LULC of 2050. This anamoly for 2050 LULC is may be due to increase in core runoff area; also the rate of increase of surface runoff is higher upto this time period which may be the cause of this or may be due to some error as the rate of increase of sediment yield is only 0.9% than that of base year period. The overall decrease of sediment yield for the projected LULC will enhanced the watershed resiliency and therby improving the health of downstream aquatic ecosystems.

2. Seasonal Impact Analysis

The seasonal impact assessment of sediment yield is done similarly to the water balance components. The sediment yield shows the increasing trend for pre-monsoon and post monsoon season for all LULC scenarios. But for monsoon season sediment yield shows the decreasing trend. The higher rate of increase of surface runoff for pre-monsoon and post-monsoon season and lower rate of increase in monsoon season is may be the cause of this result.

Table 19: Seasonal Impacts of LULC change on sediment yield considering baseline data of 2000 A.D LULC

Year	Sediment Yield (T/Ha)		
	S1	S2	S3
2000	0.06	1.28	0.05
2025	0.07	1.26	0.05
2050	0.08	1.28	0.06
2075	0.09	1.21	0.06
2100	0.11	1.10	0.06

Year	Sediment Yield (%)		
	S1	S2	S3
2025	16.7	-2.1	4.0
2050	33.3	0.0	12.0
2075	55.6	-5.7	12.0
2100	83.3	-14.4	24.0

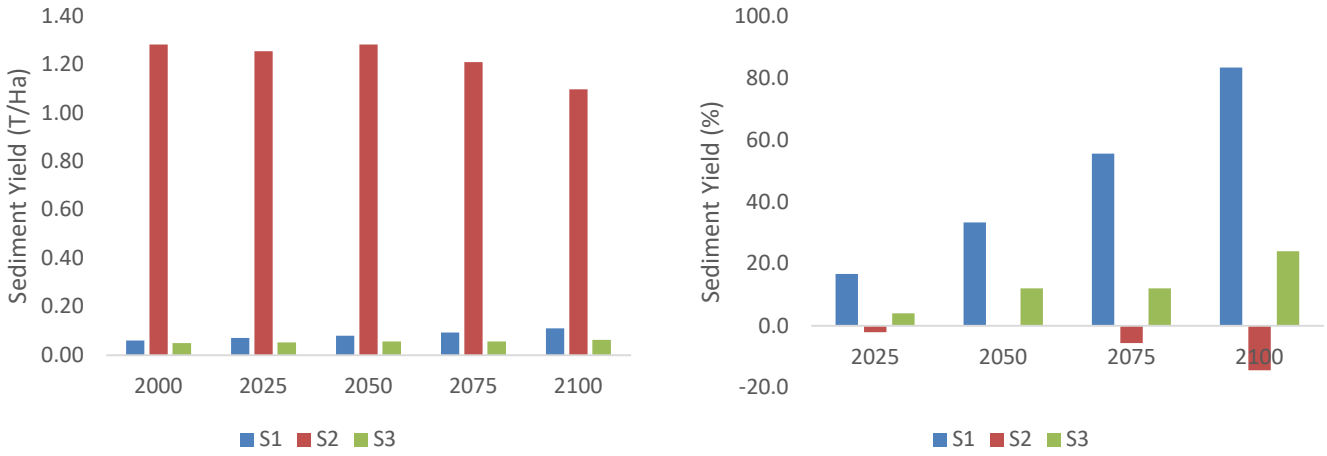

Figure 29: Averge seasonal sediment yield values for different LULC considering baseline LULC of 2000 A.D

3. Monthly Impact Analysis

The average monthly impact assessment of sediment yield for different projected LULC scenarios is shown in Table 20 and Figure 30 below. The sediment yield shows the increasing trend from month of february to may. In this period the agricultural land remains more or less barren and planting started only form may. Also this is the period of pre-monsoon season so the precipitaion in this period may cause the rapid erosion of land. For month of june to october, the sediment yield shows the decreasing trend. In this period the rate of increase of surface runoff is low and the agricultural & forest land remains covered by vegetation. These may be the cause of decresing sediment yield but the sediment yield remains high in this period as this is the period of monsoon season. The month of november and december shows zero sediment yield and also the month of january shows almost zero

sediment yield. These are the driest period and the flow in the river also remains very low. The occurance of precipitation in this period is also low. Because of these reasons the sediment yield is negligible in these months.

Table 20: Monthly impact assessment of LULC change on sediment yield

Year	Sediment Yield (T/Ha/Month)											
	Jan	Feb	Mar	Apr	May	Jun	Jul	Aug	Sep	Oct	Nov	Dec
2000	0	0.03	0.03	0.03	0.12	0.36	1.81	1.76	1.2	0.22	0	0
2025	0.01	0.04	0.05	0.04	0.12	0.35	1.76	1.74	1.17	0.21	0	0
2050	0.01	0.05	0.06	0.05	0.13	0.36	1.79	1.79	1.19	0.22	0	0
2075	0.01	0.06	0.08	0.07	0.13	0.35	1.68	1.7	1.11	0.21	0	0
2100	0.02	0.08	0.11	0.09	0.13	0.33	1.52	1.54	1	0.21	0	0

Year	Sediment Yield (%)											
	Jan	Feb	Mar	Apr	May	Jun	Jul	Aug	Sep	Oct	Nov	Dec
2025	0.0	33.3	66.7	33.3	0.0	-2.8	-2.8	-1.1	-2.5	-4.5	0.0	0.0
2050	0.0	66.7	100.0	66.7	8.3	0.0	-1.1	1.7	-0.8	0.0	0.0	0.0
2075	0.0	100.0	166.7	133.3	8.3	-2.8	-7.2	-3.4	-7.5	-4.5	0.0	0.0
2100	0.0	166.7	266.7	200.0	8.3	-8.3	-16.0	-12.5	-16.7	-4.5	0.0	0.0

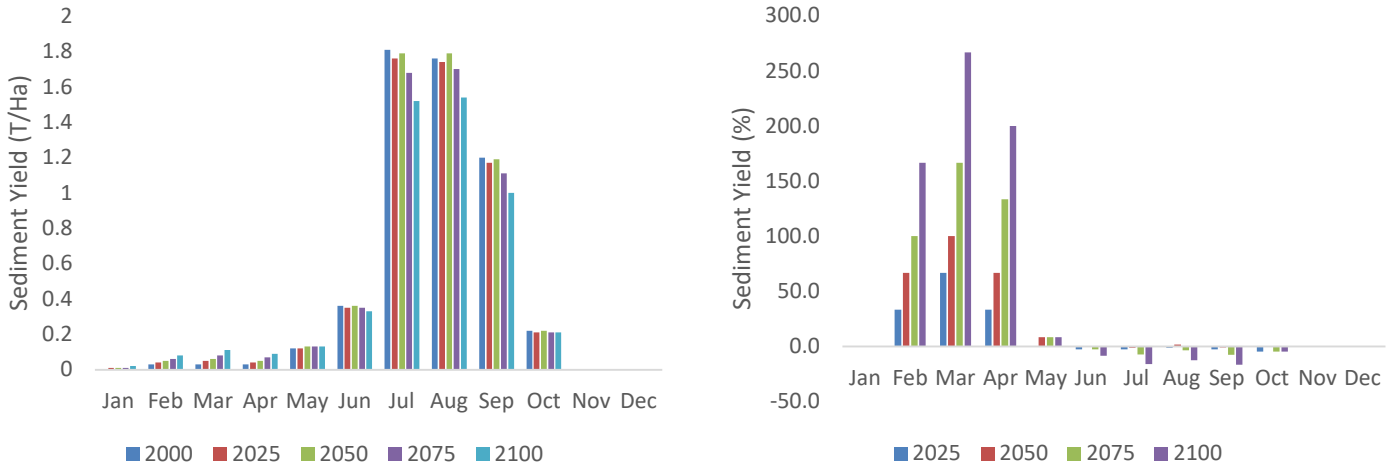

Figure 30: Average monthly sediment yield values for different LULC

5.6. **Practical Implications of the Results**

The impact analysis for all the LULC change scenarios shows the negative impacts of urbanization of KV in the natural hydrological processes of the Bagmati river. The result from this study resonates similarly to the various studies conducted in this river before as explained in the literature reviw section.

The central core area of KV covers highly dense built up area where there is no space available for further development. So the builtup are is rapidly increasing towards the outer periferi of the KV. The patches of forest areas in the central parts have been completely destroyed; only remaining were the forest of religious importance. The presence of Shivapuri Nagarjun National parks in hills surrounding the valley somehow keeps the forest areas safe from deforestation. This will keep the forest area more or less constant in the future and protect them from conversion to built-up area. However some community forest areas are still seeing deforestation, so proper awareness and protection will be necessary.

The areas of water body of the valley seems to remain more or less constant from the analysis. But the encroachment of the rivers and the increase of impervious surfaces due to urbanization have been casusing serious flooding events and will continue to cause such problems if the necessary steps is not taken now. The high intensity of even very short duration rainfall seems to cause flooding events in the low lying areas of the valley. To prevent this, the encroachment of the river should be controlled and the construction of high embankments which has been going on should be further extended to the upper parts of the tributaries of the Bagmati river also.

The increase of impervious surfaces due to rapid rate of urbanization have been causing serious problems in the groundwater flows. The insufficient water supply in the valley, reduction of recharge areas and the dependance to groundwater for drinking water will further accelerates the depletion of groundwater table. So the Bagmati river will experience very low flow during the dry seasons and flash floods during monsoon seasons. This will further complicates the hydrology of the basin. So the developement of proper watershed management strategies and its implementation should be the priority of the decision makers and is highly recommended.

Chapter 6: Conclusions

In this study, the impacts of LULC change on discharge and sediment yield of the Bagmati watershed in the Kathmandu valley was explored which is under stress due to rapid increase of urbanization. The SUFI-2 algorithm of SWAT-CUP was used for the calibration and validation of the SWAT model in a monthly time step at Khokana station. Freely available datasets and information were used for the model setup as well as model calibration and validation runs. Parameters for the model calibration and validation were selected based on the literature review, preliminary sensitivity analysis, study area conditions and their known role on hydrologic processes. Global sensitivity analysis was performed with 2000 iterations to finalized the parameters for the model. The Manning's roughness coefficient for the main channel (CH N2), soil evaporation compensation factor (ESCO) and saturated hydraulic conductivity (SOL-K) were the three most sensitive parameters influencing the discharge. Similarly, linear parameter (SPCON) & exponent parameter (SPEXP) for calculating the maximum amount of sediment that can be re-entrained during channel sediment routing followed by channel erodibility factor (CH-ERODMO) were the three most sensitive parameters influencing the sediment yield.

The statistical parameters for both calibration and validation of Discharge and Sediment flow shows the reasonable results for the parameters selected for the analysis. For both calibration and validation all the statistical parameters shows the accuracy of above 70%. The performance rating during calibration period for discharge is very good and that for sediment flow is good. Similarly, the performance rating during validation period for both discharge and sediment flow is good. Overall, the model shows good agreement between observed and simulated discharge & sediment values.

Projection of LULC is done using CA Markov model to assess the impact of LULC change in the Bagmati basin of Kathmandu valley. First the LULC is projected for 2010 A.D using 1990 and 2000 A.D LULC map from ICIMOD which is validated with LULC map of ICIMOD for 2010 A.D. The accuracy assessement of the projected LULC is done by Error Matrix analysis using IDRISI image processing model. The overall Kappa Index of agreement gives 73 % accuracy. Then the LULC of 2025, 2050, 2075 and 2100 A.D is projected by assigning different driver variables. The LULC change analysis shows the rapid rate of urbanization in the Kathmandu valley

with increase of 186.709 sq.km (30.3%) from 2000 A.D to 2100 A.D. All the other landuse classes shows the decreasing trend especially agricultural area.

The impact of LULC change is evaluated for annual, seasonal and monthly time scale. The impact of LULC change for annual time scale shows the increasing trend of surface runoff and decreasing trend of lateral flow, groundwater flow & evapotranspiration, which may be the result of conversion of landuse from agricultural and forest land to built-up area resulting in increase of impervious surfaces. The overall water yield also shows the increasing trend but the rate of increase is very small. The water yield, surface runoff, lateral flow, groundwater flow and evapotranspiration is expected to change by +1.1 %, +48 %, -9 %, -17.7 % and -1.2 % respectively from 2000 to 2100 A.D. The sediment yield also shows the decreasing trend which changes by -10 % from 2000 to 2100 A.D. The decreasing trend of sediment yield is may be due to the extensive conversion of agricultural land into residential areas.

The impact of LULC change on seasonal time scale shows the inceasing trend of river dishcarge for pre-monsoon and monsoon season and decreasing trend for post-monsoon season. This indicate the possibility of occurance of flooding in wet season and very low flow in dry season. Other water balance components like surface runoff shows the increasing trend for all seasons while lateral flow and groudwater flow shows the decreasing trend. The sediment yield shows the increasing trend for pre-monsoon and post monsoon season for all LULC scenarios. But for monsoon season sediment yield shows the decreasing trend. Evapotranspiration shows very small changes for all seasons and for all LULC scenarios.

The analysis for monthly time scale for all the projected LULC shows the similar trend. Overall the wetter month flows will be in increasing trends and dry flows will be in decreasing trend with corresponding increase in surface flow and reduction in sub-surface flows.

In the future the pressure for land use change seems to grow more rapidly in the Kathmandu valley. So the evaluation of its impact and implementation of sustainable land & water management practices are recommended and should be integrated in the decision making. Major findings of this study can be very useful for future policy making process

Future scope of the study is to incorporate projected climate data for future dynamics of the overall hydrology of the basin.

REFERENCES

Abbaspour, K. C., Johnson, C. A., & van Genuchten, M. T. (2004). Estimating Uncertain Flow and Transport Parameters Using a Sequential Uncertainty Fitting Procedure. *Vadose Zone Journal*, *3*(4), 1340–1352. https://doi.org/10.2136/vzj2004.1340

Abbaspour, Karim C. (2015). SWAT-CUP: SWAT Calibration and Uncertainty Programs - A User Manual. In *Eawag: Swiss Federal Institute of Aquatic Science and Technology*. https://swat.tamu.edu/media/114860/usermanual_swatcup.pdf

Aghsaei, H., Mobarghaee Dinan, N., Moridi, A., Asadolahi, Z., Delavar, M., Fohrer, N., & Wagner, P. D. (2020). Effects of dynamic land use/land cover change on water resources and sediment yield in the Anzali wetland catchment, Gilan, Iran. *Science of the Total Environment*, *712*. https://doi.org/10.1016/j.scitotenv.2019.136449

Ampomah, R., Hosseiny, H., Zhang, L., Smith, V., & Sample-Lord, K. (2020). A regression-based prediction model of suspended sediment yield in the Cuyahoga river in Ohio using historical satellite images and precipitation data. *Water (Switzerland)*, *12*(3). https://doi.org/10.3390/w12030881

Arnold, J. G., & Fohrer, N. (2005). SWAT2000: Current capabilities and research opportunities in applied watershed modelling. *Hydrological Processes*, *19*(3), 563–572. https://doi.org/10.1002/hyp.5611

Arnold, J. G., Kiniry, J. R., Srinivasan, R., Williams, J. R., Haney, E. B., & Neitsch, S. L. (2012). *Input/Output Documentation Soil & Water Assessment Tool*. 1–650.

Aryal, A., Shrestha, S., & Babel, M. S. (2019). Quantifying the sources of uncertainty in an ensemble of hydrological climate-impact projections. *Theoretical and Applied Climatology*, *135*(1–2), 193–209. https://doi.org/10.1007/s00704-017-2359-3

Bocquier, P. (2005). World urbanization prospects: An alternative to the UN model of projection compatible with the mobility transition theory. *Demographic Research*, *12*, 197–236. https://doi.org/10.4054/DemRes.2005.12.9

Briak, H., Moussadek, R., Aboumaria, K., & Mrabet, R. (2016). Assessing sediment yield in Kalaya gauged watershed (Northern Morocco) using GIS and SWAT model. *International*

Soil and Water Conservation Research, *4*(3), 177–185. https://doi.org/10.1016/j.iswcr.2016.08.002

Chaplot, V. (2005). Impact of DEM mesh size and soil map scale on SWAT runoff, sediment, and NO3-N loads predictions. *Journal of Hydrology*, *312*(1–4), 207–222. https://doi.org/10.1016/j.jhydrol.2005.02.017

Choto, M., & Fetene, A. (2019). Impacts of land use/land cover change on stream flow and sediment yield of Gojeb watershed, Omo-Gibe basin, Ethiopia. *Remote Sensing Applications: Society and Environment*, *14*(January), 84–99. https://doi.org/10.1016/j.rsase.2019.01.003

Costa, M. H., Botta, A., & Cardille, J. A. (2003). Effects of large-scale changes in land cover on the discharge of the Tocantins River, Southeastern Amazonia. *Journal of Hydrology*, *283*(1–4), 206–217. https://doi.org/10.1016/S0022-1694(03)00267-1

D. K. Borah, M. Bera, & S. Shaw. (2003). WATER, SEDIMENT, NUTRIENT, AND PESTICIDE MEASUREMENTS IN AN AGRICULTURAL WATERSHED IN ILLINOIS DURING STORM EVENTS. *Transactions of the ASAE*, *46*(3). https://doi.org/10.13031/2013.13601

D. N. Moriasi, J. G. Arnold, M. W. Van Liew, R. L. Bingner, R. D. Harmel, T. L. V., & ABSTRACT. (2007). MODEL EVALUATION GUIDELINES FOR SYSTEMATIC QUANTIFICATION OF ACCURACY IN WATERSHED SIMULATIONS. *Soil & Water Division of ASABE*, *39*(3), 227–234. https://doi.org/doi: 10.13031/2013.23153

Easton, Z. M., Fuka, D. R., White, E. D., Collick, A. S., Biruk Ashagre, B., McCartney, M., Awulachew, S. B., Ahmed, A. A., & Steenhuis, T. S. (2010). A multi basin SWAT model analysis of runoff and sedimentation in the Blue Nile, Ethiopia. *Hydrology and Earth System Sciences*, *14*(10), 1827–1841. https://doi.org/10.5194/hess-14-1827-2010

Getachew, B., Manjunatha, B. R., & Bhat, H. G. (2021). Modeling projected impacts of climate and land use/land cover changes on hydrological responses in the Lake Tana Basin, upper Blue Nile River Basin, Ethiopia. *Journal of Hydrology*, *595*(January), 125974. https://doi.org/10.1016/j.jhydrol.2021.125974

Gomes, M., & de Magalhaes, L. P. C. (2010). Urban Flood Control, Simulation and Management - an Integrated Approach. *Federal University of Rio de Janeiro (UFRJ)*. https://doi.org/10.5772/9574

ICIMOD. (2013). *Land cover of Nepal 2010*. 1–2. http://apps.geoportal.icimod.org/ArcGIS/rest/services/Nepal/Landcover2010/MapServer/0

J Ronald, E. (2020). *Manual: TerraSet 2020: Geospatial Monitoring and Modeling System*. www.clarklabs.org clarklabs@clarku.edu. www.clarklabs.org

Jokar Arsanjani, J., Helbich, M., Bakillah, M., Hagenauer, J., & Zipf, A. (2013). Toward mapping land-use patterns from volunteered geographic information. *International Journal of Geographical Information Science*, *27*(12), 2264–2278. https://doi.org/10.1080/13658816.2013.800871

Kashaigili, J. J. (2008). Impacts of land-use and land-cover changes on flow regimes of the Usangu wetland and the Great Ruaha River, Tanzania. *Physics and Chemistry of the Earth*, *33*(8–13), 640–647. https://doi.org/10.1016/j.pce.2008.06.014

Khalid, K., Ali, M. F., Rahman, N. F. A., Mispan, M. R., Haron, S. H., Othman, Z., & Bachok, M. F. (2016). Sensitivity Analysis in Watershed Model Using SUFI-2 Algorithm. *Procedia Engineering*, *162*, 441–447. https://doi.org/10.1016/j.proeng.2016.11.086

Lamichhane, S., & Shakya, N. M. (2019a). Alteration of groundwater recharge areas due to land use/cover change in Kathmandu Valley, Nepal. *Journal of Hydrology: Regional Studies*, *26*(November 2019), 100635. https://doi.org/10.1016/j.ejrh.2019.100635

Lamichhane, S., & Shakya, N. M. (2019b). Integrated assessment of climate change and land use change impacts on hydrology in the Kathmandu Valley watershed, Central Nepal. *Water (Switzerland)*, *11*(10). https://doi.org/10.3390/w11102059

Lamichhane, S., & Shakya, N. M. (2020). Shallow aquifer groundwater dynamics due to land use/cover change in highly urbanized basin: The case of Kathmandu Valley. *Journal of Hydrology: Regional Studies*, *30*(March), 100707. https://doi.org/10.1016/j.ejrh.2020.100707

Legesse, D., Vallet-Coulomb, C., & Gasse, F. (2003). Hydrological response of a catchment to climate and land use changes in Tropical Africa: Case study south central Ethiopia. *Journal of Hydrology*, *275*(1–2), 67–85. https://doi.org/10.1016/S0022-1694(03)00019-2

Li, Z., Liu, W., Zhang, X., & Zheng, F. (2009a). Impacts of land use change and climate variability

on hydrology in an agricultural catchment on the Loess Plateau of China. *Journal of Hydrology*, *377*(1–2), 35–42. https://doi.org/10.1016/j.jhydrol.2009.08.007

Li, Z., Liu, W. zhao, Zhang, X. chang, & Zheng, F. li. (2009b). Impacts of land use change and climate variability on hydrology in an agricultural catchment on the Loess Plateau of China. *Journal of Hydrology*, *377*(1–2), 35–42. https://doi.org/10.1016/J.JHYDROL.2009.08.007

M.B. Abbott , J.C. Bathurst, J.A. Cunge, P. E. O. and J. R. (1986). AN INTRODUCTION TO THE E U R O P E A N HYDROLOGICAL SYSTEM - - SYSTEME HYDROLOGIQUE E U R O P E E N , " SHE ", 2 : MODELLING SYSTEM The Syst ~ me Hydrologique Europ ~ en , or European Hydrological System (SHE), is an advanced , physically-based , distri. *Journal of Hydrology*, *87*, 61–77.

Manandhar, R., Odehi, I. O. A., & Ancevt, T. (2009). Improving the accuracy of land use and land cover classification of landsat data using post-classification enhancement. *Remote Sensing*, *1*(3), 330–344. https://doi.org/10.3390/rs1030330

Moradkhani, H., & Sorooshian, S. (2008). General Review of Rainfall-Runoff Modeling: Model Calibration, Data Assimilation, and Uncertainty Analysis. *Hydrological Modelling and the Water Cycle*, 1–24. https://doi.org/10.1007/978-3-540-77843-1_1

Naikoo, M. W., Rihan, M., Ishtiaque, M., & Shahfahad. (2020). Analyses of land use land cover (LULC) change and built-up expansion in the suburb of a metropolitan city: Spatio-temporal analysis of Delhi NCR using landsat datasets. *Journal of Urban Management*, *9*(3), 347–359. https://doi.org/10.1016/j.jum.2020.05.004

Ndulue, E. L., Mbajiorgu, C. C., Ugwu, S. N., Ogwo, V., & Ogbu, K. N. (2015). Assessment of land use/cover impacts on runoff and sediment yield using hydrologic models: A review. In *Journal of Ecology and The Natural Environment* (Vol. 7, Issue 2). https://doi.org/10.5897/jene2014.0482

Nyatuame, M., Amekudzi, L. K., & Agodzo, S. K. (2020). Assessing the land use/land cover and climate change impact on water balance on Tordzie watershed. *Remote Sensing Applications: Society and Environment*, *20*(March), 100381. https://doi.org/10.1016/j.rsase.2020.100381

P. W. Gassman, M. R. Reyes, C. H. Green, & J. G. Arnold. (2007). The Soil and Water Assessment Tool: Historical Development, Applications, and Future Research Directions. *Transactions*

of the ASABE, *50*(4), 1211–1250. https://doi.org/10.13031/2013.23637

Peng, S., Wang, C., Eguchi, S., Kuramochi, K., Kohyama, K., Yoshikawa, S., Itahashi, S., Igura, M., Ohkoshi, S., & Hatano, R. (2021). Response of hydrological processes to climate and land use changes in Hiso River watershed, Fukushima, Japan. *Physics and Chemistry of the Earth*, *123*(February), 103010. https://doi.org/10.1016/j.pce.2021.103010

Pokhrel, B. K. (2018). Impact of land use change on flow and sediment yields in the Khokana outlet of the Bagmati River, Kathmandu, Nepal. *Hydrology*, *5*(2). https://doi.org/10.3390/hydrology5020022

Quyen, N. T. N., Liem, N. D., & Loi, N. K. (2014). Effect of land use change on water discharge in Srepok watershed, Central Highland, Viet Nam. *International Soil and Water Conservation Research*, *2*(3), 74–86. https://doi.org/10.1016/S2095-6339(15)30025-3

Rahman, M. S., Mohiuddin, H., Kafy, A. Al, Sheel, P. K., & Di, L. (2019). Classification of cities in Bangladesh based on remote sensing derived spatial characteristics. *Journal of Urban Management*, *8*(2), 206–224. https://doi.org/10.1016/j.jum.2018.12.001

Santos, J. Y. G. dos, Montenegro, S. M. G. L., Silva, R. M. da, Santos, C. A. G., Quinn, N. W., Dantas, A. P. X., & Ribeiro Neto, A. (2021). Modeling the impacts of future LULC and climate change on runoff and sediment yield in a strategic basin in the Caatinga/Atlantic forest ecotone of Brazil. *Catena*, *203*(March). https://doi.org/10.1016/j.catena.2021.105308

Sharma, R. H., & Shakya, N. M. (2006). Hydrological changes and its impact on water resources of Bagmati watershed, Nepal. *Journal of Hydrology*, *327*(3–4), 315–322. https://doi.org/10.1016/J.JHYDROL.2005.11.051

Shrestha, S., Shrestha, M., & Babel, M. S. (2016). Modelling the potential impacts of climate change on hydrology and water resources in the Indrawati River Basin, Nepal. *Environmental Earth Sciences*, *75*(4), 1–13. https://doi.org/10.1007/s12665-015-5150-8

Singh, L., & Saravanan, S. (2020). Simulation of monthly streamflow using the SWAT model of the Ib River watershed, India. *HydroResearch*, *3*, 95–105. https://doi.org/10.1016/j.hydres.2020.09.001

Tang, F. F., Xu, H. S., & Xu, Z. X. (2012). Model calibration and uncertainty analysis for runoff

in the Chao River Basin using sequential uncertainty fitting. *Procedia Environmental Sciences*, *13*(2011), 1760–1770. https://doi.org/10.1016/j.proenv.2012.01.170

Thapa, B. R., Ishidaira, H., Pandey, V. P., & Shakya, N. M. (2017). A multi-model approach for analyzing water balance dynamics in Kathmandu Valley, Nepal. *Journal of Hydrology: Regional Studies*, *9*, 149–162. https://doi.org/10.1016/j.ejrh.2016.12.080

Thapa, R. B., & Murayama, Y. (2010). Drivers of urban growth in the Kathmandu valley, Nepal: Examining the efficacy of the analytic hierarchy process. *Applied Geography*, *30*(1), 70–83. https://doi.org/10.1016/j.apgeog.2009.10.002

Tufa, D. F., Abbulu, Y., & Srinivasarao, G. V. R. (2014). Watershed Hydrological Response To Changes in Land Use / Land Covers Patterns of River Basin : a Review. *International Journal of Civil, Structural, Environmental and Infrastructure Engineering Research and Development (IJCSEIERD)*, *4*(2), 157–170.

Zhang, H., Wang, B., Liu, D. L., Zhang, M., Leslie, L. M., & Yu, Q. (2020). Using an improved SWAT model to simulate hydrological responses to land use change: A case study of a catchment in tropical Australia. *Journal of Hydrology*, *585*(February), 124822. https://doi.org/10.1016/j.jhydrol.2020.124822

ANNEXES

Annex 1: Rain Gauge Stations used for the Study Area

S.N	Rain Gauge Station		District	Coordinates	
	Station no.	Station Name		Latitude	Departure
1	PPT_1082	Nangkhel	Bhaktapur	$27^0$39’	$85^0$28’
2	PPT_1081	Jetpurphedi	Kathmandu	$27^0$47’	$85^0$17’
3	PPT_1080	Tikathali	Lalitpur	$27^0$39’	$85^0$21’
4	PPT_1079	Nagarjun	Kathmandu	$27^0$45’	$85^0$15’
5	PPT_1077	Sundarijal	Kathmandu	$27^0$45’	$85^0$25’
6	PPT_1076	Naikap	Kathmandu	$27^0$41’	$85^0$15’
7	PPT_1075	Lele	Lalitpur	$27^0$35’	$85^0$17’
8	PPT_1074	Sundarijal	Kathmandu	$27^0$46’	$85^0$25’
9	PPT_1073	Khokana	Lalitpur	$27^0$38’	$85^0$17’
10	PPT_1060	Chapa Gaun	Lalitpur	$27^0$36’	$85^0$20’
11	PPT_1059	Changu Narayan	Bhaktapur	$27^0$42’	$85^0$25’
12	PPT_1052	Bhaktapur	Bhaktapur	$27^0$40’	$85^0$25’
13	PPT_1049	Khopasi	Panauti	$27^0$35’	$85^0$31’
14	PPT_1043	Nagarkot	Bhaktapur	$27^0$42’	$85^0$31’
15	PPT_1039	Panipokhari	Kathmandu	$27^0$44’	$85^0$20’
16	PPT_1035	Sankhu	Kathmandu	$27^0$45’	$85^0$29’
17	PPT_1030	Kathmandu Airport	Kathmandu	$27^0$42’	$85^0$22’
18	PPT_1029	Khumaltar	Lalitpur	$27^0$40’	$85^0$20’
19	PPT_1022	Godavari	Lalitpur	$27^0$35’	$85^0$24’
20	PPT_1015	Thankot	Kathmandu	$27^0$41’	$85^0$12’
21	PPT_1007	Kakani	Nuwakot	$27^0$48’	$85^0$15’

Annex 2: Metereological Stations used for the Study Area

S.N	Meteorological Station		District	Coordinates	
	Station no.	Station Name		Latitude	Departure
1	1007	Kakani	Nuwakot	$27^0$48’	$85^0$15’
2	1022	Godavari	Lalitpur	$27^0$35’	$85^0$24’
3	1029	Khumaltar	Lalitpur	$27^0$40’	$85^0$20’
4	1030	Kathmandu Airport	Kathmandu	$27^0$42’	$85^0$22’
5	1039	Panipokhari	Kathmandu	$27^0$44’	$85^0$20’
6	1043	Nagarkot	Bhaktapur	$27^0$42’	$85^0$31’
7	1073	Khokana	Lalitpur	$27^0$38’	$85^0$17’

Annex 3: Precipitation Stations used for the Study Area with weighted average value

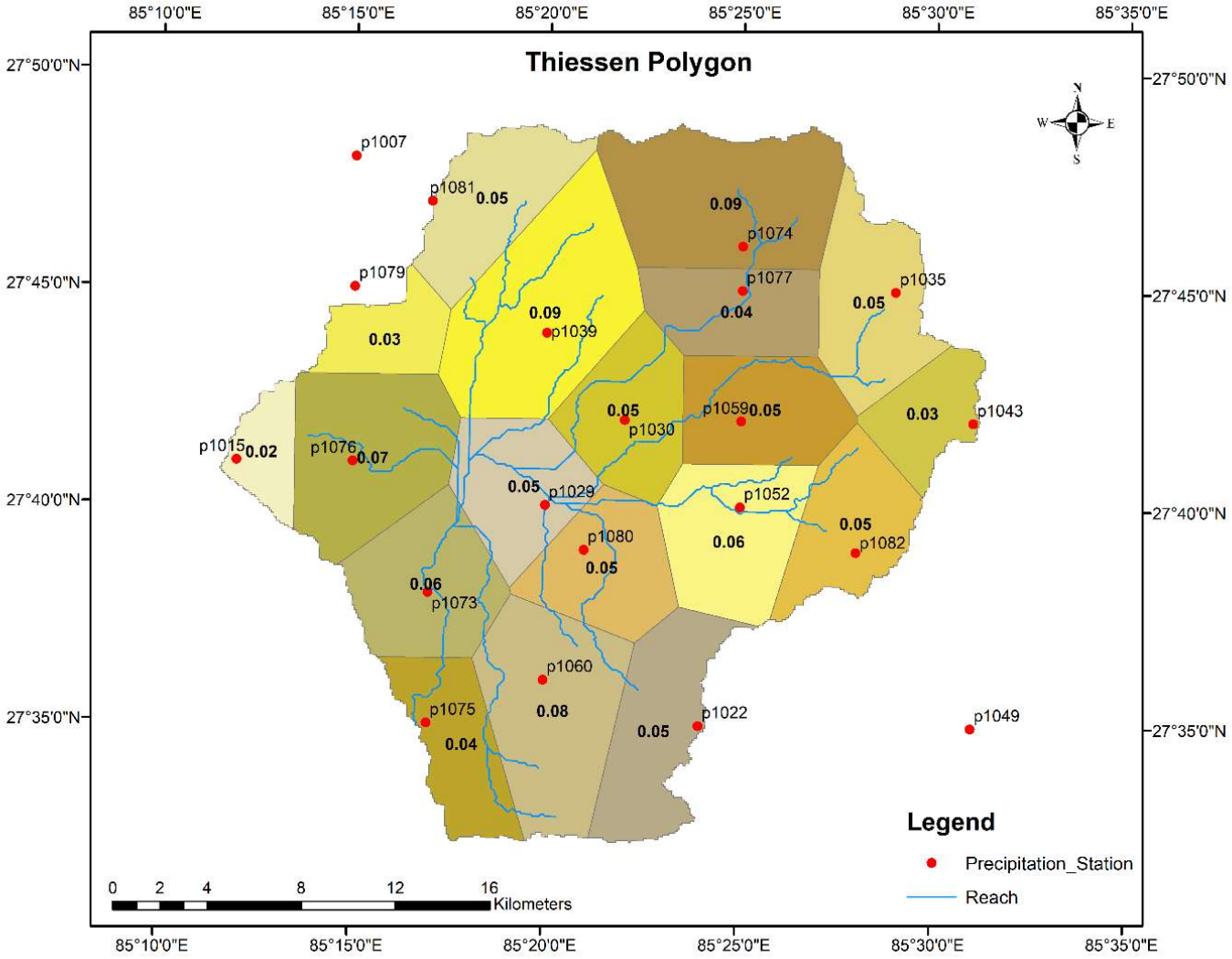

Annex 4: Transition Potential Maps for LULC Projection

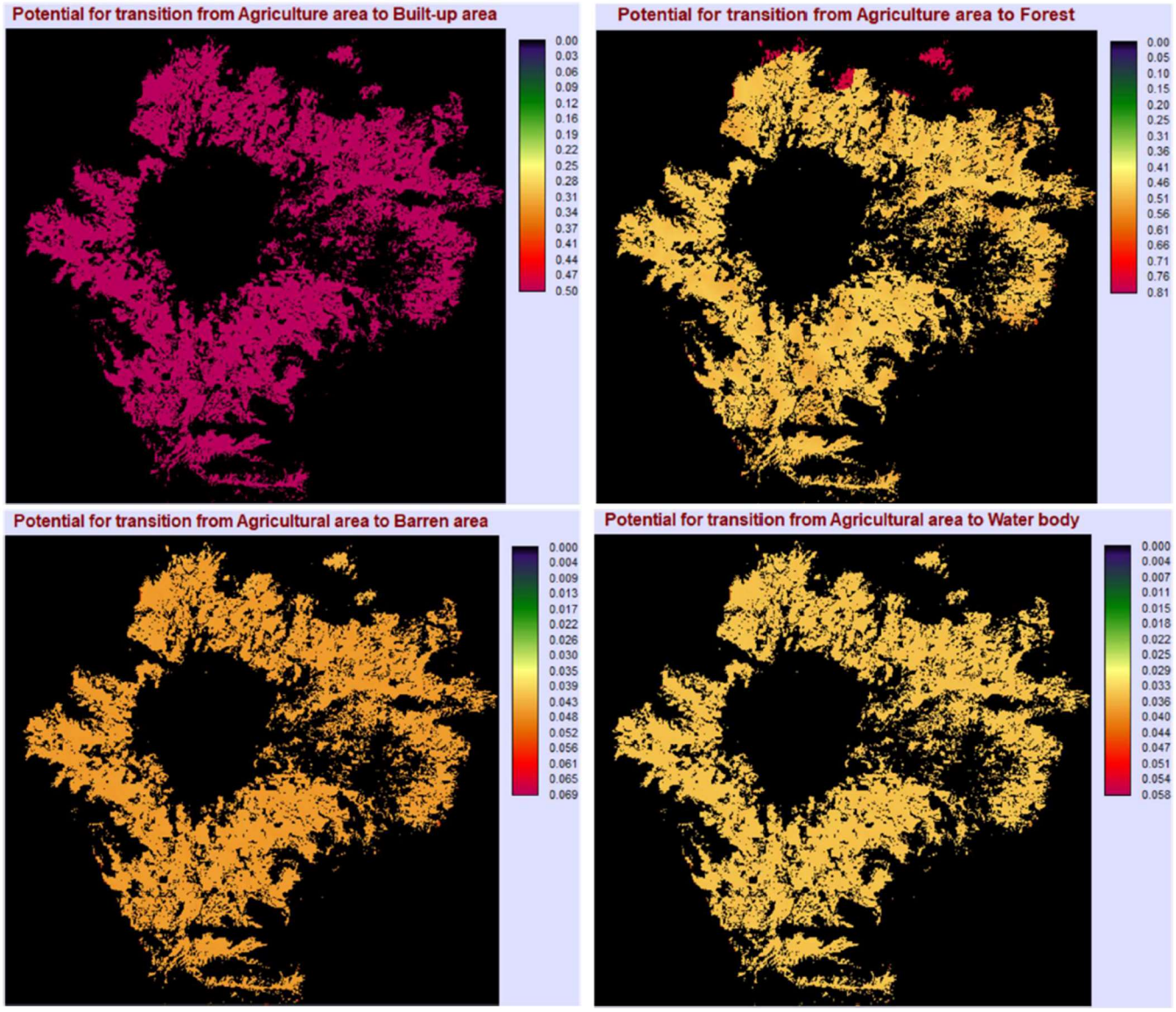

Figure 31: Transition Potential Maps for Agriculture area

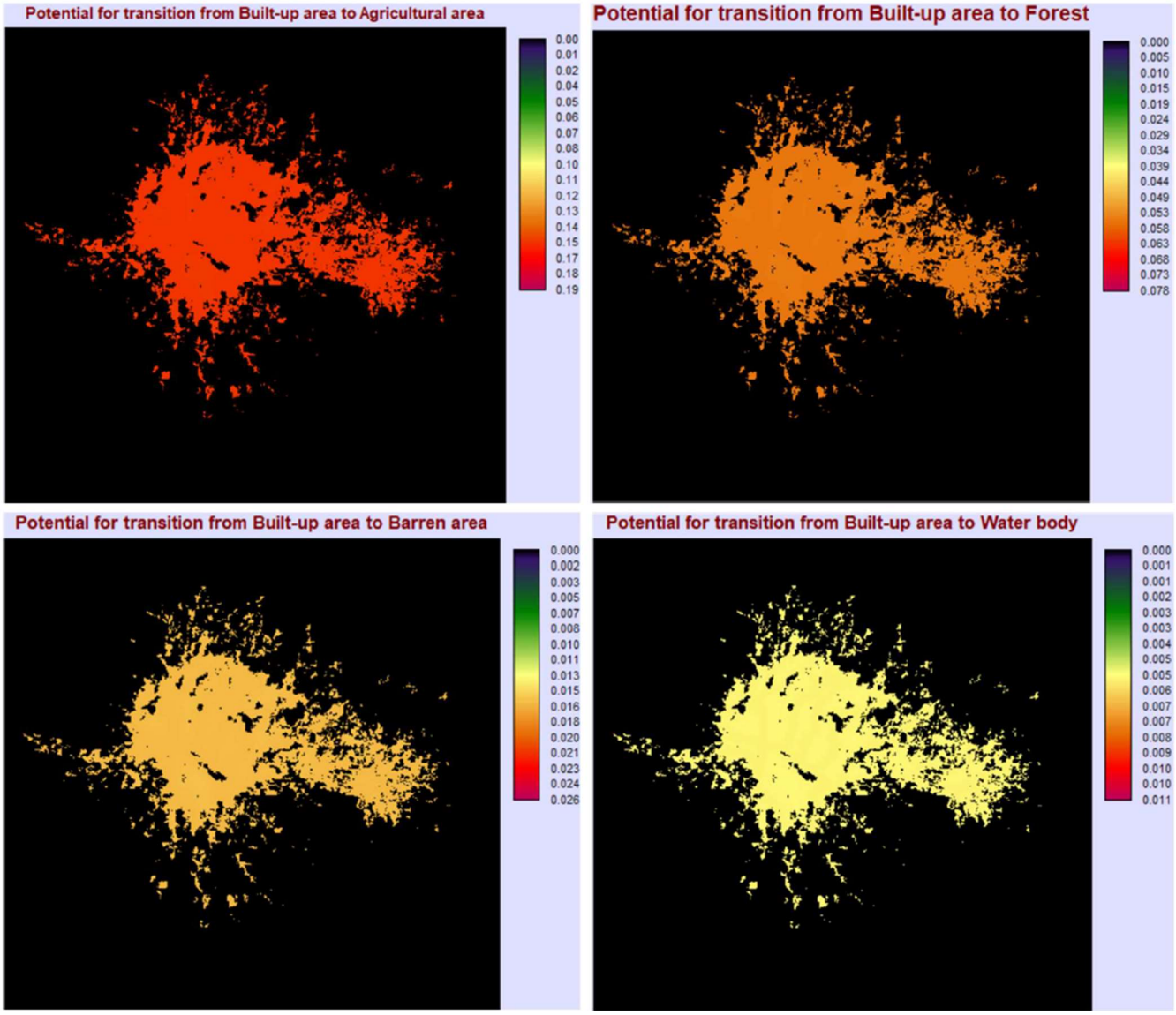

Figure 32: Transition Potential Maps for Built-up area

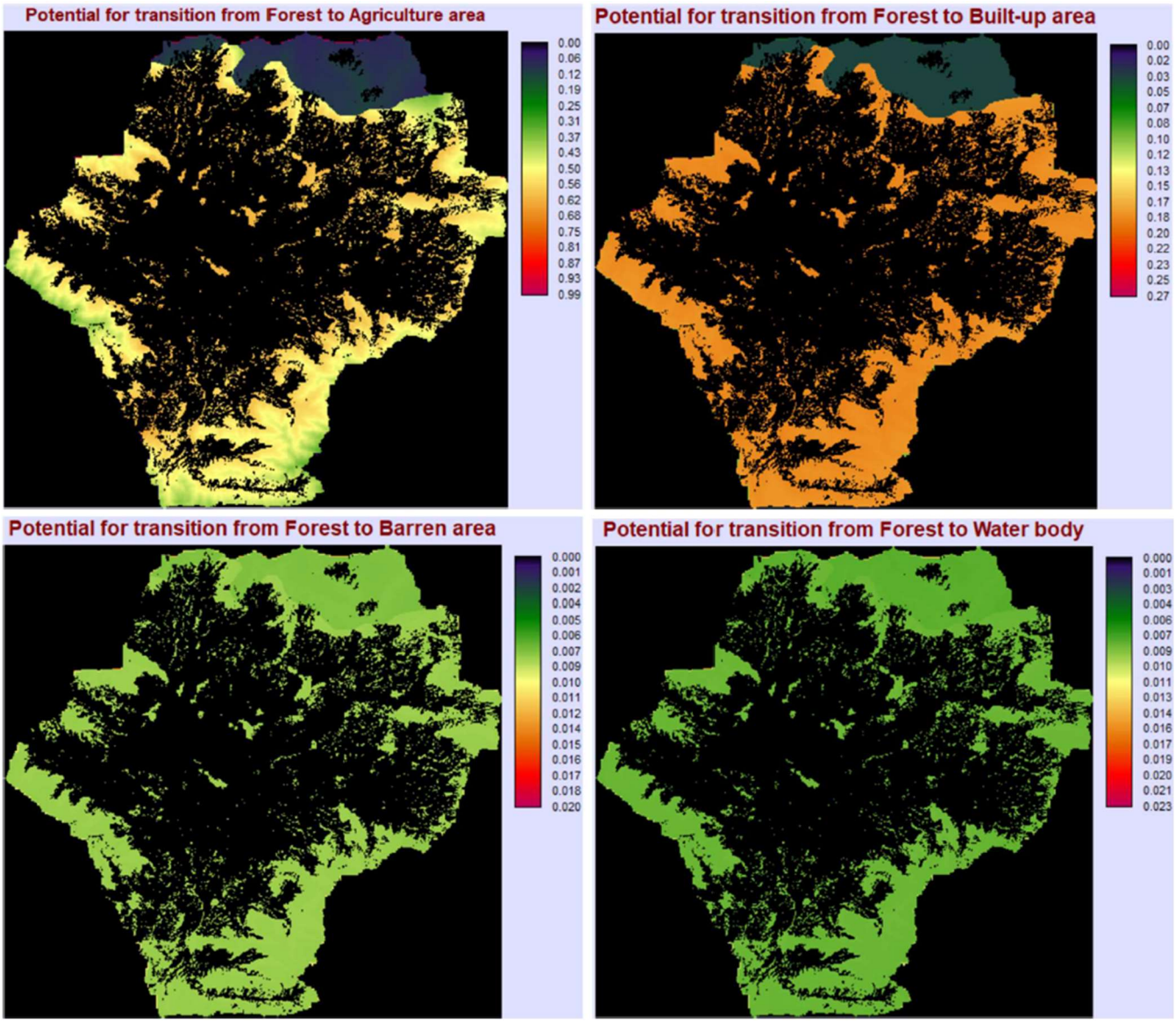

Figure 33: Transition Potential Maps for Forest Area

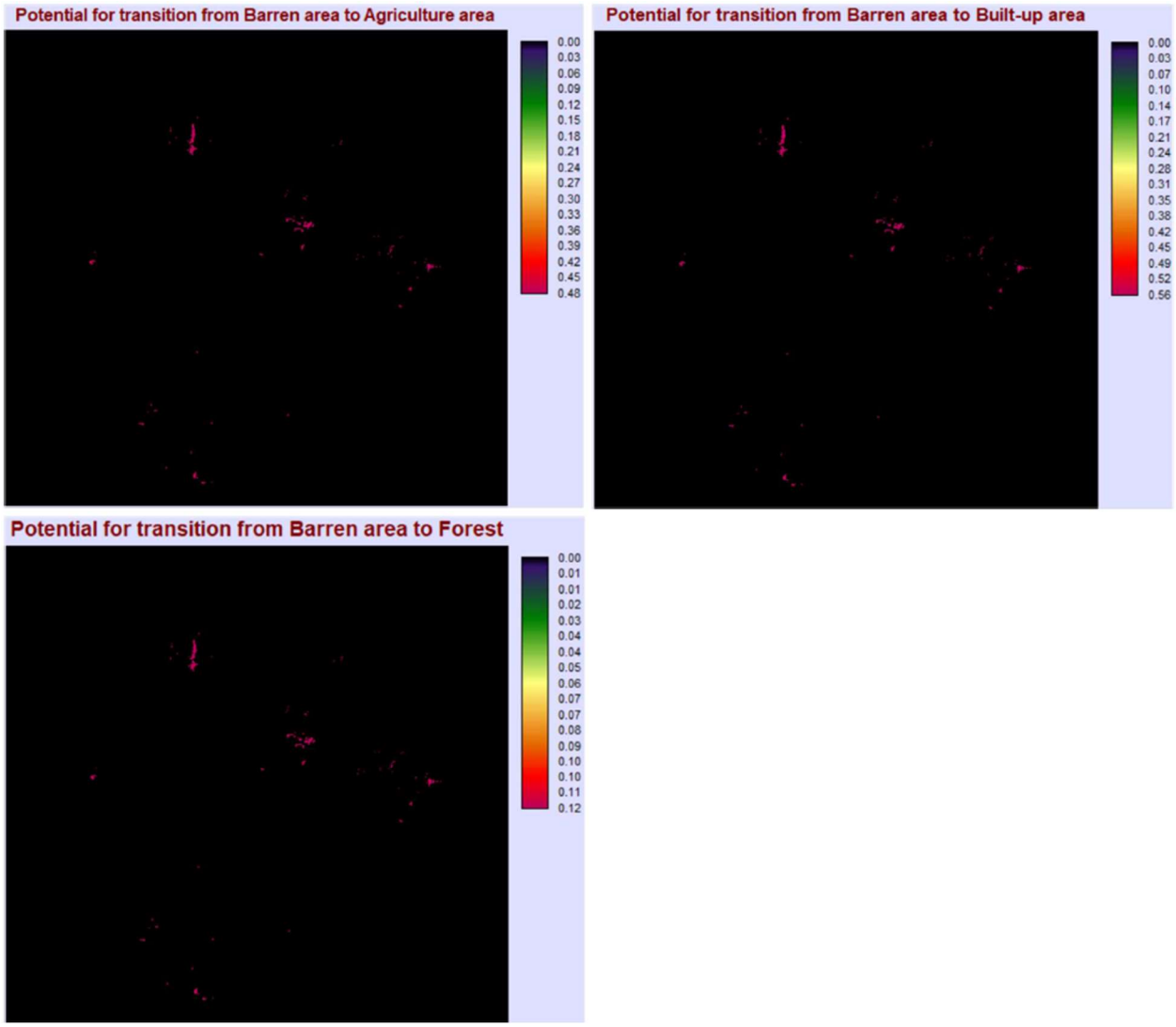

Figure 34: Transition Potential Maps for Barren area

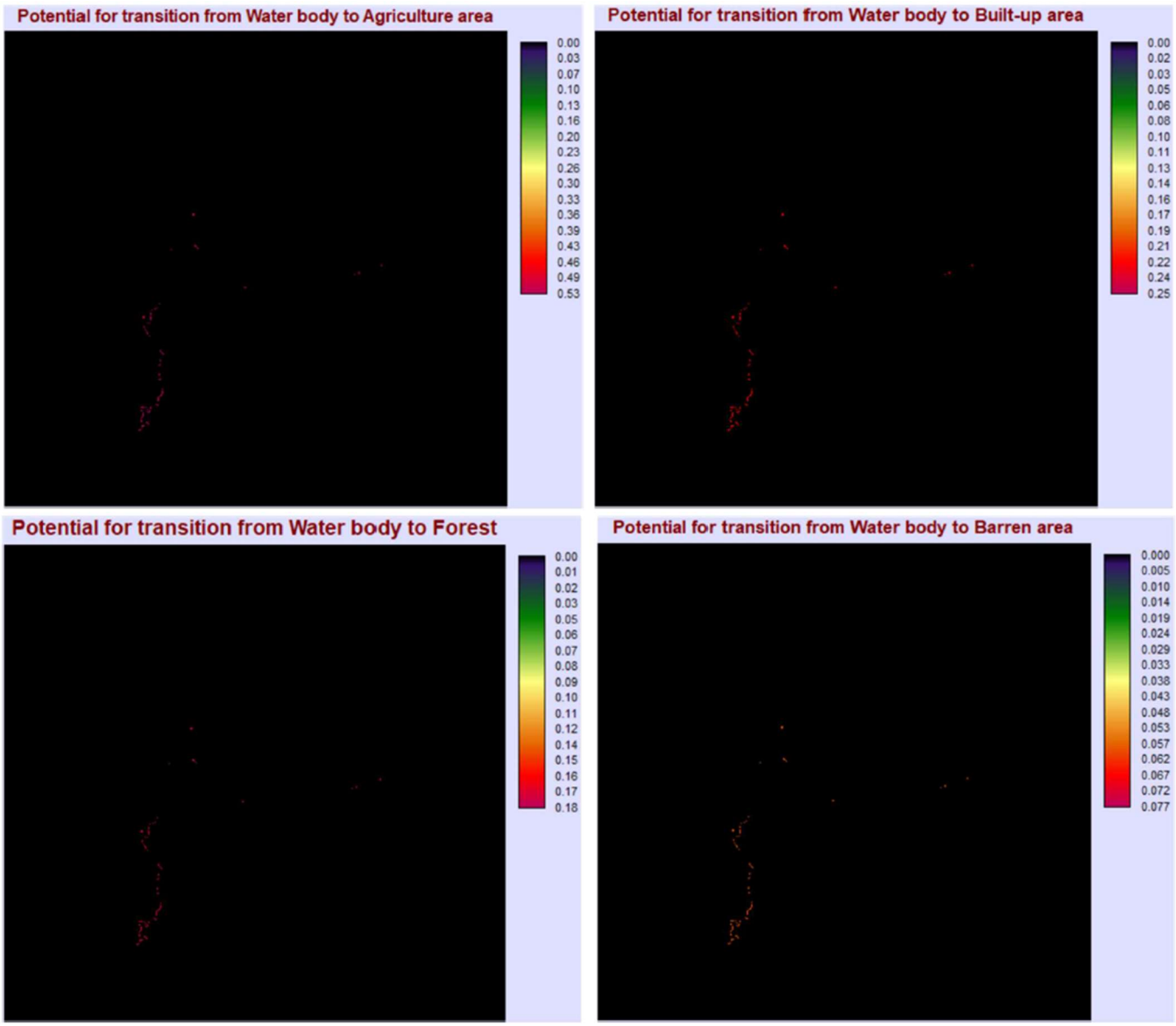

Figure 35: Transition Potential Maps for Water Body

Annex 5: Error Matrix Analysis

Error Matrix Analysis of LULC_2010_NEW (columns : truth) against LANDCOV_PREDICT_2010

	1	2	3	4	5	Total	ErrorC
1	198541	35959	28887	719	24	**264130**	**0.248321**
2	26034	150889	1125	62	0	**178110**	**0.152833**
3	23485	2947	209150	310	45	**235937**	**0.113535**
4	134	1274	19	290	2	**1719**	**0.831297**
5	353	161	7	0	58	**579**	**0.899827**
Total	**248547**	**191230**	**239188**	**1381**	**129**	**680475**	
Error0	**0.201193**	**0.210955**	**0.125583**	**0.790007**	**0.550388**		**0.178621**

ErrorO = Errors of Omission (expressed as proportions)
ErrorC = Errors of Commission (expressed as proportions)

90% Confidence Interval = +/- 0.000764 (0.177857 - 0.179385)
95% Confidence Interval = +/- 0.000910 (0.177711 - 0.179531)
99% Confidence Interval = +/- 0.001198 (0.177423 - 0.179819)

KAPPA INDEX OF AGREEMENT (KIA)

Using LANDCOV_PREDICT_2010 as the reference image ...

Category	KIA
1	0.608786
2	0.787430
3	0.824927
4	0.167012
5	0.100002

LULC_2010_NEW

Category	KIA
1	0.671169
2	0.714252
3	0.807764
4	0.207992
5	0.449144

Overall Kappa = 0.730501

Annex 6: Water Balance for Base and Projected Year LULC

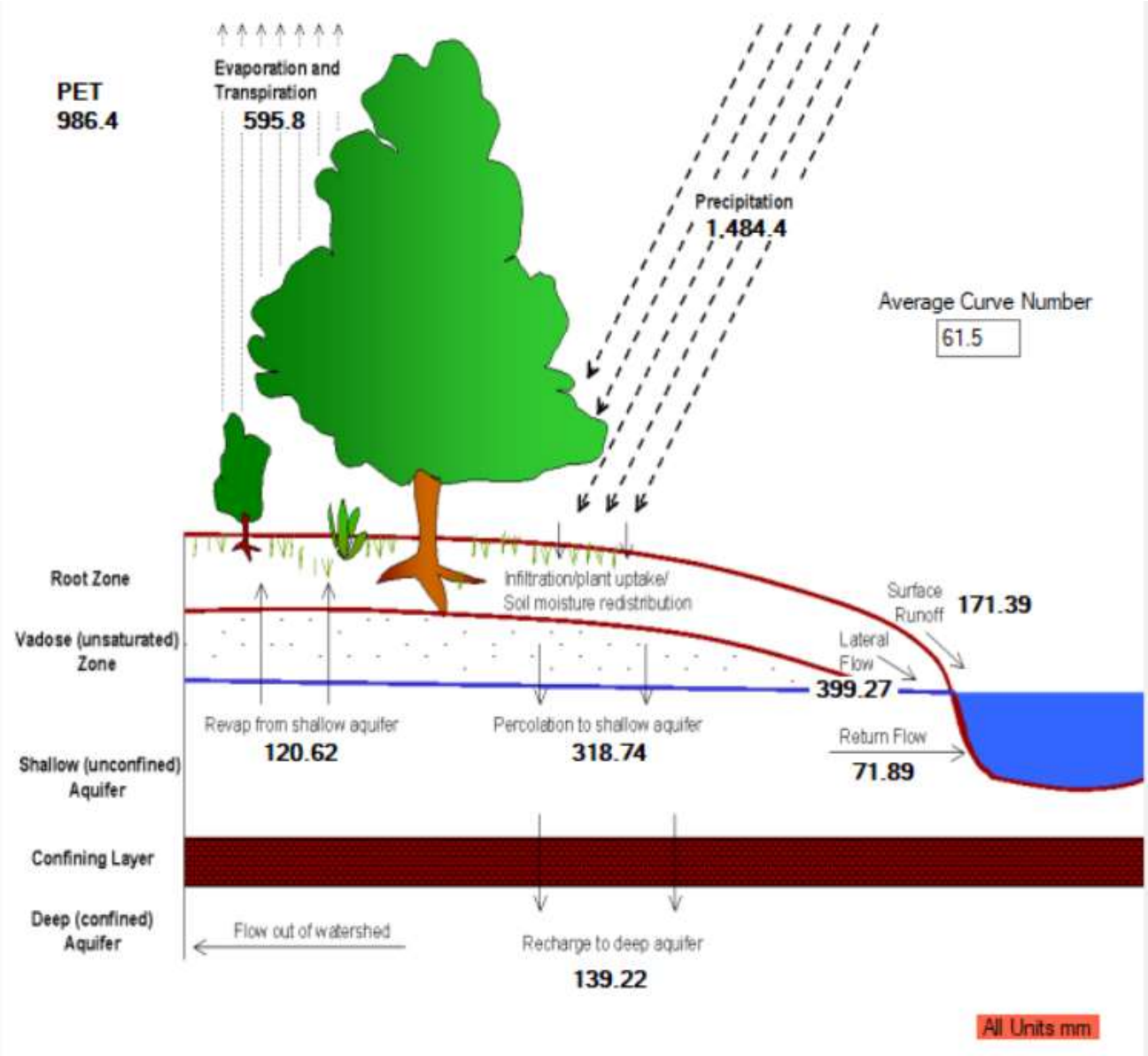

Figure 36: Water Balance for LULC 2000

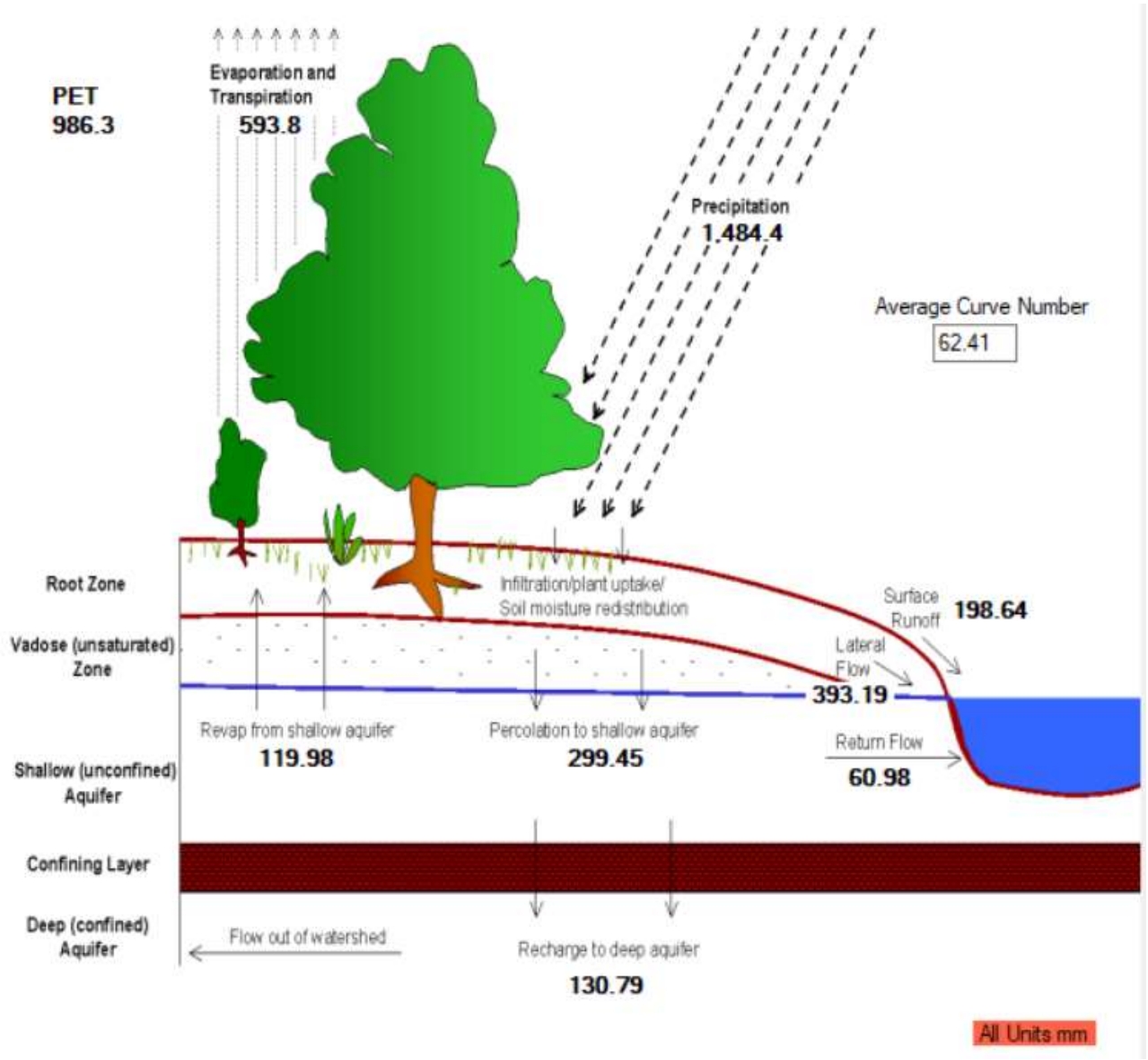

Figure 37: Water Balance for LULC 2025

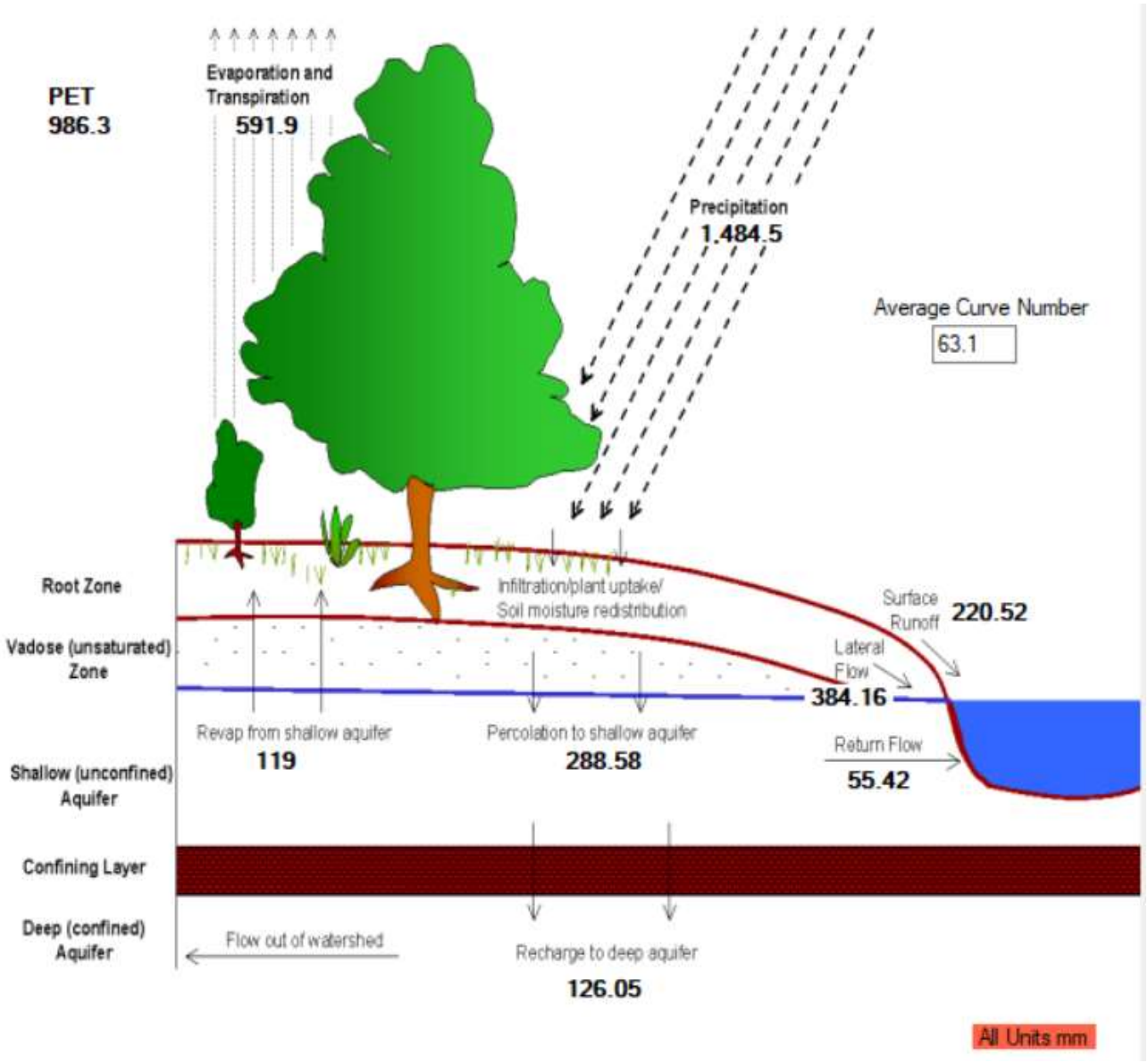

Figure 38: Water Balance for LULC 2050

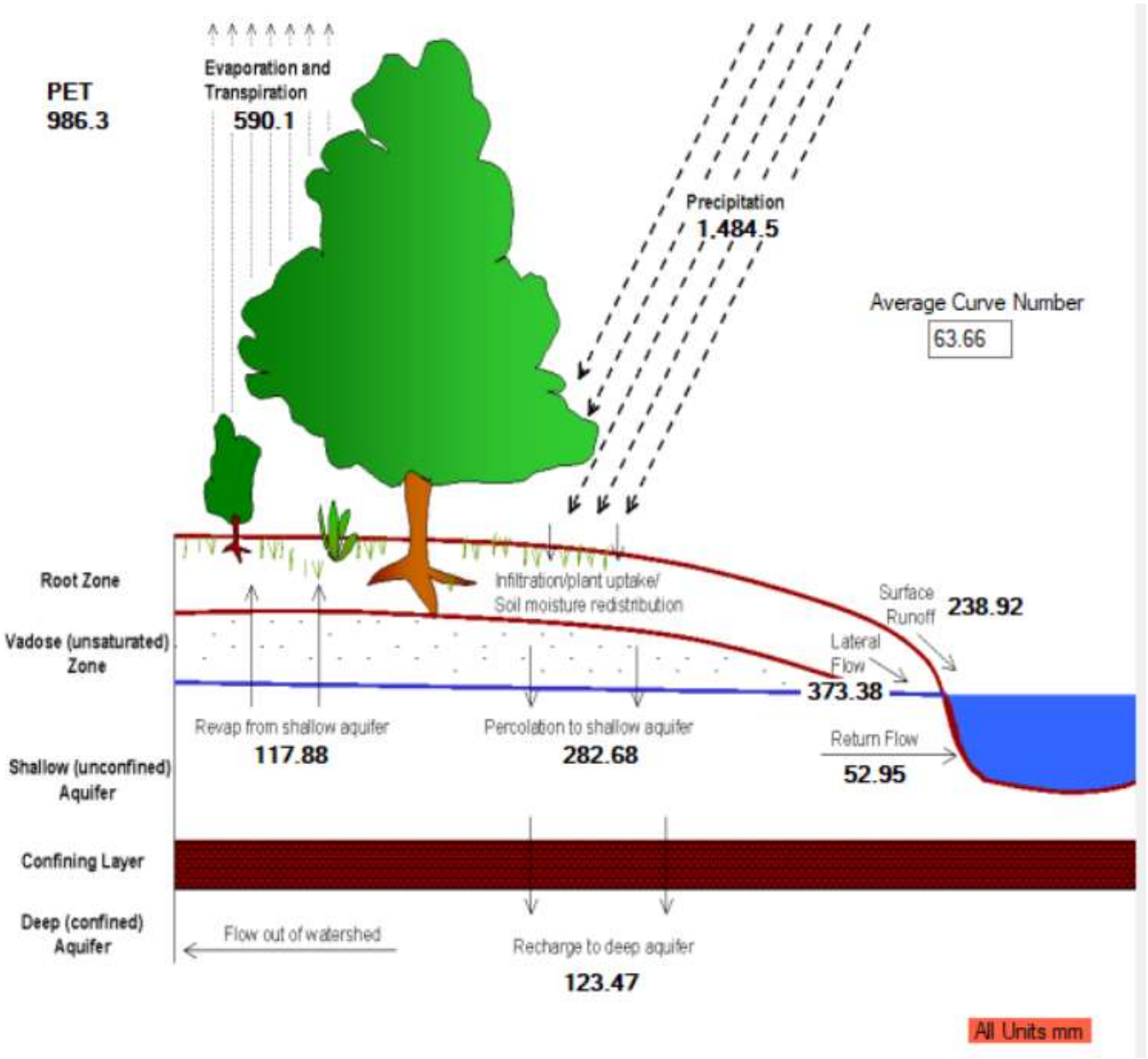

Figure 39: Water Balance for LULC 2075

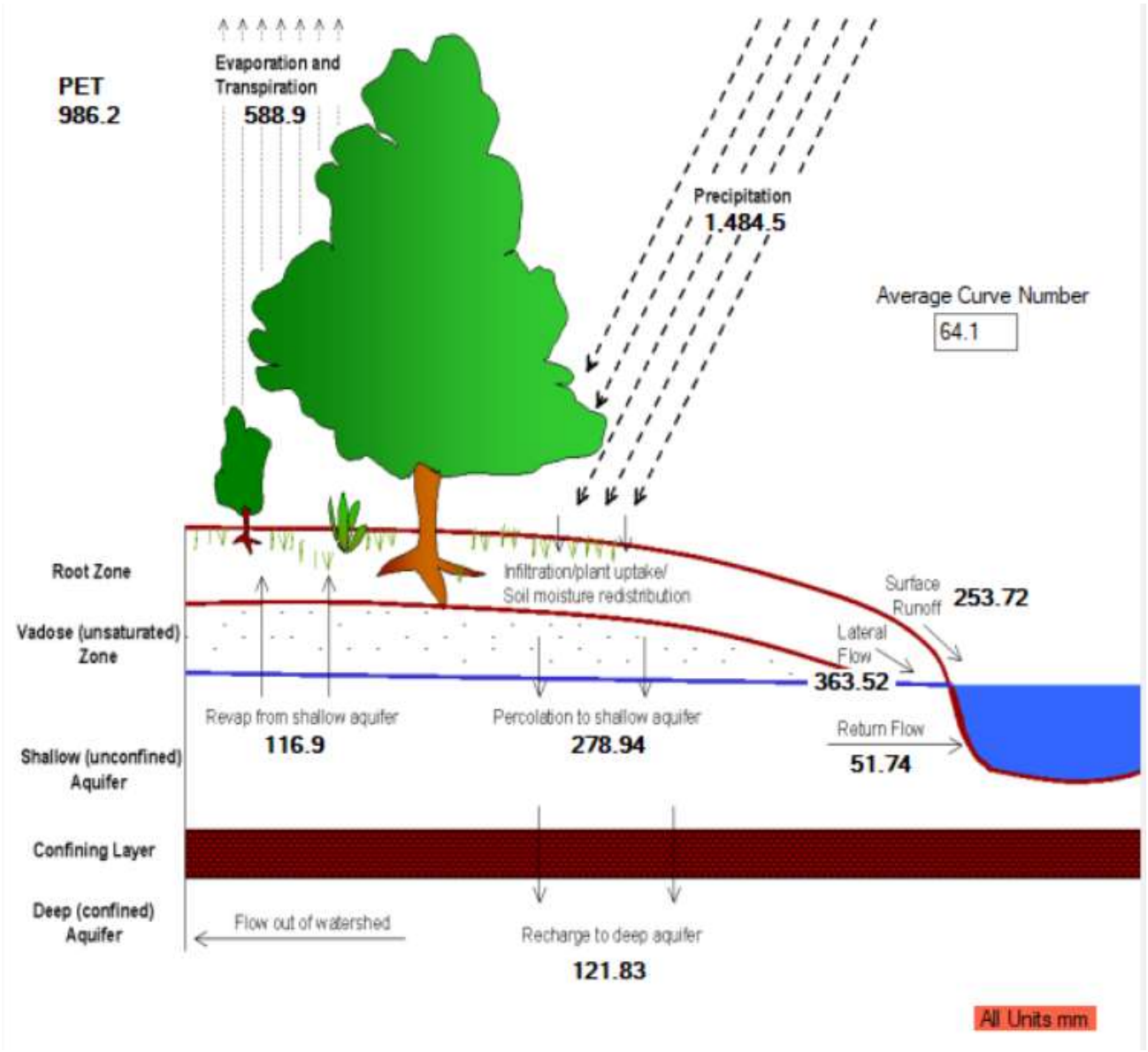

Figure 40: Water Balance for LULC 2100